Improvements in molecular diagnostics and image analysis for detecting and managing cervical cancer

Benjamin William Wormald

A thesis submitted to the Institute of Cancer Research, University of London

Degree: MD (Res)

September 2020

Word Count: 29052

Declaration

I declare that this thesis has been composed solely by myself and that it has not been submitted, in whole or in part, in any previous application for a degree. Except where states otherwise by reference or acknowledgment, the work presented is entirely my own.

Acknowledgements

This thesis would not have been possible without the support and encouragement of all my supervisors and colleagues at The Institute of Cancer Research, The Royal Marsden Hospital and Imperial College London.

I am deeply grateful to Professor Nandita deSouza for her guidance, perseverance and patience. She has provided me with a thorough grounding in research methodology and management. She has helped me at every step of the way in this project, through thick and thin.

I am indebted to Mr Thomas Ind for all his support in recommending me for the project, through to testing ideas, patient recruitment and advice throughout the project and beyond.

I would like to thank Dr Pantelis Georgiou for his encouragement and support throughout my time in his department.

I am especially grateful to Dr Jesus Rodriguez Manzano, his wisdom, encouragement and tolerance of 10 minute meetings lasting an hour, which allowed me to thrive and develop my understanding of the technology and techniques underpinning the bulk of the work completed in the thesis.

I would also like to thank Dr Simon Doran for his support and help, especially when needing to test ideas and guiding me through the machine learning and technical aspects of the project.

Ben Wormald 2020

Abstract

This thesis addresses improvements in molecular diagnostics and in image analysis, and their combination for managing cervical cancer.

Screening cytology has transformed early diagnosis but is resource intensive and highly dependent on skilled cytopathologists. Current tests focus on HPV detection but lack specificity. Multiplexing HPV PCR methods with identification of tumour nucleic acid markers would increase specificity. Also, following diagnosis, staging may be supplemented by quantitative image analytics; tumour texture information can be used alongside traditional histological assessments to provide prognostic information and enable optimal management planning at the outset. I therefore explored molecular and imaging biomarkers for improved early detection and characterisation of cervical cancer.

Chapter 2 focuses on selecting tumour markers and HPV markers relevant to cervical cancer and designing appropriate primers for tumour (hTERT, TERC, MYC) and HPV 16 and 18 marker detection on the lab-on-a-chip (LOC) platform. The analytical sensitivity of each of the markers was determined and found to be in the clinically relevant range. It then goes on to validate the lab-on-a-chip platform using banked tissue biopsy samples from patients with cervical cancer.

Chapter 3 establishes the sensitivity and specificity of HPV 16 and 18 DNA and RNA compared to MRI for early detection of cervical cancer. Finally, it trials the LOC platform prospectively using cytology samples from patients with newly diagnosed and recurrent cervical cancer and in normal controls.

Chapter 4 identifies radiomic features of cervical cancers on endovaginal MRI that differ between tumours below and above the volume threshold of eligibility

for trachelectomy and determines their value in predicting lymph node metastasis and recurrence in patients in the low-volume tumour group. It shows that in patients with low-volume tumours, ADC-radiomic texture analysis is potentially useful for predicting tumour recurrence.

Finally, Chapter 5 indicates how molecular and imaging diagnostics may be integrated into the clinical pathway of patients with cervical cancer to achieve early diagnosis and “test of cure” at the time of treatment.

Table of contents

List of figures

List of tables

List of abbreviations

ADC	Apparent diffusion coefficient
AIC	Akaike information criterion
APOBEC	Apolipoprotein
CBIT	Centre for bio-inspired technology
CIN	Cervical intraepithelial neoplasia
CMOS	Complementary metal-oxide semiconductor
DWI	Diffusion weighted imaging
FIGO	The International federation of gynecology and obstetrics
HPV	Human papillomavirus
HRA	Health research authority
IQR	Interquartile range
IRB	Internal research board
ISFET	Ion-sensitive field effect transistor
LAMP	Loop mediated isothermal amplification
LLETZ	Large loop excision of transformation zone
LMIC	Low middle income country
LN	Lymph node
LOC	Lab on a chip
LVSI	Lymphovascular space invasion
MUSCLE	Multiple sequence alignment
PCR	Polymerase chain reaction
PET	Positron emission tomography
PFS	Progression free survival
ROC	Receiver operating curve
ROI	Region of interest
SNP	Single nucleotide polymorphism
SNR	Signal to noise ratio

CHAPTER 1 Introduction

This thesis focuses on methods for improved diagnosis in early stage cervical cancer, which will ultimately impact its management and outcomes. It addresses improvements in molecular diagnostics and in image analysis, and their combination that should impact the diagnostic pathway of women with cervical cancer.

1.1 The scale of the problem- epidemiology of cervical cancer

Cervical cancer is the fourth most common cancer among women and the fourth leading cause of cancer deaths worldwide with an estimated 570000 new cases and 311,000 new deaths in 2018, with a worldwide lifetime risk of developing the disease of 1.36% (1). Most of the cases are diagnosed in less developed regions, with cervical cancer ranking second, only after breast cancer. The highest incidence and mortality rates are seen in Africa. It is the most commonly diagnosed cancer in 28 countries and the leading cause of cancer death in 42 countries, the vast majority of which are in Sub-Saharan Africa and South Eastern Asia. In comparison, in more developed areas, cervical cancer accounts for less than 1% of all cancers in women. At the extremes the age-standardised incidence and mortality shows an almost ten-fold difference between Southern Africa (43.1/20.0 per 100,000) and Western Asia (4.1/2.5 per 100,000), with figures more broadly comparing low/middle income countries against high-income countries being 18.2/12.0 per 100,000 versus 10.4/4.1 per 100,000. There is a downward trend in the incidence of invasive cervical cancer. The global age-standardised risk of disease

development and death in 2012 was 14.0 and 7.9 per 100,000 compared with 2018 estimates of 13.1 and 6.9 per 100,000 respectively. This is largely due to the implementation of screening in high-income countries, although there is a suggestion that improvements in genital hygiene, lower parity and a reducing prevalence of sexually transmitted disease may be contributing to this too. In countries with little to no screening programme incidence is either static or indeed rising, as in Eastern Europe (2-4).

Chronic infection by high-risk oncogenic subtypes of human papillomavirus (HPV) causes almost all cases of cervical cancer. Risk factors are related to acquiring an HPV infection or an impaired immune response to the infection. These risk factors include: age at sexual initiation, multiple sexual partners, history of sexually transmitted infection, immunosuppression, history of HPV-related vulvar or vaginal dysplasia and non-attendance for screening in countries with established cervical screening programmes. Additionally, smoking status, duration, and amount smoked are associated with a two-fold risk of high-grade dysplasia and carcinoma after adjustment for HPV status. This risk reduces two-fold with the cessation of smoking (5-7).

1.2 Mechanism of carcinogenesis

Infection with the human papillomavirus is recognised as the single most important causative factor in developing cervical cancer. In 2008 Harald zur Hausen was awarded the Nobel Prize in physiology and medicine for his discovery that human papillomavirus caused cervical cancer. He postulated that HPV-DNA could exist in a non-productive state in the tumours and should be detectable by specific searches for viral DNA. He found HPV to be a

heterogeneous family of viruses. Only some HPV types cause cancer. His discovery has led to characterization of the natural history of HPV infection, an understanding of mechanisms of HPV-induced carcinogenesis and the development of prophylactic vaccines against HPV acquisition (8, 9).

1.2.1 HPV prevalence, acquisition and clearance

According to the International Agency for Research on Cancer there are 12 high-risk HPV types (16,18,31,33, 35, 39, 45, 51, 52, 56, 58 and 59), which are carcinogenic to humans. HPV16 is consistently the most prevalent type in all of the world regions, detected in 60% of cases of cervical cancer with a range from 49% in Africa to 59% in Europe (10). After HPV16, the most prevalent HPV types, are HPVs 18/45/31/33/52/58, with variations between regions. HPV16 is detected more often in cases of squamous cell carcinoma (62%) than in adenocarcinoma (50%), while HPV18 and HPV45 are detected more often in adenocarcinoma (32% and 12%, respectively) than in squamous cell carcinoma (8% and 5%, respectively).

The risk of sexual transmission of HPV peaks early in sexual life and declines with age. Therefore, younger women more frequently test positive for high-risk HPV than women over 30 years of age (11). High-risk HPV screening is highly sensitive for detection of pre-malignant disease (cervical intraepithelial neoplasia (CIN) grades 2 or 3- CIN2/CIN3), but has reduced specificity, resulting in a high risk of over referral (12). Persistence of high-risk HPV infection is a key determinant of progression to disease. Infections lasting more than 2 years have a much greater risk of progression, up to 20% (13) with any high-risk HPV but could be as high as 47% with HPV 16 infections (14). The cumulative cervical cancer risks following persistent carcinogenic HPV

infections increase with age: The risks are 5.5%, 14.4%, and 18.1% for women aged 30–44 years, 45–54 years, and 55 years and older, respectively. However, newly acquired infections were associated with a low risk of cervical cancer regardless of age (15).

CIN 2 and 3 can be effectively treated by excision or ablation of the lesion on the cervix. Over a period of 30 years, untreated CIN 3 has a risk of progressing to invasive disease in approximately 25% to 30% of cases (16).

1.2.2 HPV mechanism of carcinogenesis

HPV infection alone is insufficient to cause carcinogenesis. Most HPV infections become undetectable after 6 months and never result in malignancies, with over 90% cleared by two years (17). High-risk HPV types persist longer on average than low-risk types. For HPV16, non-European viral variants are significantly more likely than European variants to cause persistence and CIN3+(18). A failure to clear the virus results in viral persistence, but many persistent infections never develop into precancerous lesions.

E6 and E7, account for most carcinogenic effects of high-risk HPV types. They promote carcinogenesis in several ways. E6 inhibits the p53 tumour suppressor by promoting its proteasomal degradation, while E7 disrupts the retinoblastoma pathway resulting in uncontrolled activation of the cell cycle and induction of p16INK4A, a cyclin-dependent kinase inhibitor, through a disrupted feedback loop (19, 20). E6 and E7 directly promote genomic instability (19, 21, 22), which can result in large chromosomal rearrangements and copy number variations, by interfering with centromere duplication during mitosis.

The apolipoprotein B mRNA editing catalytic polypeptide-like (APOBEC) mutation signature in particular is very common in HPV-positive cancers, triggered by the host response to HPV infection (23). The APOBEC family of cytosine deaminases cause cytosine to thymine or guanine mutations. APOBEC3B, a subclass of these proteins, causes characteristic mutations that are present in many cervical and head and neck cancers (24). During DNA repair, APOBEC-mediated cytosine deamination can result in characteristic mutational signatures. Upregulation of APOBEC proteins in response to viral infection can cause collateral damage to host DNA leading to carcinogenic mutations.

A key event in HPV-associated carcinogenesis is integration of the virus genome into the host chromosome. More than 50% of HPV16-positive and almost all HPV18-positive cases are associated with integration of virus genomes (25, 26). Integration of HPV into the host genome occurs leading to a break in the E2 gene, losing the main repressor of the expression of the E6 and E7 oncogenes. Integration is more likely to occur at integration hotspots, such as 3q28,4q13, 8q24, 13q22 and 17q21 (27).

1.3 Cervical Cancer diagnosis

Screening for precancerous lesions (cervical intraepithelial neoplasia) is appropriate as these lesions are common and treatable, and if they progress to invasive disease there is significant associated mortality. Screening and effective early diagnosis ensures that treatment addresses pre-invasive or early invasive disease. This means that disease detected is of low volume disease before it becomes symptomatic (28) with potential for better outcomes.

1.3.1 Screening cytology

Organised screening programmes based on the Papanicolaou cytological test have been successful in reducing the incidence of and mortality from the disease. However, the sensitivity of this test is such that women with abnormal results can be missed. A systematic review of cervical screening failures in countries with organised screening programmes showed that, among the women who developed cervical cancer, 20% to 55% had had false-negative smears 0 to 6 years prior to the diagnosis (29). Example cytology appearances are illustrated in Figure 1.1(30)

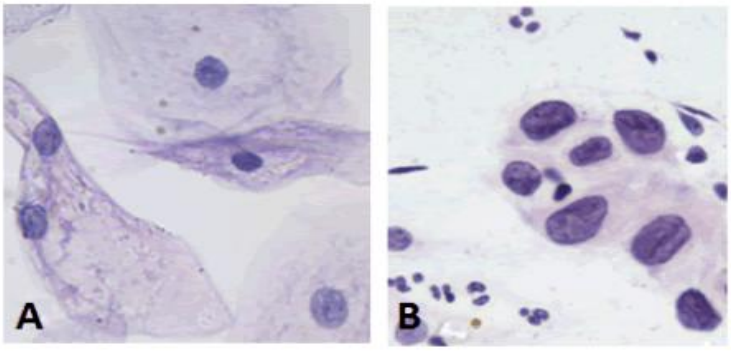

Figure 1-1 Cytology from a cervical smear showing normal cells (A) and malignant cells (B). Adapted from Deepak et al.

1.3.2 Colposcopic evaluation

Visual inspection of the cervix using acetic acid (VIA) or Lugol's iodine (VILI) is typically practised in low/middle income countries as it can be performed by trained midwives and nurses with relatively simple equipment. However, there is wide variation in its performance. A benefit of visual inspection is the opportunity to deliver immediate management when abnormalities are present. In a meta-analysis of 21 studies from sub-Saharan Africa and India among over

58 000 women,(31, 32) VIA showed moderate sensitivity for the detection of CIN2+ (pooled estimate: 79.2%–82.4%) and specificity (84.7%–87.4%). VILI

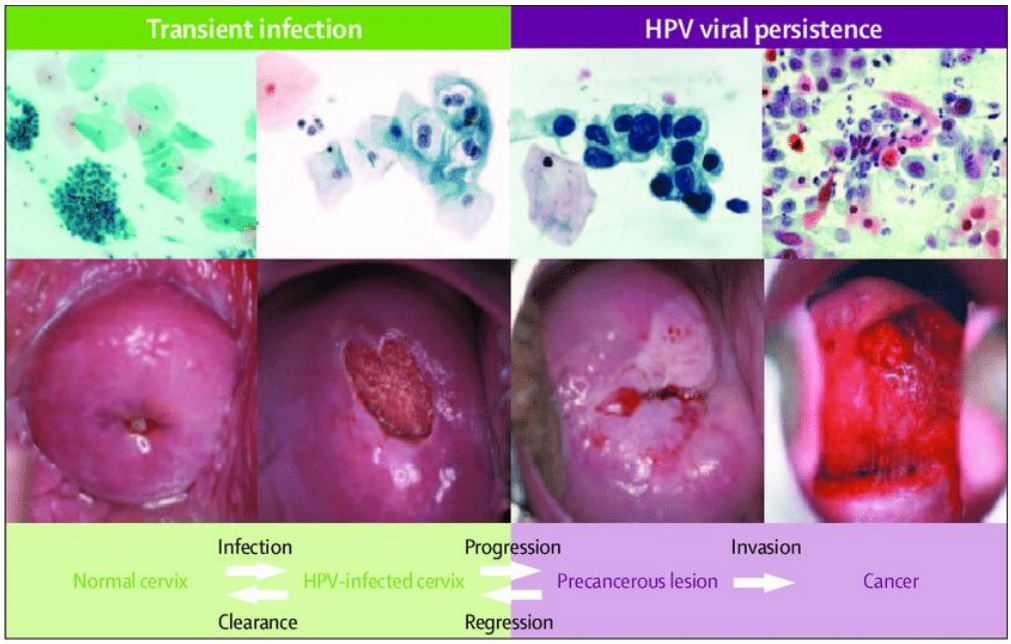

Figure 1-2 Appearances and associated cytological changes in the pathway to cervical carcinogenesis. Adapted from Crosbie et al.

performed even better with higher sensitivity (CIN2+: 91.2%–95.1%; CIN3+: 93.8%) and similar specificity (CIN2+: 84.5%–87.2%; CIN3+: 83.8%). Despite this, a single round of VIA screening has been associated with a 25%–35% reduction in cervical cancer incidence, cervical cancer mortality and the frequency of CIN2+ lesions, in studies in Thailand, Ghana and Zambia (33). Example appearance is shown in Figure 1.2 (34).

Colposcopy is a secondary test to evaluate for the presence of pre-malignant cervical disease and to determine appropriate biopsy site/s to confirm histological diagnosis. It is established as the primary procedure to assess abnormal cervical screening tests. The success of colposcopy is determined by the skill of the operator and influenced by the number of directed biopsies (35-38). The prevalence of the disease is also key – the discriminative ability of colposcopy to detect pre-malignant disease in low prevalence settings is poor

(39). In highly experienced centres the effectiveness of colposcopy to distinguish between normal and low-grade lesions from high-grade or worse lesions have a mean weighted sensitivity of 85% and specificity of 69% with a negative predictive value of 85% (40). However, this performance may not be seen in standard settings where poor sensitivity has been showed to range between 30-70%. The important distinction is represented by the false negatives of colposcopy. It is a secondary test which should aim to rule out a pre-malignant disease (41). In a recent study a cytology result of low grade dyskaryosis low grade colposcopy still had a risk of CIN2+ of 18% from associated biopsy (42). In the setting of a patient with low grade dyskaryosis and untreated following colposcopy, a 5-year risk of CIN2+ was 10% (43).

1.3.3 Screening for HPV

As over 99% of cervical cancers test positive for HPV DNA, a test for the detection of HPV DNA is a much more sensitive screening for cervical cancer precursors. A randomised controlled trial showed that a single round of HPV DNA screening in India halved mortality related to invasive cervical cancer (44). Diagnosis of HPV infection requires the detection of its genome in cellular samples by collecting exfoliated cervical cells. Specimens can be collected either by a healthcare provider during a pelvic examination, or through self-sampling (45).

Follow up of four randomised controlled trials comparing HPV DNA screening versus cytology, (POBASCAM, ARTISTIC, NTCC and Swedescreen) for a median of 6.5 years showed the rate-ratio for invasive cervical carcinoma from recruitment to end of follow-up was 0.60 (0.40-0.89) with a rate-ratio of 0.30

(0.15-0.60) for those women testing negative at entry (46). The HPV assays used in these trials were the Hybrid Capture-2 (HC2) and the GP5+/6+ PCR–enzyme immunoassay (EIA).

Molecular technologies for the detection of HPV DNA can be broadly divided into amplified and non-amplified. The tests mainly used in clinical research use amplification methods, which are further divided into signal amplified and target amplified. The main representative techniques of each category are the hybrid capture 2 (HC2; Digene Corporation, Gainthersburg, MD, USA) assay and polymerase chain reactions (PCR), respectively. Current PCR techniques involve consensus primers, so that they can be used to amplify a broad spectrum of HPV genotypes. They focus on the L1 gene. However, as 10% of integrated HPV genomes have lost the L1 gene a negative test may result despite active disease (47).

In 2009 and international expert committee proposed that any new HPV DNA assay should be at least as accurate as the HC2 or GP5+/6+ assays as these had been clinically validated (48). The Meijer criteria determine that any new test should have a relative sensitivity of at least 0.90 and relatively specificity of 0.98. This should be derived from a representative set of consecutively collected samples (minimally 60 CIN2+ cases, 800 CIN1 cases) from a population-based screening cohort of women aged 30 to 60 years (49). To assess assay performance for those that have the capability to genotype an additional set of criteria was proposed. The VALGENT (VALidation of HPV GENotyping tests), currently on its 4th iteration, involves 1000 consecutive screening samples and 300 enriched abnormal screening samples.

Women with active HPV infection will express E6/E7 oncogenes. The E6/E7 mRNA transcripts are detected by mRNA-based tests and may therefore be of higher prognostic value, improving the specificity and positive predictive value compared with the HPV DNA testing used in screening. In a large meta-analysis for CIN 2+, pooled sensitivity estimates for HPV DNA, Aptima mRNA, cytology and liquid based cytology were 89.9%, 92.7%, 62.5% and 72.9%, respectively, and pooled specificity estimates were 89.9%, 96%, 96.6%, and 90.3%, respectively (50).

Cervical screening programmes are transferring to HPV-based system and across Europe, for example, are at various stages of implementation. The Netherlands completed the transition in 2017 and recently reported increased CIN2+ detection from 11 to 14 per 1000 women screened (51). A cost analysis of the Dutch system suggested the new system was more cost effective than a cytology based approach, partly through retained protection at longer intervals between screening episodes allowing for fewer screening rounds to take place. This is despite the increase in referrals to colposcopy for low-grade lesions (12). The addition of good-performance, rapid and affordable point-of-care (POC) tests would considerably enhance access to HPV testing in low/middle income countries. An example is the careHPV test (Qiagen) is based on a simplification of the HC2 test platform. It detects 14 HR-HPV types. It has a sensitivity of 88.1% and specificity of 83.7% for CIN2+ detection using clinician-collected cervical swabs and a sensitivity of 73.6% and specificity of 88.0% using self-collected vaginal swabs (33).

1.3.4 Cervical cancer staging

The 2009 staging system(52) (Figure 1.3) was used for the studies described in this thesis.

It has since been superseded by the 2018 staging system which is included for completeness.

Stage I	The carcinoma is strictly confined to the cervix (extension to the corpus would be disregarded)
IA	Invasive carcinoma that can be diagnosed only by microscopy, with deepest invasion ≤5 mm and largest extension ≤7 mm
IA1	Measured stromal invasion of ≤3 mm in depth and extension of ≤7 mm
IA2	Measured stromal invasion of >3 mm and not >5 mm with an extension of not >7 mm
IB	Clinically visible lesions limited to the cervix uteri or preclinical cancers greater than stage IA[a]
IB1	Clinically visible lesion ≤4 cm in greatest dimension
IB2	Clinically visible lesion >4 cm in greatest dimension
Stage II	Cervical carcinoma invades beyond the uterus, but not to the pelvic wall or to the lower third of the vagina
IIA	Without parametrial invasion
IIA1	Clinically visible lesion ≤4 cm in greatest dimension
IIA2	Clinically visible lesion >4 cm in greatest dimension
IIB	With obvious parametrial invasion
Stage III	The tumor extends to the pelvic wall and/or involves lower third of the vagina and/or causes hydronephrosis or nonfunctioning kidney[b]
IIIA	Tumor involves lower third of the vagina, with no extension to the pelvic wall
IIIB	Extension to the pelvic wall and/or hydronephrosis or nonfunctioning kidney
Stage IV	The carcinoma has extended beyond the true pelvis or has involved (biopsy proven) the mucosa of the bladder or rectum. A bullous edema, as such, does not permit a case to be allotted to Stage IV.
IVA	Spread of the growth to adjacent organs
IVB	Spread to distant organs

[a]All macroscopically visible lesions—even with superficial invasion—are allotted to stage IB carcinomas. Invasion is limited to a measured stromal invasion with a maximal depth of 5 mm and a horizontal extension of not >7 mm. Depth of invasion should not be >5 mm taken from the base of the epithelium of the original tissue—squamous or glandular. The depth of invasion should always be reported in mm, even in those cases with "early (minimal) stromal invasion" (–1 mm). The involvement of vascular/lymphatic spaces should not change the stage allotment.

[b]On rectal examination, there is no cancer-free space between the tumor and the pelvic wall. All cases with hydronephrosis or nonfunctioning kidney are included, unless they are known to be due to another cause.

FIGO Committee on Gynecologic Oncology. Revised FIGO staging for carcinoma of the vulva, cervix, and endometrium. *Int J Gynecol Obstet.* 2009;105:103–104.

Figure 1-3 FIGO 2009 staging system for cervical cancer. Adapted from Pecorelli et al

The revised FIGO 2018 staging scheme (53) made several adjustments to the FIGO 2009 system namely:

- Allowing the use of any imaging modality and/or pathological findings for allocating the stage.
- In stage I, amendments to microscopic pathological findings and to size designations, allowing the use of imaging and/or pathological assessment of the size of the cervical tumour.
- In stage II, allowing the use of imaging and/or pathological assessment of size and extent of the cervical tumour.

- In stages I through III, allowing assessment of retroperitoneal lymph nodes by imaging and/or pathological findings and, if deemed metastatic, the case is designated as stage IIIC as those with lymph node metastasis have worse stage adjusted overall survival

Stage I:

The carcinoma is strictly confined to the cervix uteri (extension to the corpus should be disregarded)

- **IA** Invasive carcinoma that can be diagnosed only by microscopy, with maximum depth of invasion <5 mm
  - ○**IA1** Measured stromal invasion <3 mm in depth
  - ○**IA2** Measured stromal invasion ≥3 mm and <5 mm in depth
- **IB** Invasive carcinoma with measured deepest invasion ≥5 mm (greater than stage IA), lesion limited to the cervix uteri
  - ○**IB1** Invasive carcinoma ≥5 mm depth of stromal invasion and <2 cm in greatest dimension
  - ○**IB2** Invasive carcinoma ≥2 cm and <4 cm in greatest dimension
  - ○**IB3** Invasive carcinoma ≥4 cm in greatest dimension

Stage II:

The carcinoma invades beyond the uterus, but has not extended onto the lower third of the vagina or to the pelvic wall

- **IIA** Involvement limited to the upper two-thirds of the vagina without parametrial involvement
  - ○**IIA1** Invasive carcinoma <4 cm in greatest dimension
  - ○**IIA2** Invasive carcinoma ≥4 cm in greatest dimension
- **IIB** With parametrial involvement but not up to the pelvic wall

Stage III:

The carcinoma involves the lower third of the vagina and/or extends to the pelvic wall and/or causes hydronephrosis or non-functioning kidney and/or involves pelvic and/or paraaortic lymph nodes

- **IIIA** Carcinoma involves the lower third of the vagina, with no extension to the pelvic wall
- **IIIB** Extension to the pelvic wall and/or hydronephrosis or non-functioning kidney (unless known to be due to another cause)
- **IIIC** Involvement of pelvic and/or paraaortic lymph nodes, irrespective of tumour size and extent
  - ○**IIIC1** Pelvic lymph node metastasis only
  - ○**IIIC2** Paraaortic lymph node metastasis

Stage IV**:**

The carcinoma has extended beyond the true pelvis or has involved (biopsy proven) the mucosa of the bladder or rectum. A bullous oedema, as such, does not permit a case to be allotted to stage IV

- **IVA** Spread of the growth to adjacent organs
- **IVB** Spread to distant organs

Figure 1-4 FIGO staging system for cervical cancer 2018. Adapted from Bhatia et al

1.4 Imaging in cervical cancer

Imaging is now recognised as a fundamental part of assessment of a patient with cervical cancer. Imaging is used to stage the disease, to plan treatment, to assess response to therapy and for follow-up to identify disease recurrence. Available imaging modalities encompass ultrasound, CT, MRI and PET-CT using an 18F-FDG radiotracer. Ultrasound and CT lack the soft-tissue contrast for defining tumour within the cervix, and ultrasound is operator dependent. MRI is the first-line imaging modality for this purpose and has been shown to be superior to CT in several studies (54). Its superior image contrast also makes it the mainstay of treatment planning, response assessment and follow-up of disease within the pelvis. For assessment of extrapelvic disease, CT or PET-CT are preferred.

1.4.1 MRI

The development of improved MRI diagnostics for cervical cancer described in this thesis warrants a more detailed background to this imaging method.

1.4.1.1 Principles of MRI

When placed in a strong magnetic field (~15-30,000 times stronger than the Earth's magnetic field) hydrogen protons in tissue water align themselves parallel or anti-parallel to the direction of the magnetic field, whilst precessing (rotating) about their own axis at a frequency that is related to the strength of the magnetic field (Larmor frequency, 63.86 MHz at 1.5T, 127.71 MHz at 3T, where Tesla (T) is a unit of magnetic flux density). Radiofrequency (rf) excitation delivered at the Larmor frequency causes protons to resonate and tips the net magnetization away from their alignment along the magnetic field. When the excitation stops, protons return to their alignment in their equilibrium position. In

doing so they emit an rf signal which relates to their T1 and T2 relaxation properties. These relaxation properties are determined by tissue structure and molecular interactions. T1 relaxation refers to signal decay that is influenced by interaction of the spins with the surrounding lattice structure; T2 relaxation refers to signal decay that relates to interaction with neighbouring spins.

To generate an MR image therefore, a static magnetic field is required. Clinical systems primarily operate at 1.5T and 3.0T. Gradient coils are used to generate local magnetic field gradients that enable recognition of the position of a signal in space (spatial localisation) from its frequency and phase. This is crucial for the re-construction of an image from the emitted signals. Hardware to generate the rf pulses, receiver coils to collect the emitted signal and amplify it and computational capability for image reconstruction are essential components that are integrated within clinical MR systems. For early stage disease specialist receiver coils may be used that are placed endovaginally. This is detailed further in section 4.3.3.

1.4.1.2 Sequences used for cervical MRI

Imaging cervical cancer is heavily dependent on T2W sequences. T2W contrast is determined by the different T2 values between tissues (different rates of signal decay dependent on spin-spin interactions) which therefore depend on their molecular structure and the interaction of water protons within this molecular environment.

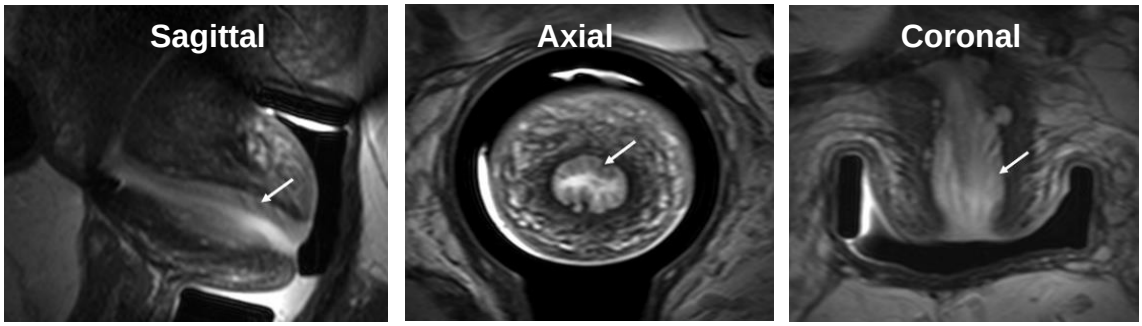

Figure 1-5 Sagittal (left), axial (middle) and coronal (right) T2W images. The intermediate signal intensity mucosa (arrows) is seen in contrast to the bright

Fluids generally have the longest T2 values (~700-1200 ms) and are hyper-intense (bright) on T2W imaging, compared to other soft tissues (~40-200 ms), which can be relatively hypo-intense (dark) depending on their water content. Cancer tissues for instance have longer T2 values than normal muscle and are brighter than the surrounding dark normal fibromuscular cervix or myometrium.

Figure 1-6 Sagittal T2W image showing a large intermediate signal-intensity cancer within the cervix (marked) in comparison to the low signal intensity myometrium and bright signal from fluid in the bladder.

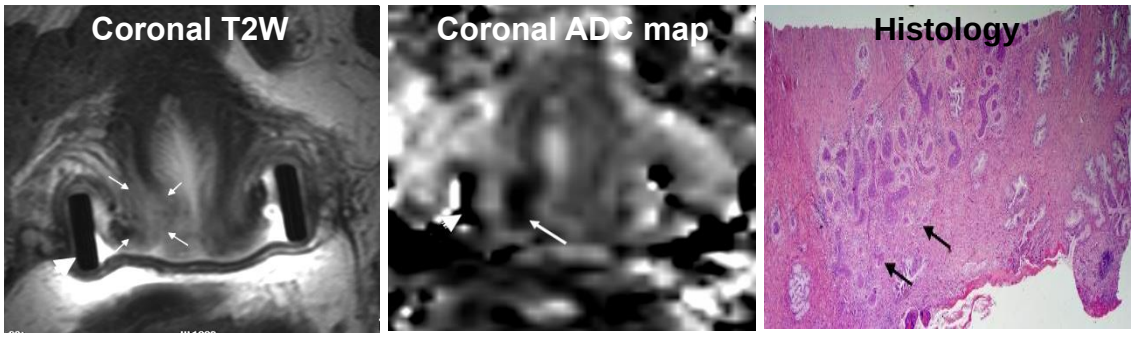

Figure 1-7 Coronal T2W image (left) and ADC map derived from diffusion-weighted images (middle) show a poorly defined tumour in the former and a well-defined restricted diffusion mass in the latter (arrows), The right-hand image shows the corresponding histological area

Another key sequence used for cervical cancer delineation is diffusion-weighted imaging (DWI)(55) . DWI depends on the thermally induced random movement /of molecules, which is affected by the presence of cellular structures that provide barriers to movement (56). DWI is sensitive to changes in the diffusion of water molecules within intra-cellular and extra-cellular spaces (56). The DWI signal can be quantified by calculating the apparent diffusion coefficient (ADC), which describes the distances diffused by water molecules over time, and is measured in units mm^2/s. ADC calculation requires the diffusion signal to be measured at least twice, using different b values, which describe the diffusion-weighting of the sequence and are defined by the strength, duration and separation of the diffusion gradients (56). Lower b-values (<50 s/mm^2) are sensitive to longer distances travelled by protons, such as those within the microvascular compartment; higher b-values (>500 s/mm^2) are sensitive to shorter distances travelled by protons in molecular environments restricted by larger molecules such as those bound in cell membranes. The requirement to measure the DWI signal multiple times means that acquisitions can be lengthy. ADC values derived for each image voxel are used to create ADC maps. Tumours are densely cellular and appear as areas of restricted diffusion (bright

on diffusion-weighted images where the signal has not decayed, and dark on ADC maps where the rate of decay of signal is low).

1.4.1.3 Protocols for cervical imaging

MRI offers a multiplanar facility, and the orientation of slices can be performed at any prescribed angle. It is usual to image with T2W sequences in at least 2 planes, with DWI in 1 or 2 planes that best demonstrate the lesion. The planes advocated are normally along the long axis and the short axis of the cervix (sagittal and axial respectively). However, as surgical visualisation of the uterus is normally done in the coronal plane, it is helpful to visualise the uterus and cervix in the coronal plane also. The coronal and axial planes are used for determining parametrial invasion, the axial plane is used for determining extension into the bladder and rectum, and the sagittal plane is used for determining extension into the uterine body, bladder and rectum (57). In the sagittal plane it is also possible to determine the relationship of the superior tumour margin to the cervical os and hence the patient's suitability for trachelectomy.

1.4.1.4 Interpretation of cervical MRI

Identification of an intermediate signal-intensity mass within the cervix necessitates a measurement of its volume, as this is the strongest prognostic factor in cervical cancer(58). Accurate estimates are possible by outlining the whole tumour area on all slices and multiplying by slice thickness. Tumour extent in terms of local extension-laterally into the parametria and anteriorly and posteriorly into fat planes between cervix and bladder and cervix and rectosigmoid colon respectively and pelvic side-wall involvement are noted as part of MRI staging. Vaginal involvement is usually noted at examination under

anaesthesia. Pelvic nodal involvement is assessed on axial T2W images through the pelvis. Use of contrast agents (weakly paramagnetic agents such as gadolinium chelates or lymph node specific contrast agents is not warranted routinely as they do not improve diagnostic accuracy (59). Assessment of abdominal or more distant metastatic spread remains the domain of CT/PET-CT.

1.4.2 Imaging extracervical disease with CT and PET-CT

As with other cancer types, the sensitivity and specificity of detecting involved lymph nodes on CT has been shown to be 57% and 91% respectively in a meta-analysis of 22 studies (60). This is because CT is fundamentally an x-ray technique whose contrast is determined by tissue density alone. Involved nodes are the same tissue density as uninvolved nodes and their involvement can only be surmised from an increase in size. Size criteria for recognizing nodes as abnormal are established; these require short axis measurements, which are sometimes dependent on the obliquity of the node in relation to the plane of image acquisition.

PET-CT has replaced CT for assessing nodal status in gynaecological cancers. It has a reported sensitivity and specificity of 66% and 97% in a meta-analysis of 46 studies (60). Tumour containing nodes have a high glucose turn over and take up the fluorodeoxyglucose tracer. This undergoes intracellular phosphorylation and is trapped. Signal recognition is via the gamma-emission of 2 coincidental photons. As the technique involves a whole-body scan, it offers the potential for recognition of unexpected or additional sites of metastases. It is also used as the technique of choice for follow-up and surveillance of cervical

cancers 3 months post treatment (61, 62) because of its high sensitivity for detecting residual or recurrent disease and its whole-body visualisation.

1.5 Management of cervical cancer

The management of cervical cancer depends on disease stage at diagnosis, patient age, morbidity and desire for fertility preservation. The broad strategies for treatment are surgery for Stage 1 disease and chemoradiotherapy for locally advanced disease, Stages 2-4.

1.5.1 Surgical treatment

1.5.1.1 Radical hysterectomy

The standard surgical procedure for patients with early-stage cervical cancer is radical hysterectomy and pelvic lymphadenectomy. However, this treatment does not preserve fertility.

Key principles of treatment include avoiding a combination of radical surgery and radiotherapy due to the additive morbidity associated with this treatment (63). If a combination of risk factors is known at diagnosis (e.g. lymphovascular space invasion or lymphadenopathy), which would require an adjuvant treatment, primary chemoradiotherapy would be indicated. Systematic lymph node dissection includes the removal of lymphatic tissue from regions with the most frequent occurrence of positive nodes such as obturator fossa, external iliac regions, common iliac regions bilaterally, and presacral region. Removal of ovaries is unnecessary in premenopausal women but an opportunistic salpingectomy at hysterectomy is reasonable.

Modified radical hysterectomy (Piver Class II) encompasses of removal of the uterus, the cervix and upper 1 cm to 2 cm of the vagina. The limits of resection include the medial half of the parametria and proximal uterosacral ligaments. Radical hysterectomy (Piver Class III), consists of removal of the uterus with the upper third of the vagina and parametrial tissues. The uterine vessels are ligated at their origin, and the whole width of the parametrium removed on both sides, along with the removal of as much of the uterosacral ligaments as possible.

1.5.1.2 Use of neoadjuvant chemotherapy

Traditionally, early cervical cancers have been treated with surgery and advanced cancers with chemoradiotherapy. However, there is no consensus regarding the ideal treatment for stage IB2 cervical cancers. In the UK, stage IB2 is treated mainly by chemoradiotherapy, due to a high likelihood of risk factors requiring adjuvant chemoradiotherapy (64). However, another approach recently studied show that neoadjuvant chemotherapy followed by surgery for cervical cancer stage IB2 to IIB, result in similar survival, but less long term toxicity compared to chemo-radiotherapy (65). A Cochrane database review done nearly a decade ago of 6 trials (1072 women). Whilst PFS was significantly improved with neoadjuvant chemotherapy (HR = 0.76, 95% CI = 0.62 to 0.94, p = 0.01), no OS benefit was observed (HR = 0.85, 95% CI = 0.67 to 1.07, p = 0.17). There was also no difference in the effect of neoadjuvant chemotherapy according to total cisplatin dose, chemotherapy cycle length or by cervical cancer stage (66). A more recent randomised phase 3 trial indicated that in patients with locally advanced disease, chemoradiotherapy had a better disease-free survival than

neoadjuvant therapy followed by surgery (67). In patients suitable for surgery, neoadjuvant chemotherapy is not routinely used.

1.5.1.3 Fertility sparing surgery

As a significant proportion of women are diagnosed with early cervical cancer during their reproductive years, fertility sparing options have been explored, including, conisation and radical trachelectomy, of which there are vaginal and abdominal varieties. Radical trachelectomy means removing the cervix with parametrium and upper vagina but retaining the uterus.

For stages 1a1 and 1a2, lymph node-negative, LVSI-negative patients a conisation is typically performed. A pelvic lymphadenectomy is recommended in women with stage 1a2 and LVSI. Radical trachelectomy is the treatment of choice for women with stage T1b1 with tumours less than 2cm in diameter and lymph node negative. Women have a risk of adjuvant therapy being required, and therefore fertility sacrificing, following histological analysis of 11%.

In a recent meta-analysis of 60 observational studies analysed by a random-effects model and a meta-regression to assess heterogeneity conisation was associated with a recurrence rate of 0.4% with no reported deaths and a pregnancy rate of 36.1%, a miscarriage rate of 14.8% and a preterm delivery rate of 6.8%. Radical trachelectomy had a recurrence rate of 2.3% with a pregnancy rate of 20.5%, a miscarriage rate of 24.0% and a preterm delivery rate of 26.6%. To reduce the risk of pre-term labour an intraoperative placement of permanent cerclage should be performed (68).

However, data can be confounded by women not attempting pregnancy. Figures quoted in the most recent BGCS guideline suggest women attempting a pregnancy 54.5% achieved one and 54.2% achieved at least one birth.

Following radical trachelectomy 38.3% are born prematurely and some 17% are born before 32 weeks (69).

1.5.1.4 Adjuvant treatment

Adjuvant radiotherapy is offered when a combination of risk factors at final pathology such as tumour size, LVSI, and depth of stromal invasion is present. GOG 92 (Gynaecology Oncology Group 92- a phase III randomized trial of postoperative pelvic irradiation in Stage IB cervical carcinoma with poor prognostic features) compared radiotherapy after surgery with surgery alone in an intermediate-risk group. There was a reduction in the recurrence rate from 28% to 15% with the addition of radiotherapy (63). Typically, a dose between 45-50 Gy is applied over 4-5 weeks and should commence within 8 weeks. The clinical treatment volume should include the common, external, and internal iliac lymph node regions and the upper 3 cm of vagina and paravaginal soft tissue lateral to the vagina (70-72).

In patients with high-risk prognostic factors such as lymph node metastasis, parametrial invasion or positive surgical margins the addition of chemotherapy to radiotherapy significantly improves progression-free and overall survival by almost a half (73, 74).

1.5.1.5 Pelvic Exenteration

Pelvic exenteration is a rare radical surgical procedure to remove the visceral pelvic organs en-bloc and is performed for recurrent disease located in the central pelvis. Survival rates after pelvic exenteration have been reported as high as 48-54% (75, 76). This procedure is an option for salvage therapy with a therapeutic intent. Pelvic exenteration, however, is associated with high perioperative morbidity due to the nature and extent of surgery, with

complication rates previously quoted as 51–88% with a perioperative mortality of 1.9% (77).

1.5.2 Chemoradiotherapy

Results of 18 trials from 11 countries worldwide shows there is clear evidence that adding chemotherapy to radiotherapy improves both overall and disease-free survival, with a 6% absolute survival benefit and an 8% disease-free survival benefit at 5 years (78).

Primary chemoradiotherapy consists of concomitant pelvic chemoradiotherapy, which is platinum based, and brachytherapy. Overall treatment time is typically between 6-8 weeks. External beam radiotherapy (EBRT) is applied as concomitant chemoradiotherapy with a total dose of 45 to 50 Gy. Targets for treatment include the primary cervical tumour and the adjacent tissues such as parametria, uterine corpus, upper vagina, and the lymphatic chain (obturator, internal, external and common iliac, presacral). Brachytherapy is offered in large tumours toward the end of treatment or after concomitant chemoradiotherapy with a dose of 40 to 45 Gy to reach a total EBRT + brachytherapy dose of equal to or greater than 85 to 90 Gy (79).

1.6 Outcomes of treatment

According to the most recent survival data for the UK the expected 5-year overall survival for stages 1-4 is, 95%, 50%, 40% and 5% respectively (80). However, there are several prognostic factors, especially affecting early stage disease which can have a profound effect on risk of recurrence and ultimately death.

Pelvic lymph node metastases decrease the 5-year survival from 82-90% to 38-61% in patients with positive lymph nodes in Stage 1 disease. In Stage 1A disease LVSI is present in 2.1-5.5% of cases with positive lymph node metastasis present in 2% with a recurrence rate of 0.4-2% and overall survival between 98-99% (81-83). Additional risk factors for recurrence are large tumour diameter, deep stromal invasion, and lymphovascular space invasion, a combination of which are present in up to 25% of Stage 1B tumours. These factors increase the risk of recurrence at 3 years from 2 to 31% (63, 84).

1.7 Gaps in knowledge

Disease detection: The most powerful way to influence outcomes in cervical cancer is through early disease detection. Screening cytology has made huge in-roads in this regard, making cervical cancer a rare cancer in the developed world. However, the means to carry out large scale screening in the developing world where the incidence of cervical cancer is high, is resource limited. Having a robust point-of-care test, that is cheap and easily administered would be a huge advantage. Current tests focus on HPV detection and use Hybrid Capture 2 or PCR based assays. The methodology is robust, but they remain difficult to analyse and lack specificity. Multiplexing HPV PCR methods with identification of tumour nucleic acid markers would increase specificity.

Disease prognosis: Once the diagnosis of cervical cancer has been made on biopsy, imaging is used for staging. Advances in quantitative image analytics mean that tumour texture information can be extracted from the data. This image quantitation could be used alongside traditional histological assessments to provide predictive information and enable optimal management planning at

the outset. Imaging biomarkers can be derived from the whole tumour (unlike the sampling variation intrinsic to biopsy) and have the advantage of being available prior to treatment planning.

Derivation of an apparent diffusion coefficient (ADC) from the DW images (85) and analysis of first order histogram distribution of ADC values has been shown to predict histological subtype (86, 87), staging (88), parametrial invasion (89), LVSI (90), the response to chemo-radiotherapy [19] and to aid surgical decision-making (91)[20]. However, these first-order statistical quantitative imaging data remain limited in their prediction of likely recurrence (92). It is possible to refine image analysis and convert the T2-W (93) and DW (94) imaging data into a high-dimensional feature space using algorithms to extract a more extensive set of statistical features within the data. This type of analysis, referred to as “radiomics”, requires that the data have a high signal-to-noise ratio to reduce error in the analysis from image noise; this is achievable in cervical cancer using an endovaginal MRI technique (95).

I therefore explored molecular and imaging biomarkers for improved early detection and characterisation of cervical cancer.

1.8 Hypothesis

Development of molecular and imaging-based markers for cervical cancer enables early detection of disease and its characterisation.

1.9 Aims

- To select a panel of DNA/RNA tumour markers sensitive to diagnosing cervical cancer and design an optimal lab-on-a chip for this purpose

- To establish the value of HPV testing in addition to MRI for detecting cervical cancer prior to definitive surgical treatment
- To validate the lab-on-a-chip (LOC) technology for detecting HPV and tumour markers by comparing its performance against standard polymerase chain reaction (PCR) systems.
- To establish the sensitivity and specificity of LOC technology for detecting cervical cancer (HPV DNA/RNA and hTERT TERC and Myc testing) in a prospective trial using cytology samples and validate the results by comparing them with those from a standard polymerase chain reaction (PCR) system.
- To establish the diagnostic benefit of the LOC testing in patients with endovaginal MRI scans that are negative vs. positive for tumour.
- To identify radiomic features of poor prognosis in early stage cervical cancer and to determine their value in predicting lymph node metastasis and recurrence in patients in the low-volume tumour group.

1.10 References

1. Bray F, Ferlay J, Soerjomataram I, Siegel RL, Torre LA, Jemal A. Global cancer statistics 2018: GLOBOCAN estimates of incidence and mortality worldwide for 36 cancers in 185 countries. CA: A Cancer Journal for Clinicians.0(0).
2. Bray F, Ferlay J, Soerjomataram I, Siegel RL, Torre LA, Jemal A. Global cancer statistics 2018: GLOBOCAN estimates of incidence and mortality worldwide for 36 cancers in 185 countries. CA: A Cancer Journal for Clinicians. 2018;68(6):394-424.
3. Vaccarella S, Lortet-Tieulent J, Plummer M, Franceschi S, Bray F. Worldwide trends in cervical cancer incidence: Impact of screening against changes in disease risk factors. European Journal of Cancer. 2013;49(15):3262-73.
4. Ferlay J, Soerjomataram I, Dikshit R, Eser S, Mathers C, Rebelo M, et al. Cancer incidence and mortality worldwide: sources, methods and major patterns in GLOBOCAN 2012. Int J Cancer. 2015;136(5):E359-86.
5. Roura E, Castellsagué X, Pawlita M, Travier N, Waterboer T, Margall N, et al. Smoking as a major risk factor for cervical cancer and pre-cancer: Results from the EPIC cohort. International Journal of Cancer. 2014;135(2):453-66.
6. Comparison of risk factors for invasive squamous cell carcinoma and adenocarcinoma of the cervix: collaborative reanalysis of individual data on 8,097 women with squamous cell carcinoma and 1,374 women with adenocarcinoma from 12 epidemiological studies. Int J Cancer. 2007;120(4):885-91.
7. Cohen PA, Jhingran A, Oaknin A, Denny L. Cervical cancer. The Lancet. 2019;393(10167):169-82.
8. Durst M, Gissmann L, Ikenberg H, zur Hausen H. A papillomavirus DNA from a cervical carcinoma and its prevalence in cancer biopsy samples from different geographic regions. Proc Natl Acad Sci U S A. 1983;80(12):3812-5.
9. zur Hausen H. Papillomaviruses in the causation of human cancers - a brief historical account. Virology. 2009;384(2):260-5.
10. de Sanjose S, Quint WG, Alemany L, Geraets DT, Klaustermeier JE, Lloveras B, et al. Human papillomavirus genotype attribution in invasive cervical cancer: a retrospective cross-sectional worldwide study. The Lancet Oncology. 2010;11(11):1048-56.
11. Argyri E, Papaspyridakos S, Tsimplaki E, Michala L, Myriokefalitaki E, Papassideri I, et al. A cross sectional study of HPV type prevalence according to age and cytology. BMC Infect Dis. 2013;13:53.
12. Jansen EEL, Naber SK, Aitken CA, de Koning HJ, van Ballegooijen M, de Kok I. Cost-effectiveness of HPV-based cervical screening based on first year results in the Netherlands : A modelling study. Bjog. 2020.
13. Ebisch RMF, Ketelaars PJW, van der Sanden WMH, Schmeink CE, Lenselink CH, Siebers AG, et al. Screening for persistent high-risk HPV infections may be a valuable screening method for young women; A retrospective cohort study. PLoS One. 2018;13(10):e0206219.
14. Kjaer SK, Frederiksen K, Munk C, Iftner T. Long-term absolute risk of cervical intraepithelial neoplasia grade 3 or worse following human papillomavirus infection: role of persistence. Journal of the National Cancer Institute. 2010;102(19):1478-88.
15. Chen H-C, Schiffman M, Lin C-Y, Pan M-H, You S-L, Chuang L-C, et al. Persistence of Type-Specific Human Papillomavirus Infection and Increased Long-term Risk of Cervical Cancer. JNCI: Journal of the National Cancer Institute. 2011;103(18):1387-96.
16. McCredie MR, Sharples KJ, Paul C, Baranyai J, Medley G, Jones RW, et al. Natural history of cervical neoplasia and risk of invasive cancer in women with cervical intraepithelial neoplasia 3: a retrospective cohort study. The Lancet Oncology. 2008;9(5):425-34.

17. Ho GYF, Bierman R, Beardsley L, Chang CJ, Burk RD. Natural History of Cervicovaginal Papillomavirus Infection in Young Women. New England Journal of Medicine. 1998;338(7):423-8.
18. Schiffman M, Rodriguez AC, Chen Z, Wacholder S, Herrero R, Hildesheim A, et al. A Population-Based Prospective Study of Carcinogenic Human Papillomavirus Variant Lineages, Viral Persistence, and Cervical Neoplasia. Cancer research. 2010;70(8):3159-69.
19. Vande Pol SB, Klingelhutz AJ. Papillomavirus E6 oncoproteins. Virology. 2013;445(1-2):115-37.
20. Roman A, Munger K. The papillomavirus E7 proteins. Virology. 2013;445(1-2):138-68.
21. Songock WK, Kim S-m, Bodily JM. The human papillomavirus E7 oncoprotein as a regulator of transcription. Virus Research. 2017;231:56-75.
22. Eldakhakhny S, Zhou Q, Crosbie EJ, Sayan BS. Human papillomavirus E7 induces p63 expression to modulate DNA damage response. Cell Death & Disease. 2018;9(2):127.
23. Integrated genomic and molecular characterization of cervical cancer. Nature. 2017;543(7645):378-84.
24. Warren CJ, Westrich JA, Doorslaer KV, Pyeon D. Roles of APOBEC3A and APOBEC3B in Human Papillomavirus Infection and Disease Progression. Viruses. 2017;9(8).
25. Bodelon C, Vinokurova S, Sampson JN, den Boon JA, Walker JL, Horswill MA, et al. Chromosomal copy number alterations and HPV integration in cervical precancer and invasive cancer. Carcinogenesis. 2016;37(2):188-96.
26. Oyervides-Muñoz MA, Pérez-Maya AA, Rodríguez-Gutiérrez HF, Gómez-Macias GS, Fajardo-Ramírez OR, Treviño V, et al. Understanding the HPV integration and its progression to cervical cancer. Infection, Genetics and Evolution. 2018;61:134-44.
27. Gimenes F, Souza RP, de Abreu AL, Pereira MW, Consolaro ME, da Silva VR. Simultaneous detection of human papillomavirus integration and c-MYC gene amplification in cervical lesions: an emerging marker for the risk to progression. Archives of gynecology and obstetrics. 2016;293(4):857-63.
28. deSouza NM, Soutter WP, McIndoe GA, Gilderdale DJ, Krausz T. Stage I cervical cancer: tumor volume by magnetic resonance imaging of screen-detected versus symptomatic lesions. Journal of the National Cancer Institute. 1997;89(17):1314-5.
29. Spence AR, Goggin P, Franco EL. Process of care failures in invasive cervical cancer: systematic review and meta-analysis. Preventive medicine. 2007;45(2-3):93-106.
30. Rajasekharan D, Kumar R, Balakrishnan B, Sharathkumar P, Pournami C, Sibi S, et al. Computer Assisted Pap Smear Analyser for Cervical Cancer Screening using Quantitative Microscopy. J Cytol Histol. 2015;S:3.
31. Arbyn M, Sankaranarayanan R, Muwonge R, Keita N, Dolo A, Mbalawa CG, et al. Pooled analysis of the accuracy of five cervical cancer screening tests assessed in eleven studies in Africa and India. International Journal of Cancer. 2008;123(1):153-60.
32. Fokom-Domgue J, Combescure C, Fokom-Defo V, Tebeu PM, Vassilakos P, Kengne AP, et al. Performance of alternative strategies for primary cervical cancer screening in sub-Saharan Africa: systematic review and meta-analysis of diagnostic test accuracy studies. BMJ : British Medical Journal. 2015;351:h3084.
33. Kelly H, Mayaud P, Segondy M, Pant Pai N, Peeling RW. A systematic review and meta-analysis of studies evaluating the performance of point-of-care tests for human papillomavirus screening. Sexually Transmitted Infections. 2017;93(S4):S36-S45.
34. Crosbie EJ, Einstein MH, Franceschi S, Kitchener HC. Human papillomavirus and cervical cancer. The Lancet. 2013;382(9895):889-99.
35. Khan MJ, Werner CL, Darragh TM, Guido RS, Mathews C, Moscicki A-B, et al. ASCCP Colposcopy Standards: Role of Colposcopy, Benefits, Potential Harms, and Terminology for Colposcopic Practice. Journal of Lower Genital Tract Disease. 2017;21(4).

36. Massad LS, Jeronimo J, Schiffman M. Interobserver agreement in the assessment of components of colposcopic grading. Obstetrics and gynecology. 2008;111(6):1279-84.
37. Gage JC, Hanson VW, Abbey K, Dippery S, Gardner S, Kubota J, et al. Number of cervical biopsies and sensitivity of colposcopy. Obstetrics and gynecology. 2006;108(2):264-72.
38. Pretorius RG, Belinson JL, Burchette RJ, Hu S, Zhang X, Qiao YL. Regardless of skill, performing more biopsies increases the sensitivity of colposcopy. J Low Genit Tract Dis. 2011;15(3):180-8.
39. Cantor SB, Cárdenas-Turanzas M, Cox DD, Atkinson EN, Nogueras-Gonzalez GM, Beck JR, et al. Accuracy of colposcopy in the diagnostic setting compared with the screening setting. Obstetrics and gynecology. 2008;111(1):7-14.
40. Mitchell MF, Schottenfeld D, Tortolero-Luna G, Cantor SB, Richards-Kortum R. Colposcopy for the diagnosis of squamous intraepithelial lesions: a meta-analysis. Obstetrics and gynecology. 1998;91(4):626-31.
41. Giannella L. The clinical problem of colposcopy is represented by false-negatives. Archives of gynecology and obstetrics. 2015;291(4):711-2.
42. Silver MI, Andrews J, Cooper CK, Gage JC, Gold MA, Khan MJ, et al. Risk of Cervical Intraepithelial Neoplasia 2 or Worse by Cytology, Human Papillomavirus 16/18, and Colposcopy Impression: A Systematic Review and Meta-analysis. Obstetrics and gynecology. 2018;132(3):725-35.
43. Costa-Fagbemi M, Yakubu M, Meggetto O, Moffatt J, Walker MJ, Koné AP, et al. Risk of Cervical Dysplasia After Colposcopy Care and Risk-Informed Return to Population-Based Screening: A Systematic Review. J Obstet Gynaecol Can. 2020;42(5):607-24.
44. Sankaranarayanan R, Nene BM, Shastri SS, Jayant K, Muwonge R, Budukh AM, et al. HPV screening for cervical cancer in rural India. N Engl J Med. 2009;360(14):1385-94.
45. Toliman PJ, Kaldor JM, Badman SG, Gabuzzi J, Silim S, Kumbia A, et al. Performance of clinical screening algorithms comprising point-of-care HPV-DNA testing using self-collected vaginal specimens, and visual inspection of the cervix with acetic acid, for the detection of underlying high-grade squamous intraepithelial lesions in Papua New Guinea. Papillomavirus Research. 2018;6:70-6.
46. Ronco G, Dillner J, Elfström KM, Tunesi S, Snijders PJ, Arbyn M, et al. Efficacy of HPV-based screening for prevention of invasive cervical cancer: follow-up of four European randomised controlled trials. Lancet. 2014;383(9916):524-32.
47. Tjalma WA, Depuydt CE. Cervical cancer screening: which HPV test should be used--L1 or E6/E7? European journal of obstetrics, gynecology, and reproductive biology. 2013;170(1):45-6.
48. Meijer CJ, Berkhof H, Heideman DA, Hesselink AT, Snijders PJ. Validation of high-risk HPV tests for primary cervical screening. Journal of clinical virology : the official publication of the Pan American Society for Clinical Virology. 2009;46 Suppl 3:S1-4.
49. Arbyn M, Snijders PJ, Meijer CJ, Berkhof J, Cuschieri K, Kocjan BJ, et al. Which high-risk HPV assays fulfil criteria for use in primary cervical cancer screening? Clinical microbiology and infection : the official publication of the European Society of Clinical Microbiology and Infectious Diseases. 2015;21(9):817-26.
50. Koliopoulos G, Nyaga VN, Santesso N, Bryant A, Martin-Hirsch PP, Mustafa RA, et al. Cytology versus HPV testing for cervical cancer screening in the general population. Cochrane Database Syst Rev. 2017;8:CD008587.
51. Aitken CA, van Agt HME, Siebers AG, van Kemenade FJ, Niesters HGM, Melchers WJG, et al. Introduction of primary screening using high-risk HPV DNA detection in the Dutch cervical cancer screening programme: a population-based cohort study. BMC Med. 2019;17(1):228.
52. Pecorelli S, Zigliani L, Odicino F. Revised FIGO staging for carcinoma of the cervix. International Journal of Gynecology & Obstetrics. 2009;105(2):107-8.

53. Bhatla N, Berek JS, Cuello Fredes M, Denny LA, Grenman S, Karunaratne K, et al. Revised FIGO staging for carcinoma of the cervix uteri. International Journal of Gynecology & Obstetrics. 2019;145(1):129-35.
54. Woo S, Atun R, Ward ZJ, Scott AM, Hricak H, Vargas HA. Diagnostic performance of conventional and advanced imaging modalities for assessing newly diagnosed cervical cancer: systematic review and meta-analysis. Eur Radiol. 2020.
55. Charles-Edwards EM, deSouza NM. Diffusion-weighted magnetic resonance imaging and its application to cancer. Cancer Imaging. 2006;6:135-43.
56. Le Bihan D. Apparent diffusion coefficient and beyond: what diffusion MR imaging can tell us about tissue structure. Radiology. 2013;268(2):318-22.
57. Sala E, Wakely S, Senior E, Lomas D. MRI of malignant neoplasms of the uterine corpus and cervix. AJR Am J Roentgenol. 2007;188(6):1577-87.
58. Soutter WP, Hanoch J, D'Arcy T, Dina R, McIndoe GA, DeSouza NM. Pretreatment tumour volume measurement on high-resolution magnetic resonance imaging as a predictor of survival in cervical cancer. BJOG. 2004;111(7):741-7.
59. Balleyguier C, Sala E, Da Cunha T, Bergman A, Brkljacic B, Danza F, et al. Staging of uterine cervical cancer with MRI: guidelines of the European Society of Urogenital Radiology. Eur Radiol. 2011;21(5):1102-10.
60. Liu B, Gao S, Li S. A Comprehensive Comparison of CT, MRI, Positron Emission Tomography or Positron Emission Tomography/CT, and Diffusion Weighted Imaging-MRI for Detecting the Lymph Nodes Metastases in Patients with Cervical Cancer: A Meta-Analysis Based on 67 Studies. Gynecologic and obstetric investigation. 2017;82(3):209-22.
61. Liu FY, Su TP, Wang CC, Chao A, Chou HH, Chang YC, et al. Roles of posttherapy (18)F-FDG PET/CT in patients with advanced squamous cell carcinoma of the uterine cervix receiving concurrent chemoradiotherapy. European journal of nuclear medicine and molecular imaging. 2018;45(7):1197-204.
62. Phippen NT, Havrilesky LJ, Barnett JC, Hamilton CA, Stany MP, Lowery WJ. Does Routine Posttreatment PET/CT Add Value to the Care of Women With Locally Advanced Cervical Cancer? International journal of gynecological cancer : official journal of the International Gynecological Cancer Society. 2016;26(5):944-50.
63. Sedlis A, Bundy BN, Rotman MZ, Lentz SS, Muderspach LI, Zaino RJ. A randomized trial of pelvic radiation therapy versus no further therapy in selected patients with stage IB carcinoma of the cervix after radical hysterectomy and pelvic lymphadenectomy: A Gynecologic Oncology Group Study. Gynecologic oncology. 1999;73(2):177-83.
64. Nama V, Angelopoulos G, Twigg J, Murdoch JB, Bailey J, Lawrie TA. Type II or type III radical hysterectomy compared to chemoradiotherapy as a primary intervention for stage IB2 cervical cancer. Cochrane Database of Systematic Reviews. 2018(10).
65. Kenter G, Greggi S, Vergote I, Katsaros D, Kobierski J, Massuger L, et al. Results from neoadjuvant chemotherapy followed by surgery compared to chemoradiation for stage Ib2-IIb cervical cancer, EORTC 55994. Journal of Clinical Oncology. 2019;37(15_suppl):5503-.
66. Rydzewska L, Tierney J, Vale CL, Symonds PR. Neoadjuvant chemotherapy plus surgery versus surgery for cervical cancer. Cochrane Database Syst Rev. 2012;12:CD007406.
67. Gupta S, Maheshwari A, Parab P, Mahantshetty U, Hawaldar R, Sastri S, et al. Neoadjuvant Chemotherapy Followed by Radical Surgery Versus Concomitant Chemotherapy and Radiotherapy in Patients With Stage IB2, IIA, or IIB Squamous Cervical Cancer: A Randomized Controlled Trial. Journal of Clinical Oncology. 2018;36(16):1548-55.
68. Zhang Q, Li W, Kanis MJ, Qi G, Li M, Yang X, et al. Oncologic and obstetrical outcomes with fertility-sparing treatment of cervical cancer: a systematic review and meta-analysis. Oncotarget. 2017.
69. Society BGC. Cervical Cancer Guidelines: Recommendations for Practice. 2020.

70. Small W, Jr., Mell LK, Anderson P, Creutzberg C, De Los Santos J, Gaffney D, et al. Consensus guidelines for delineation of clinical target volume for intensity-modulated pelvic radiotherapy in postoperative treatment of endometrial and cervical cancer. Int J Radiat Oncol Biol Phys. 2008;71(2):428-34.
71. Radiologists TRCo. Radiotherapy dose fractionation, Third edition. 2019.
72. Jhawar S, Hathout L, Elshaikh MA, Beriwal S, Small W, Mahmoud O. Adjuvant Chemoradiation Therapy for Cervical Cancer and Effect of Timing and Duration on Treatment Outcome. International Journal of Radiation Oncology*Biology*Physics. 2017;98(5):1132-41.
73. Peters WA, 3rd, Liu PY, Barrett RJ, 2nd, Stock RJ, Monk BJ, Berek JS, et al. Concurrent chemotherapy and pelvic radiation therapy compared with pelvic radiation therapy alone as adjuvant therapy after radical surgery in high-risk early-stage cancer of the cervix. Journal of clinical oncology : official journal of the American Society of Clinical Oncology. 2000;18(8):1606-13.
74. Falcetta FS, Medeiros LRF, Edelweiss MI, Pohlmann PR, Stein AT, Rosa DD. Adjuvant platinum-based chemotherapy for early stage cervical cancer. Cochrane Database of Systematic Reviews. 2016(11).
75. Berek JS, Howe C, Lagasse LD, Hacker NF. Pelvic exenteration for recurrent gynecologic malignancy: survival and morbidity analysis of the 45-year experience at UCLA. Gynecologic oncology. 2005;99(1):153-9.
76. Goldberg GL, Sukumvanich P, Einstein MH, Smith HO, Anderson PS, Fields AL. Total pelvic exenteration: the Albert Einstein College of Medicine/Montefiore Medical Center Experience (1987 to 2003). Gynecologic oncology. 2006;101(2):261-8.
77. Matsuo K, Mandelbaum RS, Adams CL, Roman LD, Wright JD. Performance and outcome of pelvic exenteration for gynecologic malignancies: A population-based study. Gynecologic oncology. 2019;153(2):368-75.
78. Reducing Uncertainties About the Effects of Chemoradiotherapy for Cervical Cancer: A Systematic Review and Meta-Analysis of Individual Patient Data From 18 Randomized Trials. Journal of Clinical Oncology. 2008;26(35):5802-12.
79. Cibula D, Pötter R, Planchamp F, Avall-Lundqvist E, Fischerova D, Haie Meder C, et al. The European Society of Gynaecological Oncology/European Society for Radiotherapy and Oncology/European Society of Pathology guidelines for the management of patients with cervical cancer. Radiotherapy and Oncology. 2018;127(3):404-16.
80. Cancer Research UK. Cervical cancer survival statistics [Available from: https://www.cancerresearchuk.org/about-cancer/cervical-cancer/survival.
81. Hou J, Goldberg GL, Qualls CR, Kuo DY, Forman A, Smith HO. Risk factors for poor prognosis in microinvasive adenocarcinoma of the uterine cervix (IA1 and IA2): a pooled analysis. Gynecologic oncology. 2011;121(1):135-42.
82. Tseng J, Sonoda Y, Gardner GJ, Zivanovic O, Abu-Rustum N, Leitao MM. Stage IA2 cervical cancer: Long-term outcomes with less radical as opposed to more radical surgical management. Journal of Clinical Oncology. 2016;34(15_suppl):e17011-e.
83. Wright JD, NathavithArana R, Lewin SN, Sun X, Deutsch I, Burke WM, et al. Fertility-conserving surgery for young women with stage IA1 cervical cancer: safety and access. Obstetrics and gynecology. 2010;115(3):585-90.
84. Delgado G, Bundy B, Zaino R, Sevin BU, Creasman WT, Major F. Prospective surgical-pathological study of disease-free interval in patients with stage IB squamous cell carcinoma of the cervix: a Gynecologic Oncology Group study. Gynecologic oncology. 1990;38(3):352-7.
85. Guan Y, Shi H, Chen Y, Liu S, Li W, Jiang Z, et al. Whole-Lesion Histogram Analysis of Apparent Diffusion Coefficient for the Assessment of Cervical Cancer. J Comput Assist Tomogr. 2016;40(2):212-7.
86. Downey K, Riches SF, Morgan VA, Giles SL, Attygalle AD, Ind TE, et al. Relationship between imaging biomarkers of stage I cervical cancer and poor-prognosis histologic features:

quantitative histogram analysis of diffusion-weighted MR images. AJR Am J Roentgenol. 2013;200(2):314-20.
87. Winfield JM, Orton MR, Collins DJ, Ind TE, Attygalle A, Hazell S, et al. Separation of type and grade in cervical tumours using non-mono-exponential models of diffusion-weighted MRI. Eur Radiol. 2017;27(2):627-36.
88. Guan Y, Li W, Jiang Z, Zhang B, Chen Y, Huang X, et al. Value of whole-lesion apparent diffusion coefficient (ADC) first-order statistics and texture features in clinical staging of cervical cancers. Clin Radiol. 2017;72(11):951-8.
89. Woo S, Kim SY, Cho JY, Kim SH. Apparent diffusion coefficient for prediction of parametrial invasion in cervical cancer: a critical evaluation based on stratification to a Likert scale using T2-weighted imaging. Radiol Med. 2017.
90. Yang W, Qiang JW, Tian HP, Chen B, Wang AJ, Zhao JG. Minimum apparent diffusion coefficient for predicting lymphovascular invasion in invasive cervical cancer. J Magn Reson Imaging. 2017;45(6):1771-9.
91. Downey K, Jafar M, Attygalle AD, Hazell S, Morgan VA, Giles SL, et al. Influencing surgical management in patients with carcinoma of the cervix using a T2- and ZOOM-diffusion-weighted endovaginal MRI technique. British journal of cancer. 2013;109(3):615-22.
92. Payne GS, Schmidt M, Morgan VA, Giles S, Bridges J, Ind T, et al. Evaluation of magnetic resonance diffusion and spectroscopy measurements as predictive biomarkers in stage 1 cervical cancer. Gynecologic oncology. 2010;116(2):246-52.
93. Hou Z, Li S, Ren W, Liu J, Yan J, Wan S. Radiomic analysis in T2W and SPAIR T2W MRI: predict treatment response to chemoradiotherapy in esophageal squamous cell carcinoma. Journal of thoracic disease. 2018;10(4):2256-67.
94. Wang Q, Li Q, Mi R, Ye H, Zhang H, Chen B, et al. Radiomics Nomogram Building From Multiparametric MRI to Predict Grade in Patients With Glioma: A Cohort Study. J Magn Reson Imaging. 2019;49(3):825-33.
95. Gilderdale DJ, deSouza NM, Coutts GA, Chui MK, Larkman DJ, Williams AD, et al. Design and use of internal receiver coils for magnetic resonance imaging. Br J Radiol. 1999;72(864):1141-51.

CHAPTER 2 Developing and testing a panel of DNA/RNA cervical tumour markers on a lab-on-a-chip platform

2.1 Introduction

The selection of markers for cervical cancer diagnosis in this work is based on the known characteristics of all cancer cells (chromosomal aberrations that result in uncontrolled proliferation) while considering the specific abnormalities associated with cervical cancer (presence of the human papilloma virus DNA/RNA). Based on the current literature, I selected a panel of four markers plus two housekeeping markers which were a mixture of genomic DNA and mRNA markers. The mRNA tumour markers were hTERT, MYC, and type-specific HPV E6*I. The DNA tumour marker was TERC. Genomic DNA and mRNA versions of GAPDH were used as housekeeping markers.

2.1.1 Marker selection

Proliferative capacity in cancer cells is partly attained through telomere maintenance. Telomeres, which are repetitive sequences of 5000-15000 nucleotides (96) at each end of chromosomes, protect chromosomes from degradation and end-to-end fusions, contributing to genomic stability. Telomeres are maintained by a specialised RNA-dependent DNA polymerase (telomerase) which is predominantly active during embryonic and foetal development (97). Because DNA polymerase does not fully replicate the 3' end of the lagging strands of the linear molecule, an "end replication problem"(98) results with progressive telomere loss from the ends of chromosomes each time

a cell divides. *In vitro*, this limits the proliferation of normal mammalian somatic cells (referred to as the Hayflick limit). At this limit, critically shortened telomeres trigger a permanent growth arrest known as replicative senescence or mortality stage 1 (M1). Cells which can escape replicative senescence through the inactivation of a critical cell cycle checkpoint gene such as p53 continue to divide and suffer further telomere loss until they reach a second block on proliferation known as crisis or mortality stage 2 (M2). Occasionally cells may escape from crisis and are able to maintain telomere length through the activation of telomerase, and this leads to unlimited proliferative capacity (99). As telomerase is universally expressed (100) in HPV-positive cancers, I selected two telomerase components as potential tumour markers: hTERT and TERC.

2.1.1.1 Evidence supporting hTERT selection

The hTERT gene, which encodes for a catalytic protein with reverse transcriptase activity, is located on chromosome 5 (5p15). It is significantly overexpressed in cervical lesions and tumours, being detectable in at least 90% of cervical cancers (101, 102), but has low to nil expression in normal tissue. In small studies it has been shown to have a high sensitivity and specificity in detecting cancerous and high-grade lesions, especially when combined with HPV E6/7 mRNA (103-105). The hTERT expression is proportional to the grade of cervical lesions and its activity has been found to parallel worsening cervical disease (106). hTERT is directly activated by high risk HPV E6 protein and the human E3 Ubiquitin Ligase E6 Associated Protein (E6AP)(107), whilst low risk HPV types cannot cause hTERT activation (108). HPV E7 proteins act

synergistically with E6 to activate hTERT. The alternative splicing of hTERT pre-mRNA regulates telomerase activity. Alternative splicing, which affects about 95% of genes in multicellular eukaryotes, allows for the generation of over 100,000 proteins from about 20,000 protein-coding sequences, thus greatly expanding the coding capacity of eukaryotic genomes (109). The hTERT gene spans 42kb and contains 16 exons and 15 introns. The full-length of hTERT mRNA is approximately 4.0kb. At least seven selective splicing sites are located on the hTERT pre-mRNA, including three deletion sites (α, β, and γ) and four insertion sites (110). Only the full-length hTERT mRNA shows telomerase activity (111) although this spliced version is not the most common variant(112, 113). It has been shown that even in cervical cancer cell lines only a small proportion of full-length hTERT transcripts are present compared with their spliced counterparts (114).

2.1.1.2 Evidence supporting TERC selection

The functional RNA component of telomerase (TERC) serves as a template for telomeric DNA synthesis. TERC is located on chromosome 3 (3q26). Chromosomal amplifications at 3q26 are common (25, 115). There are numerous reports of high copy numbers of TERC found in fluorescence in situ hybridisation (FISH) studies and it is universally found in cervical cancers (116, 117). Gain of 3q26 is a predictor of progression from low-grade dysplasia to high-grade dysplasia and has been shown to have a high specificity in high risk population screening studies (118-121).

Detecting an increase in TERC DNA copy numbers relative to GAPDH DNA copy number may allow for an assessment of amplification of chromosome

3q26. This requires the ability to detect small relative differences between TERC and GAPDH copy numbers as well as a large enough proportion of cells in the sample with aberrant chromosome 3q26 to provide a mean TERC amplification rate. A study of over 1000 patients indicated that in patients with at least CIN2+ 21-47% of cells from the cervical sample had abnormal TERC amplification patterns. These ranged from 2:3 copy number ratios to a high proportion of cases of squamous cell carcinoma with 5 copies of TERC detectable. The CIN2/3 cases had an average of 3.45 copies of TERC in 21% of cells and the SCC cases had an average of 4.15 copies per cell in 46% of exfoliated cells. This would indicate an average of 2.3 and 2.99 copies of TERC for the cells contained within an exfoliated cell sample in CIN2/3 and SCC cases respectively. Given an expected copy number of 2 per cell in normal cells this would require the capability to resolve a 15% and 49% difference to correctly classify disease. This is potentially possible with digital PCR technology but it has not yet been evaluated with loop-mediated isothermal amplification techniques (122).

2.1.1.3 Evidence supporting MYC selection

MYC is located on 8p24 and plays a role in cell cycle progression, apoptosis and cellular transformation. It has been found to be overexpressed in the majority of cervical cancers. It has a direct link in the over activation of telomerase and is the most common site of HPV integration (123, 124). Similar to TERC it is a site of genomic copy number gains most often found in cervical cancer and is a powerful predictor of progression and persistence of cervical dysplasia (27, 125-127).

2.1.1.4 Markers of HPV infection

HPV DNA is recognised as a marker for cervical cancer ***(128)*** and when combined with cytology a significant improvement in sensitivity is seen in detecting CIN2+ (129). The 4 most common HPV types which cause disease are 16, 18, 45 and 58 from a consensus of two large studies of HPV type distribution (10, 130). Therefore, I selected these 4 types to develop the mRNA assay around.

HPV E6/E7 mRNA testing has been advocated as screening tool, with equal sensitivity to HPV DNA (131), higher specificity and reduced rates of colposcopy referral (132-134). HPV E6*I is a splice variant of the full length E6E7 mRNA produced by all high risk HPV types (60). An intron is removed from the E6 portion of the polycistronic RNA which changes the E6 ORF and generates a new stop codon. This helps to facilitate E7 translation by increasing the distance between the E6 stop and E7 start codon (135). The E6*I splice variant has been found to be more abundant in cervical lesions (136, 137), than other transcript variants, including full length, especially in HPV 16 compared with HPV 18 (23) and correlates with the severity of disease (138). It may even correlate with prediction of progression of early pre-cancerous lesions (139, 140). This splice variant mRNA was selected as the HPV marker.

2.1.1.5 Housekeeping genes

Commonly used housekeeping genes are Glyceraldehyde-3-phosphate dehydrogenase (GAPDH), involved in glycolysis and gluconeogenesis, Beta-

actin (ACTB), involved in cytoskeletal structural protein formation, and Beta-2 microglobulin (B2M), a component of MHC Class I molecules (141-143).

GAPDH is located on chromosome 12 (12p13) and was chosen as the housekeeping marker as it has been shown to have stable expression in both cell lines and cervical cancer tissue (141, 142, 144).

2.1.2 Lab-on-a-chip methodology for marker detection: current status

The lab-on-a-chip platform uses LAMP with complementary metal oxide semi-conductor (CMOS)-based chemical sensing and builds on microchip technology. The cost of manufacture is low and there is direct communication with servers (145). The system integrates more than 1000 sensors per microchip. The fact that no fluorescent labels are needed lowers the cost per test, because the probe does not need to be "tagged", and the electronic/electrochemical readout gives scope for miniaturization without trading accuracy, so making it suitable at the point-of-care. The technology has been successfully tested in detecting treatment resistant forms of aspergillus and malaria(146-148).

2.1.2.1 Loop-mediated isothermal amplification (LAMP)

LAMP methods were originally developed by Notomi et al (149) and have been incorporated into lab-on-a-chip to allow rapid amplification of nucleic acids at a single temperature, typically between 63-65^{0}C. The reaction proceeds without thermocycling as it is required with polymerase chain reaction (PCR). This makes the technique an ideal method for point-of-care testing. The method

relies on auto-cycling strand displacement DNA synthesis conducted by a DNA polymerase with high strand displacement activity.

Initially LAMP was designed with four primers, but this was extended to six by Nagamine (150) as this accelerated the reaction. The six primers are Forward-Inner (FIP), Backward-Inner (BIP), Forward Outer (F3), Backward Outer (B3), Forward Loop (LF) and Backward Loop (LB). A stem-loop structure is constructed, in which the sequences of both DNA ends are derived from the inner primer. Subsequently, an exponential generation of inverted repeats is constructed as the inner primers anneal and cause amplification from the loops in the original structure (Figure 2.1). The addition of the loop primers LF and LB allow for hybridisation to the available stem-loops which are not hybridised by the inner primers (FIP/BIP). This markedly accelerates the reaction from 1 hour to 10-15 minutes depending upon the concentration of the starting material.

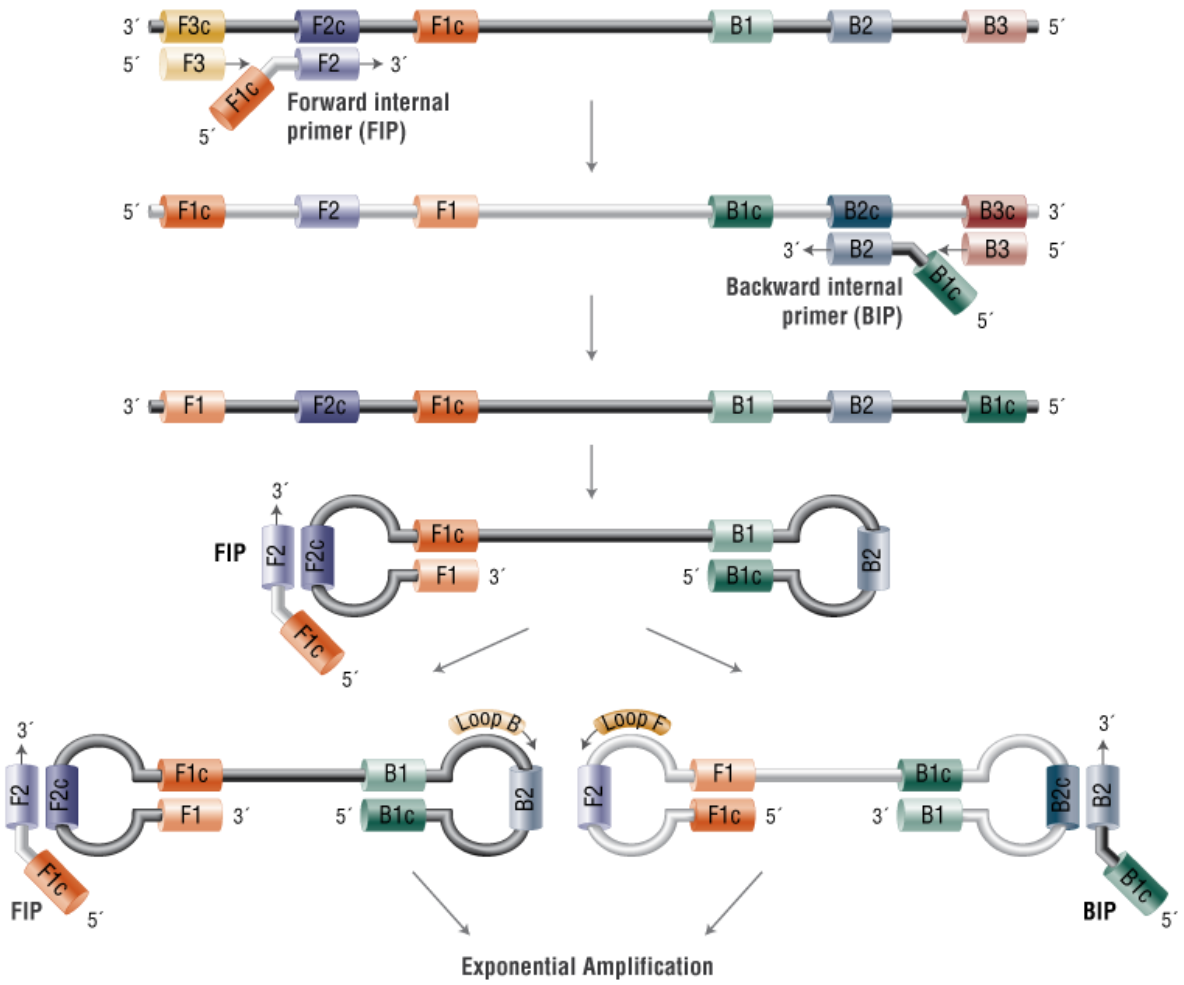

Figure 2-1 Diagram illustrating mechanism of loop mediated isothermal amplification. Courtesy of New England Biolabs

LAMP based assays have been successfully developed for a multitude of purposes, ranging from detection of infectious diseases to identification of genotype polymorphisms(151, 152). There have been assays developed to genotype HPV (153, 154) from cervical cytology samples but thus far there is no such LAMP based assay developed to detect cervical cancer from DNA/RNA markers.

2.1.2.2 CMOS-based chemical sensing

The Centre for Bio-Inspired Technology (CBIT) at Imperial College London has developed pH-sensing CMOS technology. At the heart of the system are Ion-

sensitive Field-Effect Transistors (ISFETs) which are used to measure ion concentrations in solution. The system is coupled with an embedded heater and temperature sensors so that the need for bulky external devices is removed and on-chip amplification and testing is enabled. These detection systems provide label-free nucleic acid amplification methods by measuring released hydrogen ions during nucleotide incorporation rather than relying on indirect measurements such as fluorescent dyes. A direct detection of the pH change which occurs during nucleic acid polymerisation and converts the chemical (H+) signal into an electrical one is indicative of the presence of the target nucleic acids (145).

2.2 Aim and Objectives

2.2.1 Aim:

To develop a panel of DNA/RNA tumour markers sensitive to detecting cervical cancer, incorporate them into an existing lab-on-a-chip platform and test the potential of the platform for diagnosing cervical cancer.

2.2.2 Objectives:

- To design a panel of DNA/RNA LAMP primers for the selected tumour markers using amplification chemistries compatible with CMOS
- To use synthetic DNA to determine the analytical sensitivity and quantitative performance for each primer set
- To incorporate the primers into an existing lab-on-a-chip platform
- To test the performance of the lab-on-a-chip
- platform using *ex vivo* samples from women with cervical cancer

The first 3 objectives were part of a technical development phase and the last objectives was a clinical testing phase, prior to the pilot clinical trial described in Chapter 3

2.3 Technical development- Designing and evaluating LAMP primers for selected tumour markers on a lab-on-a-chip platform

I designed four (TERC, MYC, GAPDH RNA, and all HPV types) or five (TERT and GAPDH DNA) LAMP primer sets for each target.

2.3.1 Design of primers

For each of the selected tumour markers the genomic sequences were retrieved from the National Institute of Health GenBank system and visualised with Geneious software (Table 2.1). Within Geneious the sequences were aligned with the MUSCLE method (MUltiple Sequence Comparison by Log-Expectation) (155). For the RNA markers the mRNA transcript variant sequences were also downloaded.

The splice variant locations for TERT (111) and HPV (156) types were added to the sequences prior to primer design.

Tumour marker	GenBank Accession number
TERT	NG_009265.1, NM_198253.2, NM_001193376.1, NR_149162.1, NR_149163.1
TERC	NG_016363.1
MYC	NG_007161.2, NM_002467.5, NM_001354870.1
GAPDH	NG_007073.2, NM_002046, NM_001256799, NM_001289745, NM_001289746 and NM_001357943
HPV 16	K02718.1
HPV 18	AY262282.1
HPV 45	X74479.1
HPV 58	D90400.1

Table 2-1 Human and HPV gene GenBank codes used for LAMP primer design.

LAMP primers were designed using Primer Explorer V5.

(http://primerexplorer.jp/lampv5e/index.html)

2.3.1.1 hTERT

With hTERT there are multiple transcript variants but only the full length mRNA transcript conserves telomerase activity (109). Therefore, exclusion of the two main variants, alpha and beta, that are inhibitory to telomerase function was necessary. The alpha splice variant removes the first 36bp of exon 6, while the beta splice variant removes 182bp from exons 7 and 8 (111) As the F2 primer is located within the 36bp alpha splice sequence and the B2 and B3 primers are located in the portion of exon 7 which is part of the beta splice, a primer set

specific to full length mRNA, that was unable to amplify the main inhibitory splice variants and was exon-exon spanning was designed.

2.3.1.2 TERC

TERC has a single exon to provide the template RNA for telomerase. Primers were applied to this sequence and five difference sets were designed.

2.3.1.3 MYC

In designing MYC RNA, transcript variants were aligned and mismatched nucleotides avoided in positioning the primers. Primers were designed to span exon-exon junctions and two different exon-exon pairs were selected. Two primers sets were designed for each pair.

2.3.1.4 HPV E6

The HPV E6*I mRNA primer design was more challenging to accomplish. The objective was to avoid amplifying the full-length mRNA sequence and focus solely on the specific splice variant.

The initial design centred on locating the F2-F1c or B2-B1c primer group either side of the splice junction. This would potentially result in an unstable portion of the LAMP cycling dumbbell structure and not allow amplification to proceed. Unfortunately, pilot experiments with the four HPV primer sets designed in this way yielded unreliable results. There was inconsistent amplification of full-length targets with time to positive times insufficiently different from the specific spliced variant the marker was supposed to amplifying.

Subsequently, I located the F2 primer 3-4bp across the splice junction. (Figure 2.2) However, this did not ensure specificity, as the first 3-4 base pairs at the 5' end of the spliced region shared 50-75% of the overlapped region and potentially allowed primer annealing and therefore amplification. Similarly, the last 2 base pairs at the 3' end of the spliced region were identical to the last 2 base pairs immediately before the splice junction potentially enabling the F2 primer to anneal inappropriately in this position. To solve this problem I inserted mismatched nucleotides at 3' end of the F2 primer (157, 158). This ensured that the F2 primer could only form weak bonds when annealing to the inappropriate regions in the spliced sequence. This allowed the polymerase to amplify from the preferential primer annealing site.

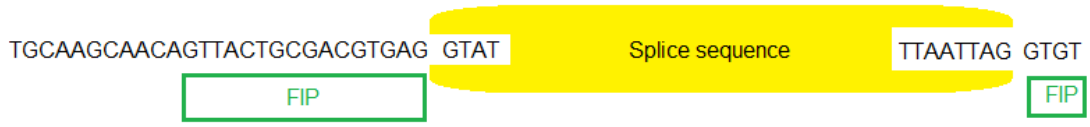

Figure 2-2 Illustration of location of FIP primer across splice region.

2.3.1.5 GAPDH

For GAPDH DNA (9 exons and 8 introns) five different primers sets were designed using two different exon locations. Primers were applied across an adjacent exon and intron to specifically select for DNA sequences. For GAPDH RNA, the process was the same as for MYC RNA.

2.3.2 Primer selection based on analytical sensitivity

2.3.2.1 Synthetic DNA samples

Synthetic double-stranded DNA containing the sequence of the target DNA or RNA was purchased from Integrated DNA Technologies (Leuven, Belgium). The synthetic DNA was quantified using a Qubit 3.0 fluorometer and the high-sensitivity double-stranded DNA assay kits (Life Technologies, Carlsbad, CA).

2.3.2.2 Experimental methods for primer set selection

The best primer sets were selected as follows:

Step 1: Primer sets for RNA based markers were tested against human genomic DNA (Thermo Fisher Scientific) to ensure the primers were specific to RNA, and not DNA.

Step 2: All primer sets were tested against a synthetic dsDNA or RNA containing the sequence of interest, including appropriate non-template controls.

In this initial primer screen the synthetic sequence was diluted to a 10^6 copy/reaction.

Step 3: The two primer set candidates that achieved the fastest time to positive were then tested in a dilution screen.

Analytical sensitivity of the assays were evaluated in serial 10-fold dilutions of synthetic DNA or RNA target. This was performed using either a 10^8-10^0, 10^6-10^0 or 10^4-10^0 serial fold dilutions to then select the most sensitive of the two primer sets candidates.

The experiments were performed on a LightCycler 96 System (Roche Molecular Systems, Pleasanton, CA).

With the TERC tumour marker candidates, one of the two selected options was faster but less sensitive than the other. The slower candidate did not have two loop primers, which affected its efficiency. I manually designed an additional loop primer for this primer set and retested it. This optimised primer set achieved a faster and more sensitive result than either of the original primer designs.

Of the four MYC RNA primer sets designed, options 2, 3 and 4 amplified genomic DNA inappropriately and were abandoned. The remaining primer set was tested in the dilution screen stage. As this primer set performed very well, additional primer designs were not sought.

The hTERT primers were also tested against a synthetic sequence specific to alpha and beta splice variants. The HPV E6*I primers were tested against a full-length sequence to ensure specificity to the spliced version.

The LAMP reaction mix composition is given in Appendix 6.1 and individual marker primer and dilution screen results can be found in Appendix 6.2-6.11.

2.3.2.3 Tumour marker sensitivity

A summary of the performance of the final human genomic tumour markers can be seen in Table 2-2 and Figure 2-3.

LAMP	RNA			DNA	
Copies/reaction	hTERT	MYC	GAPDH	TERC	GAPDH
10^8	5.61 (0.13)	-	-	-	-
10^7	7.08 (0.12)	-	-	-	-
10^6	8.52 (0.22)	6.26 (0.41)	5.83 (0.06)	-	-
10^5	9.6 (0.06)	7.51 (0.07)	6.93 (0.19)	-	-
10^4	11.04 (0.13)	9.22 (0.06)	8.14 (0.22)	8 (0.1)	6.84 (0.22)
10^3	12.91 (0.44)	10.58 (0.19)	9.35 (0.17)	9.3 (0.2)	8.13 (0.32)
10^2	-	11.81 (0.59)	-	10.15 (0.23)	9.98 (0.12)
10^1	-	14.98 (1.95)	-	11.95 (0.15)	11.33 (0.12)
10^0	-	-	-	-	13.62 (0.86)
R^2	0.99	0.97	1.00	0.97	0.99

Table 2-2 Analytical sensitivity of final primer sets for human markers. Time to positive in minutes (Standard deviation) for each synthetic DNA/RNA concentration

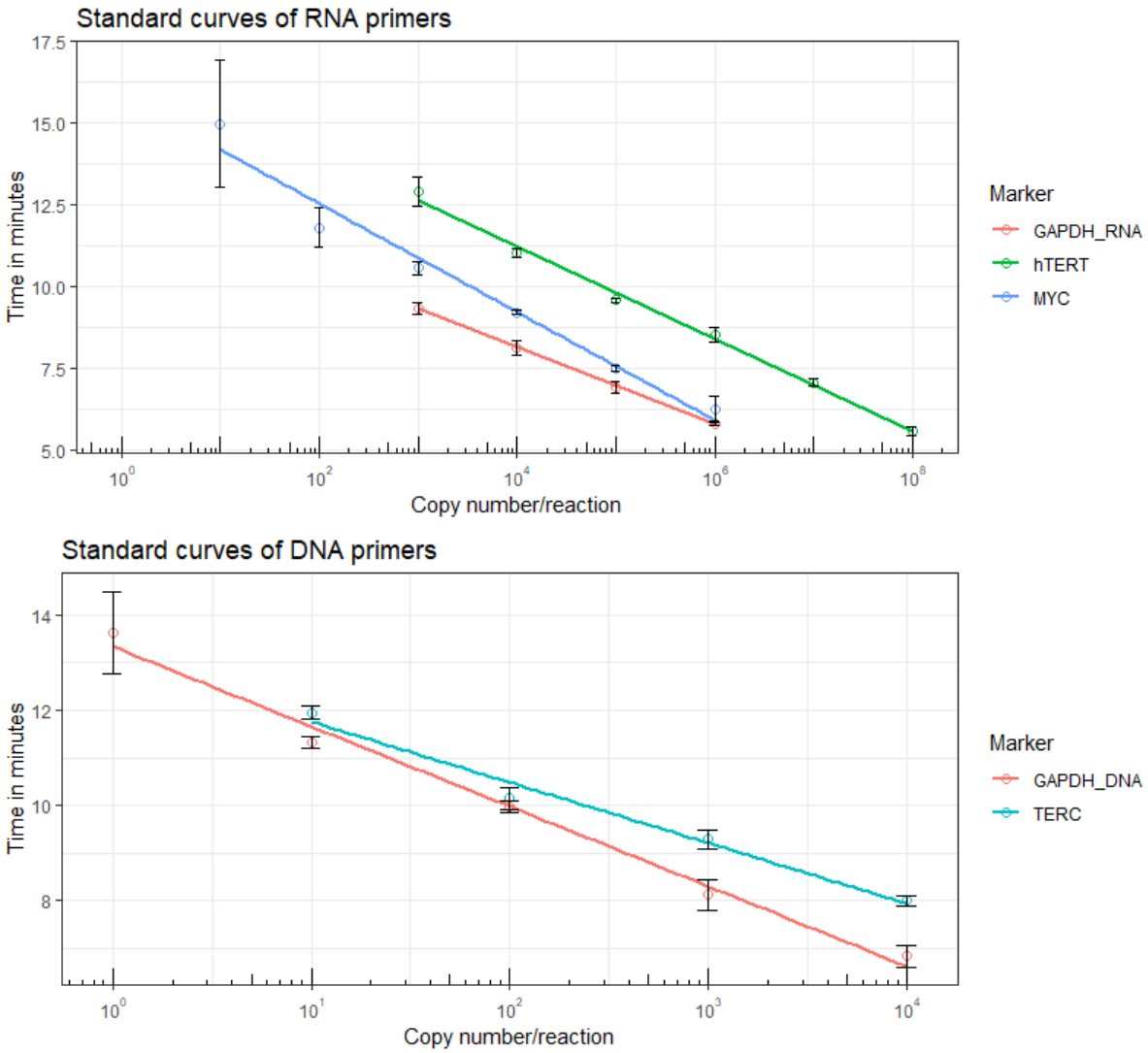

Figure 2-3 Standard curves of RNA and DNA primers designed for human tumour markers tested against synthetic DNA and RNA in standard LAMP mix. Tests performed on Lightcycler 96 benchtop device.

2.3.2.4 HPV E6*I sensitivity

The four HPV types each had four primer designs which went through an initial primer screen then a dilution screen stage (Appendix 6.11). When the chosen primer sets were tested against the non-splice sequence inappropriate amplification occurred. The design of forming an unstable stem loop was not successful in stopping non-specific amplification, although it did impede the efficiency.

I attempted to improve this specificity by removing the loop primer associated with the stable stem-loop structure (Appendix 6.11.2). The primer sets for 16, 18 and 45 responded favourably to this intervention and markedly hampered the amplification of full-length sequences. However, I discovered a secondary design issue with the primer sets and so did not run an experiment with the spliced sequences with the primer sets with a loop primer removed. Instead, I redesigned the primer sets to include mismatch nucleotides.

I present below the results of the mismatch nucleotide experiments for HPV 16. The other three HPV types are presented in Appendix 6.11.3-6.11.6).

Primer Option vs splice/full sequence	Time to positive (mins)	Error(mins)
16_1_splice	6.26	0.09
16_1_full	23.80	0.63
16_2_splice	7.36	0.08
16_2_full	27.21	1.10

Table 2-3 HPV 16 Option screen

There were two new options for HPV 16 (Table 2-3). Option 1 was chosen as it was the most efficient at amplifying the spliced sequence. The Option 1 primer set was run with different mismatched nucleotides in the FIP primer component. The mismatch primer set 16_4.1_S successfully amplified the spliced sequence but not the full-length sequence (Table 2-4).

Primer Option	Time to positive (mins)	Error(mins)
16_3.2_S	8.71	0.05
16_3.2_F	29.37	4.03
16_3.3_S	37.24	1.22
16_3.3_F	-	-
16_4.1_S	10.25	0.10
16_4.1_F	-	-
16_4.2_S	17.42	0.88
16_4.2_F	35.44	2.30
16_4.3_S	22.07	2.44
16_4.3_F	30.59	8.56

Table 2-4 HPV 16 Option 1 Mismatch screen

The top 3 mismatch primer mixes were tested in a dilution screen of both splice and non-splice sequence to determine the dynamic range of concentrations over which they are sensitive. A primer set sensitive to a splice sequence concentration of 10^0 would have a likely TTP of less than 20 minutes so that the test would be 'over' before the non-splice sequence began to amplify. Evidence from The Cancer Genome Atlas in cervical cancer(23) suggested a mean ratio of 2:1 spliced/full length in HPV 16 versus a 1:1 ratio in HPV 18 disease, with a maximum ratio of 2:1 full-length to spliced copies. An initial experiment to confirm whether the specific detection of the spliced target in an environment of mixed spliced/full length sequences with differing concentrations was performed with the HPV 58 primer set. Using a mix of 1:1, 1:3 and 1:7 splice:full length

ratios with deliberate exaggeration of the expected in vivo copy number ratios to confirm the specificity, the expected melting peak temperature of 84^{o}C, as found in pure-spliced sequence reactions, was seen in each of the mixed environment reactions, with a time to positive in line with the concentration of the spliced sequence used in each sequence mix. This is reassuring that despite the potential for non-specific amplification of full-length targets, the pragmatic reality is that, *in vivo*, both spliced and full-length sequences are always present and the spliced target will be amplified due to its more favourable reaction efficiency.

2.3.3 Quantitative performance of primers in LAMP

2.3.3.1 Synthetic DNA/RNA for primer testing

For the RNA markers, synthetic double-stranded DNA containing a T7 promotor for RNA transcription was synthesized by Integrated DNA Technologies (Leuven, Belgium). The HiScribe T7 High-yield RNA synthesis kit ((New England Biolabs, Hitchin, UK) was used to produce target specific RNA to test the designed primers. The synthetic DNA and RNA was quantified using a Qubit 3.0 fluorometer and high-sensitivity double-stranded DNA and single stranded RNA assay kits (Life Technologies, Carlsbad, CA).

Sensitivity of the assay was evaluated in serial 10-fold dilutions of synthetic DNA/RNA target, ranging from 10^{8} to 10^{0} copies per reaction with each condition run in triplicate. pH-LAMP assays were performed on a LightCycler 96 System (Roche Molecular Systems, Pleasanton, CA) and data analysed using LightCycler 96 System software version SW1.1.

2.3.3.2 Analytical sensitivity of primers in LAMP

The final primer sets defined (Table 2-5) were tested in the pH-LAMP specific reaction mix to be used on the lab-on-a-chip platform. A set of standard curves (Table 2-6, Figure 2-4) were produced using this new pH-LAMP mix. These curves were used to determine marker concentrations in the clinical samples.

Name	sequence
F3_TERT	GCCTGAGCTGTACTTTGTCA
B3_TERT	GGTGAGCCACGAACTGTC
FIP_TERT	TGGGGTTTGATGATGCTGGCGA-GGGCGCGTACGACACCATCC
BIP_TERT	GGTCCAGAAGGCCGCCCAT-GCTGGAGGTCTGTCAAGGTA
LF_TERT	ACCTCCGTGAGCCTGTCCTG
LB_TERT	CACGTCCGCAAGGCCTTCA
F3_MYC	CCATGAGGAGACACCGCC
B3_MYC	TGCTGATGTGTGGAGACGT
FIP_MYC	AGCCTGCCTCTTTTCCACAGAA-CACCACCAGCAGCGAC
BIP_MYC	CTGGATCACCTTCTGCTGGAGG-GGCACCTCTTGAGGACCA
LF_MYC	TCATCTTCTTGTTCCTCCTCAGA
LB_MYC	CAGCAAACCTCCTCACAGCC
F3_GAPRNA	GATGCTGGCGCTGAGTAC
B3_GAPRNA	GCTAAGCAGTTGGTGGTGC

FIP_GAPRNA	CTTTTGGCTCCCCCCTGCAAATGGAGTCCACTGGCGTCTT
BIP_GAPRNA	TCTGCTGATGCCCCCATGTTCGGAGGCATTGCTGATGATCT
LF_GAPRNA	AGCCTTCTCCATGGTGGTG
LB_GAPRNA	GTCATGGGTGTGAACCATGAG
F3_GAPDNA	ACCCCCATAGGCGAGATC
B3_GAPDNA	TGATGACCCTTTTGGCTCC
FIP_GAPDNA	CTCCATGGTGGTGAAGACGCC-CAAAATCAAGTGGGGCGATG
BIP_GAPDNA	CGGGAGGGGAAGCTGACTCA-ACAGCAGAGAAGCAGACAGT
LF_GAPDNA	TCCACGACGTACTCAGCG
LB_GAPDNA	GCAGGACCCGGGTTCAT
F3_TERC	TGTGAGCCGAGTCCTGG
B3_TERC	TCTCCGGAGGCACCCA
FIP_TERC	AGGAAGAGGAACGGAGCGAGTC-GTGCACGTCCCACAGCT
BIP_TERC	GAAAGGCCTGAACCTCGCCC-TGCCACCGCGAAGAGT
LB_TERC	AGAGACCCGCGGCTGACA
LF_TERC	CGGCGCGATTCCCTGA

Table 2-5 pH-LAMP primer sequences

pH LAMP	RNA			DNA	
Copies/reaction	hTERT	MYC	GAPDH	TERC	GAPDH
10^8	-	4.85 (0.07)	3.36 (0.05)	3.00 (0.15)	1.74 (0.03)
10^7	7.84 (0.17)	5.97 (0.08)	4.46 (0.21)	4.03 (0.03)	3.11 (0.15)
10^6	9.34 (0.13)	7.19 (0.06)	5.64 (0.31)	4.86 (0.24)	3.99 (0.08)
10^5	10.94 (0.33)	8.2 (0.2)	6.27 (0.07)	5.68 (0.38)	4.41 (0.17)
10^4	12.57 (0.45)	9.53 (0.18)	7.3 (0.07)	6.62 (0.29)	5.08 (0.31)
10^3	14.99 (0.64)	10.9 (0.52)	8.51 (0.1)	7.46 (0.09)	6.49 (0.38)
10^2	16.22 (0.5)	12.18 (1.16)	-	8.42 (0.12)	6.84 (0.12)
10^1	-	-	-	9.62 (0.42)	8.12 (0.15)
10^0	-	-	-	10.4 (0.03)	8.59 (0.37)
R^2	0.99	1.00	0.99	1.00	0.99

Table 2-6 Analytical sensitivity of human markers in pH-LAMP

Figure 2.4: Standard curves of RNA and DNA primers designed for human tumour markers tested against synthetic RNA and DNA in pH-LAMP mix. Tests performed on Lightcycler 96 benchtop device.

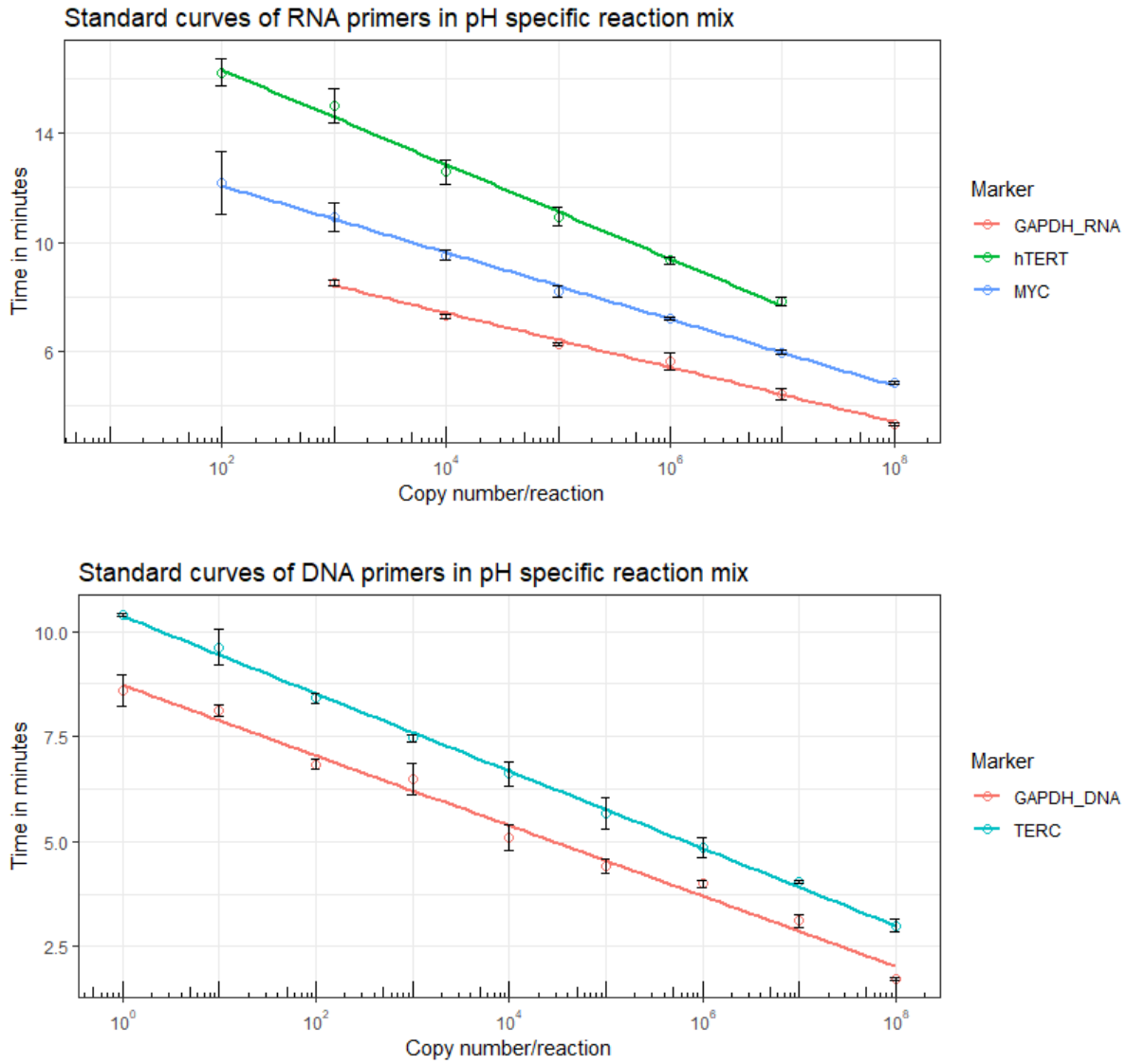

2.3.4 Incorporating the primers into an existing lab-on-a-chip platform

2.3.4.1 Amplification chemistry for lab-on-a-chip platform

In order to transfer the developed amplification chemistries to a Lab-on-Chip platform, compatibility with the sensing capabilities of ISFET sensors was needed. Since ISFETs are inherently pH sensors, the reaction mix of a standard

LAMP was modified to pH-LAMP (159) by adjusting the buffering capabilities to allow for changes in pH to be measured during DNA amplification.

Each solution was split into 5-μL reactions (triplicates) on a 96-well PCR plate and heated at 63C for 40 minutes using a real-time qPCR platform (LC96).

During nucleic acid amplification, nucleotides are incorporated by action of a polymerase resulting in the release of a proton (H^+) as described by:

$$dNTP+DNA_n \rightarrow DNA_{n+1}+PPi+H^+$$

where DNA_n indicates the *n*th nucleotide and PPi is pyrophosphate.

The release of protons into the amplification reaction induces a change in pH that ISFETs can transduce into an electrical output, thus correlating a change in pH to a change in voltage (146). Additionally, this change is regulated by the buffer capacity (β) of the solution. Overall, the change in pH is given by:

$$\Delta pH=N(H^+/\beta)$$

where *N* denotes the total number of nucleotides incorporated during amplification (159). Consequently, the pH change is proportional to the total number of nucleotides inserted and inversely proportional to the buffering capacity of the solution. DNA amplification modifies the overall pH of the solution causing a proportional change in voltage detected by the ISFETs. When no amplification occurs the pH of the solution remains unchanged therefore giving a constant voltage signal.

During an amplification reaction, the pH signal is obtained by taking the average of the active sensors that are exposed to the solution. The sensing membrane exposed to the solution undergoes hydration which manifests as a slow monotonic change on the output voltage signal, typically referred to as drift

(160). The underlying cause is the diffusion of ions from the solution to charge-trapping sites in the nitride that exist due to its structure.

2.3.4.2 Lab-on-a chip hardware and readouts

The process of nucleic acid detection on the lab-on-a-chip platform followed a clearly specified procedure. A microfluidic reaction chamber was laser cut from a 3 mm acrylic sheet by a colleague in the laboratory. I added this on top of the CMOS microchip. In addition, a silver/silver chloride reference electrode was inserted in the chamber for sensor biasing, which was obtained by chlorination of a 0.03 mm diameter silver wire in 1M KCl. 20uL of de-ionised water was loaded into the chamber and covered with PCR tape. The chip was inserted into the lab-on-a-chip platform and connected via Bluetooth to the mobile phone device which controls the platform and records the output wirelessly (Figure 2-5). An initial check of chip voltage measurement was performed to determine whether the platform peltier heated the chip to 63^{o}C. During this time the observed sample drift in voltage can be decoupled from the expected drift and the pH change due to DNA amplification obtained.

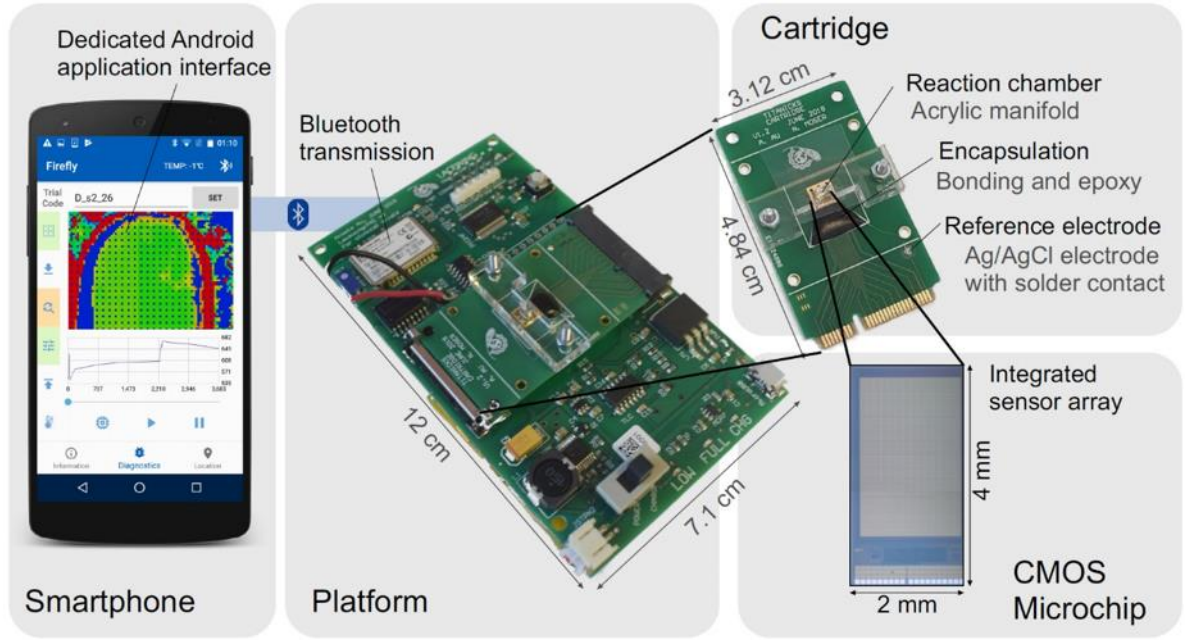

Figure 2-5 Components of the Lab-on-a-chip system connected wirelessly to a smartphone readout

To carry-out nucleic acid amplification reactions, the de-ionised water was removed from the microfluidic chamber and replaced with 20µL of pH-LAMP or pH-RT-LAMP (RT – reverse transcription) mix and sealed with PCR tape to

avoid evaporation and contamination of the amplified products. The mixture was heated to 63C for 35 minutes.

The output voltages measured by the chip were first linearised and then set to a relative scale by setting the minimum relative voltage value to 0 and the maximum value to 1. A sigmoidal curve was then fitted to this data and a corresponding threshold value of 0.2 calculated and time to positive (TTP) derived. This was similar to the technique used in the Lightcycler 96 system to establish the Cq in relation to predefined dye-specific fluorescence threshold values.

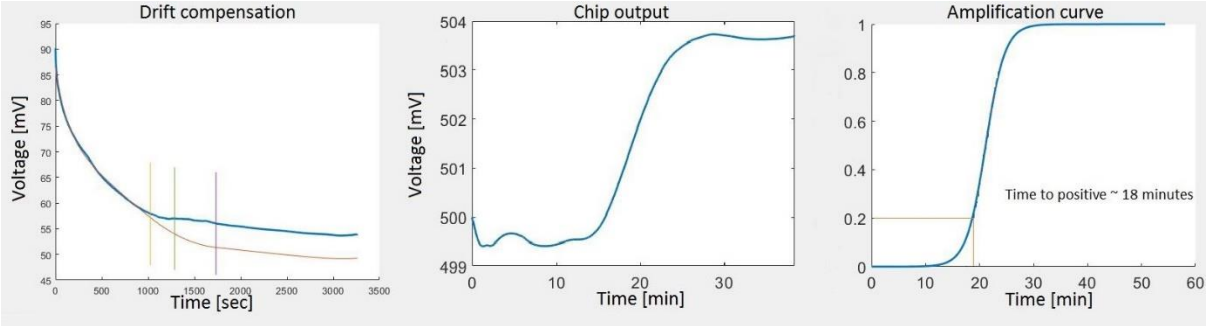

Figure 2-6 Output voltages with time showing drift compensation (left), chip output (middle) and amplification curve after correction (right).

Due to volume of extracted RNA available following RNA extraction of samples, only a single lab-on-a-chip procedure was performed for each sample.

2.4 Clinical testing- validating the lab-on-a-chip technology using banked tissue biopsies

I embarked upon validating the DNA/RNA primers which had been tested upon a standard benchtop Lightcycler device on clinical samples, and also allowing the initial testing of a selection of markers directly on the Lab-on-a-chip device.

The solid tumour samples available to me were used opportunistically but also as the solid tumours would have a high cellularity content I could reasonably assume that a negative test result wasn't due the available target copy number being below the analytical sensitivity of the primers designed.

2.4.1 Sample tissues

An existing holding of 45 cervical tissue biopsies taken in 2001 from patients with cervical cancer with their informed consent as part of a research study led by Professor Nandita deSouza was used. The biopsies were originally taken during surgery at the Hammersmith hospital and snap frozen at -80^{0}C. They were initially stored at Hammersmith Hospital at -80C and transferred to The Institute of Cancer Research and have remained frozen at -80C throughout. There was no clinical or identifying information available to me. Pathological verification of cancer was undertaken.

DNA and RNA was extracted, testing undertaken on the lab-on-a-chip platform and a comparison made with a pH-LAMP experiment on the LC96 system.

2.4.2 DNA and RNA extraction

Cervical tissue samples were separated into sections. One was embedded in paraffin and a single slide stained with Haemotoxylin and Eosin reviewed by a consultant histopathologist to classify the sample as benign or malignant tissue. The other section was homogenized in 2 mL tubes containing RLT+/BME lysis buffer solution from the AllPrep DNA/RNA Kit (Qiagen, Hilden, Germany) and zirconium oxide beads in a Precellys 24 Homogenizer (Bertin, Villeurbanne, France). Subsequently, DNA and RNA were extracted using the AllPrep kit, according to the manufacturer's instructions. Total DNA and RNA yield was

determined using a NanoDrop ND-2000 spectrophotometer (Thermo Fisher Scientific, Waltham, USA). Only those samples which yielded both DNA and RNA were selected for analysis.

Of 45 patient samples with DNA and RNA extracted, only 10 samples had both DNA and RNA suitable for analysis. In 35 cases, the RNA was not of sufficient quantity for LAMP and PCR analysis (< 9 ng/uL). Therefore, the validation of HPV markers identified using lab-on-a-chip technology was done in 10 samples only where DNA and RNA quantity and quality indicated excellent extraction due to the high number of cells. Of these 10 samples, 5 contained benign tissue only, 4 contained squamous cell carcinoma and 1 contained adenocarcinoma (identified on Haematoxylin and Eosin sections by Dr Katherine Vroobels, consultant histopathologist at the Royal Marsden Hospital).

DNA validation was done on HPV and RNA validation was done on hTERT. hTERT was selected as previous literature has suggested it is a promising tumour marker in cervical cancer (103, 161). It was not possible to evaluate both DNA and RNA from HPV or to evaluate TERC or Myc RNA as the number of experiments possible on the lab-on-a-chip was limited by the time to construct the individual chips. The volume of DNA and RNA available from the biopsies was also a limiting factor.

2.4.3 HPV marker validation

HPV 16 DNA was detected in samples H5, H7, H17 and H27 (Table 3.2) on the lab-on-a-chip platform. These results were confirmed using the LAMP mix on the LC96 thermocycler. HPV 18 DNA was detected in samples H11 and H45 on the lab-on-a-chip platform and confirmed using the LAMP mix on the LC96

thermocycler. The presence of HPV 16 DNA also was confirmed using PCR primers. Two cases (H2 and H12) were negative for HPV 16 on the LC96 device but were positive when measured on the lab-on-a-chip platform. It may be that the copy number of HPV 16 DNA in both of these samples was at the limit of detection and that the larger sample volume used on the lab-on-a-chip platform enabled detection of lower copy numbers at the edge of the detection limit.

2.4.4 Tumour marker validation

The presence of hTERT RNA was detected in 5 of 5 cancer samples and 0 of 5 benign samples thus perfectly distinguishing the benign from the tumour samples on lab-on-a-chip. This was confirmed using conventional PCR (Table 2-7). The time to positive was between 12 and 15 minutes.

These data indicate that the lab-on-a-chip platform provides equivalent results to conventional qPCR instruments for detection of HPV DNA and RNA and tumour RNA.

Sample ID	Diagnosis	DNA_conc (ng/ul)	RNA_Conc (ng/uL)	GAPDH RNA TTP (sd)	HPV 16/18* DNA TTP (sd)	HPV 16/18* LOC TTP	HPV 16/18* PCR CT (sd)	hTERT RNA TTP (sd)	hTERT LOC TTP	hTERT PCR CT (sd)
H2	Benign	322.3	22.8	9.02 (0.11)	-	17.64	35.51	-	-	-
H5	SCC	1745	1434.4	7.06 (0.11)	20.56 (0.56)	14.89	21.41 (0.02)	12.42 (0.34)	21.84	33.48 (0.03)
H7	SCC	1811.8	1576.5	5.7 (0.05)	18.87 (0.23)	14.21	35.95 (0.40)	12.83 (0.77)	21.73	33.70 (0.69)
H9	Benign	590.3	195.4	6.96 (0.04)	-	-	-	-	-	-
H11	Benign	169.5	44.4	7.96 (0.16)	12.48* (0.49)	8.18*	27.16* (0.11)	-	-	-
H12	SCC	1412.7	718.6	6.69 (0.13)	-	17.56	36.30 (0.12)	14.21 (2.79)	18.76	31.57 (0.09)
H17	Benign	2192.8	957.4	8.67 (0.12)	35.4 (5.08)	15.54	34.81 (1.93)	-	-	-
H18	Benign	22.7	9.2	9.2 (0.09)	-	-	-	-	-	-
H27	ADC	1510.5	1570.9	7.97 (0.05)	20.74 (0.26)	18.51	32.61 (0.31)	15.06 (4.01)	14.56	32.75 (0.30)
H45	SCC	1439.3	1048.2	6.47 (0.07)	18.63* (0.21)	18.72*	29.73* (0.02)	14.82 (2.22)	9.42	32.06 (0.33)

Table 2-7 Summary of HPV DNA and RNA and hTERT RNA in 10 cervical biopsy sample results using LOC compared to standard PCR. GAPDH was used as a "housekeeping" gene and is shown for comparison. TTP – time to positive, CT – cycle threshold, sd – standard deviation

2.5 Discussion

2.5.1 Selection of markers for cervical cancer detection on lab-on-a-chip

The selected markers were chosen with three criteria in mind; clear contribution to the mechanism of carcinogenesis, evidence of differentiation between normal, dysplasia and carcinoma in the expression levels and finally, consistent evidence supporting the overexpression or amplification in predicting disease (103, 123, 162). Several studies examine the mutations noted in tumour samples but this has limited use in a clinical test to predict presence of disease as the mutation present would need to be known a priori. The exploratory marker TERC/GAPDH ratio is based on solid evidence of TERC amplification in FISH experiments (116, 121, 163-165). A digital PCR test to examine the exact copy number variation would most likely offer a more accurate solution, however, this would limit the portability of the test.

2.5.2 Lab-on-a chip in non-cancer use

The Centre for Bio-Inspired Technology (CBIT) group has explored several uses for the lab-on-a-chip technique, some of which are being tested in clinics in the developing world. This can be used as a model to further develop the technology as a point-of-care diagnostic platform in countries with a high incidence of cervical cancer. For example, the lab-on-a-chip method incorporating pH-LAMP based detection of malaria has been utilised with a rapid and specific detection of P. falciparum malaria using an assay targeting the gene *kelch* 13. Detection occurred in less than 20 minutes in isothermal conditions using LAMP with direct chemical-to-electronic sensing. DNA quantification on-chip, using DNA samples derived from clinical isolates of P.

falciparum could be detected to 10^1 copies per reaction. The system was compared against a commercial instrument using fluorescence and achieved equivalent detection capability. In addition, the group demonstrated the successful detection of the C580Y single-nucleotide polymorphism (SNP) associated with artemisinin-resistant malaria, and re-enforces the potential of SNP detection in tumour samples (148).

Separately, a LAMP-based method of detecting Aspergillus fumigatus, which causes a spectrum of respiratory and invasive infections, has also been successfully developed and tested. The methodology was validated by the design of specific LAMP primers targeting dominant triazole-resistant genotypes of A. fumigatus, and the assay was shown to have high analytical sensitivity and specificity for detecting the most prevalent cyp51A mutation, TR34. This highlighted the potential of diagnosing multiazole-resistant Aspergillus, at the point-of-care using a highly sensitive assay (10 copies/reaction) with a reaction time of 30 minutes (147).

Finally, a method of HIV-1 viral load detection based on a CMOS chip platform has been developed. The chip has embedded heaters and thermal sensors which facilitate on-chip nucleic acid amplification detected with ISFET sensors. The pH RT-LAMP assay detects 10 copies of RNA per reaction within 30 minutes. The performance of the assay in almost 1000 plasma samples show a detection rate for inputs >1000 copies/reaction of 95% and for inputs of 50 to 1000 copies of 88.7% (166). These examples highlight the potential of the lab-on-a-chip technique as a diagnostic assay. My work shows for the first time that it is feasible to perform these assays using tumour-specific markers.

The current workflow still relies on using extracted DNA/RNA that is pre-prepared and ready for pipetting onto the chip. For the device to be truly point-of-care, an embedded sample preparation module will need to be created incorporating microfluidic technology that enables a seamless workflow from sample to result. Because LAMP has been shown to be more robust to reaction inhibitors found in clinical samples such as urine and blood than PCR (167) and because exfoliated cellular material from cervical smears is readily available, sample preparation should be minimal and only require lysis.

2.5.3 Sufficient for clinical purposes?

The analytical sensitivity of the selected markers is more than adequate for our purposes. The DNA markers GAPDH and TERC resolve down to 10^0 copies per reaction and have similar standard curve gradients; this should provide a reliable method of predicting copy number variation in the samples. The mRNA markers, whilst having a poorer sensitivity in comparison to the DNA markers, with a limit of detection of 10^2 for hTERT and MYC, and 10^3 for GAPDH mRNA, are comparable to other LAMP-based markers. The GAPDH mRNA limit of detection is a potential limiting factor if there are samples with low cellularity (successful amplification of GAPDH mRNA is an indicator of appropriate sample extraction and sample integrity) as this could result in those samples being rejected. However, a minimum expectation of 10^3 copies of GAPDH mRNA per 10ng of total RNA is considered a reasonable threshold (168). Given the average quantity of extracted total RNA in archived cervical samples is 27.5ng/uL (169) the limit of detection of 10^3 copies per reaction for our GAPDH mRNA test is several orders of magnitude lower than would be found in normal

clinical samples. Nevertheless, the limitations of pursuing goals of ultra-sensitivity with these assays comes at the price of loss of specificity and causes patients to be classified as positive who in truth have no clinically relevant disease. Therefore, a balance between optimal sensitivity without increasing the number of false positive classifications, which would require further (unnecessary) investigations, needs to be made. The performance of the designed markers seems to sit squarely in the clinically relevant zone. This will be further explored in the next chapter when using usual Cervex brush cervical samples and validating the markers on these samples, which will have much less cellularity than the solid tumour samples used in this chapter.

2.5.4 Validation of clinical testing against PCR

Validation of the clinical testing against conventional PCR showed largely equivalent results for both the DNA and RNA tests in the HPV and hTERT primers. The PCR primers for MYC and TERC/GAPDH performed poorly in the experiments, perhaps indicating alternative primers should be used as their technical sensitivity was below expectation in the clinical samples. Similarly, validation of the HPV-16 and the tumour markers against standard PCR was also equivalent. The lab-on-a-chip system was in close agreement with the traditional benchtop LC96 system, which indicates the potential of this platform as a diagnostic tool.

The pH-LAMP HPV Type 18 DNA marker, as developed by Luo et al (170), needs further work. This could be ameliorated by setting a very short time to positive threshold but alternative HPV 18 DNA LAMP primer sets would be available to test which may provide more reliable real-world results. The

development of a robust, sensitive set of HPV DNA type specific pH-LAMP primers would be a prerequisite to this platform being successful as a screening platform.

2.6 Summary

-
- Appropriate primers were designed for detection of selected tumour and HPV markers on a lab-on-a-chip platform.
-
- The analytical sensitivity of each of the markers was determined and found to be in the clinically relevant range.
-
- The quantitative performance of the primers was assessed using LAMP and the technology transferred to the lab-on-a-chip platform.
-
- The lab-on-a-chip platform was tested using banked tissue biopsy samples from patients with cervical cancer and shown to provide equivalent results to conventional qPCR instruments for detection of HPV DNA and RNA and tumour RNA.

2.7 References

10. de Sanjose S, Quint WG, Alemany L, Geraets DT, Klaustermeier JE, Lloveras B, et al. Human papillomavirus genotype attribution in invasive cervical cancer: a retrospective cross-sectional worldwide study. The Lancet Oncology. 2010;11(11):1048-56.

23. Integrated genomic and molecular characterization of cervical cancer. Nature. 2017;543(7645):378-84.

25. Bodelon C, Vinokurova S, Sampson JN, den Boon JA, Walker JL, Horswill MA, et al. Chromosomal copy number alterations and HPV integration in cervical precancer and invasive cancer. Carcinogenesis. 2016;37(2):188-96.

27. Gimenes F, Souza RP, de Abreu AL, Pereira MW, Consolaro ME, da Silva VR. Simultaneous detection of human papillomavirus integration and c-MYC gene amplification in cervical lesions: an emerging marker for the risk to progression. Archives of gynecology and obstetrics. 2016;293(4):857-63.

96. Schmidt JC, Cech TR. Human telomerase: biogenesis, trafficking, recruitment, and activation. Genes & development. 2015;29(11):1095-105.

97. Shay JW, Bacchetti S. A survey of telomerase activity in human cancer. European Journal of Cancer. 1997;33(5):787-91.

98. Levy MZ, Allsopp RC, Futcher AB, Greider CW, Harley CB. Telomere end-replication problem and cell aging. Journal of Molecular Biology. 1992;225(4):951-60.

99. Cong Y-S, Wright WE, Shay JW. Human Telomerase and Its Regulation. Microbiology and Molecular Biology Reviews. 2002;66(3):407-25.

100. Katzenellenbogen RA. Activation of telomerase by HPVs. Virus Res. 2017;231:50-5.

101. Mutirangura A, Sriuranpong V, Termrunggraunglert W, Tresukosol D, Lertsaguansinchai P, Voravud N, et al. Telomerase activity and human papillomavirus in malignant, premalignant and benign cervical lesions. British journal of cancer. 1998;78(7):933-9.

102. Snijders PJ, van Duin M, Walboomers JM, Steenbergen RD, Risse EK, Helmerhorst TJ, et al. Telomerase activity exclusively in cervical carcinomas and a subset of cervical intraepithelial neoplasia grade III lesions: strong association with elevated messenger RNA levels of its catalytic subunit and high-risk human papillomavirus DNA. Cancer research. 1998;58(17):3812-8.

103. Wang HY, Park S, Kim S, Lee D, Kim G, Kim Y, et al. Use of hTERT and HPV E6/E7 mRNA RT-qPCR TaqMan assays in combination for diagnosing high-grade cervical lesions and malignant tumors. Am J Clin Pathol. 2015;143(3):344-51.

104. Zejnullahu VA, Zejnullahu VA, Josifovska S, Vukovik N, Pakovski K, Panov S. Correlation of hTERT Expression with Cervical Cytological Abnormalities and Human Papillomavirus Infection. 2017;38(3):143.

105. Kailash U, Soundararajan CC, Lakshmy R, Arora R, Vivekanandhan S, Das BC. Telomerase activity as an adjunct to high-risk human papillomavirus types 16 and 18 and cytology screening in cervical cancer. British journal of cancer. 2006;95(9):1250-7.

106. Katzenellenbogen R. Telomerase Induction in HPV Infection and Oncogenesis. Viruses. 2017;9(7).

107. Liu X, Yuan H, Fu B, Disbrow GL, Apolinario T, Tomaić V, et al. The E6AP Ubiquitin Ligase Is Required for Transactivation of the hTERT Promoter by the Human Papillomavirus E6 Oncoprotein. Journal of Biological Chemistry. 2005;280(11):10807-16.

108. Van Doorslaer K, Burk RD. Association between hTERT activation by HPV E6 proteins and oncogenic risk. Virology. 2012;433(1):216-9.

109. Wong MS, Wright WE, Shay JW. Alternative Splicing Regulation of Telomerase: A New Paradigm. Trends in genetics : TIG. 2014;30(10):430-8.

110. Ulaner GA, Hu JF, Vu TH, Giudice LC, Hoffman AR. Tissue-specific alternate splicing of human telomerase reverse transcriptase (hTERT) influences telomere lengths during human development. Int J Cancer. 2001;91(5):644-9.
111. Ulaner GA, Hu JF, Vu TH, Giudice LC, Hoffman AR. Telomerase activity in human development is regulated by human telomerase reverse transcriptase (hTERT) transcription and by alternate splicing of hTERT transcripts. Cancer research. 1998;58(18):4168-72.
112. Listerman I, Sun J, Gazzaniga FS, Lukas JL, Blackburn EH. The major reverse transcriptase-incompetent splice variant of the human telomerase protein inhibits telomerase activity but protects from apoptosis. Cancer research. 2013;73(9):2817-28.
113. Colgin LM, Wilkinson C, Englezou A, Kilian A, Robinson MO, Reddel RR. The hTERTalpha splice variant is a dominant negative inhibitor of telomerase activity. Neoplasia. 2000;2(5):426-32.
114. Yi X, Shay JW, Wright WE. Quantitation of telomerase components and hTERT mRNA splicing patterns in immortal human cells. Nucleic Acids Res. 2001;29(23):4818-25.
115. Nachajova M, Brany D, Dvorska D. Telomerase and the process of cervical carcinogenesis. Tumour biology : the journal of the International Society for Oncodevelopmental Biology and Medicine. 2015;36(10):7335-8.
116. Jiang J, Wei LH, Li YL, Wu RF, Xie X, Feng YJ, et al. Detection of TERC amplification in cervical epithelial cells for the diagnosis of high-grade cervical lesions and invasive cancer: a multicenter study in China. The Journal of molecular diagnostics : JMD. 2010;12(6):808-17.
117. Wang X, Liu J, Xi H, Cai L. The significant diagnostic value of human telomerase RNA component (hTERC) gene detection in high-grade cervical lesions and invasive cancer. Tumour biology : the journal of the International Society for Oncodevelopmental Biology and Medicine. 2014;35(7):6893-900.
118. Jiang J, Wei L-H, Li Y-L, Wu R-F, Xie X, Feng Y-J, et al. Detection of TERC Amplification in Cervical Epithelial Cells for the Diagnosis of High-Grade Cervical Lesions and Invasive Cancer: A Multicenter Study in China. The Journal of molecular diagnostics : JMD. 2010;12(6):808-17.
119. Jalali GR, Herzog TJ, Dziura B, Walat R, Kilpatrick MW. Amplification of the chromosome 3q26 region shows high negative predictive value for nonmalignant transformation of LSIL cytologic finding. American journal of obstetrics and gynecology. 2010;202(6):581 e1-5.
120. Rodolakis A, Biliatis I, Symiakaki H, Kershnar E, Kilpatrick MW, Haidopoulos D, et al. Role of chromosome 3q26 gain in predicting progression of cervical dysplasia. International journal of gynecological cancer : official journal of the International Gynecological Cancer Society. 2012;22(5):742-7.
121. Ji W, Lou W, Hong Z, Qiu L, Di W. Genomic amplification of HPV, h-TERC and c-MYC in liquid-based cytological specimens for screening of cervical intraepithelial neoplasia and cancer. Oncology letters. 2019;17(2):2099-106.
122. El Khattabi LA, Rouillac-Le Sciellour C, Le Tessier D, Luscan A, Coustier A, Porcher R, et al. Could Digital PCR Be an Alternative as a Non-Invasive Prenatal Test for Trisomy 21: A Proof of Concept Study. PLOS ONE. 2016;11(5):e0155009.
123. Sagawa Y, Nishi H, Isaka K, Fujito A, Takayama M. The correlation of TERT expression with c-myc expression in cervical cancer. Cancer letters. 2001;168(1):45-50.
124. Bodelon C, Untereiner ME, Machiela MJ, Vinokurova S, Wentzensen N. Genomic characterization of viral integration sites in HPV-related cancers. International Journal of Cancer. 2016;139(9):2001-11.
125. Kubler K, Heinenberg S, Rudlowski C, Keyver-Paik MD, Abramian A, Merkelbach-Bruse S, et al. c-myc copy number gain is a powerful prognosticator of disease outcome in cervical dysplasia. Oncotarget. 2015;6(2):825-35.
126. Kuglik P, Kasikova K, Smetana J, Vallova V, Lastuvkova A, Moukova L, et al. Molecular cytogenetic analyses of hTERC (3q26) and MYC (8q24) genes amplifications in correlation with

oncogenic human papillomavirus infection in Czech patients with cervical intraepithelial neoplasia and cervical carcinomas. Neoplasma. 2015;62(01):130-9.
127. Zhu D, Jiang XH, Jiang YH, Ding WC, Zhang CL, Shen H, et al. Amplification and overexpression of TP63 and MYC as biomarkers for transition of cervical intraepithelial neoplasia to cervical cancer. International journal of gynecological cancer : official journal of the International Gynecological Cancer Society. 2014;24(4):643-8.
128. Mayrand MH, Duarte-Franco E, Rodrigues I, Walter SD, Hanley J, Ferenczy A, et al. Human papillomavirus DNA versus Papanicolaou screening tests for cervical cancer. N Engl J Med. 2007;357(16):1579-88.
129. Gustinucci D, Giorgi Rossi P, Cesarini E, Broccolini M, Bulletti S, Carlani A, et al. Use of Cytology, E6/E7 mRNA, and p16INK4a-Ki-67 to Define the Management of Human Papillomavirus (HPV)-Positive Women in Cervical Cancer Screening. Am J Clin Pathol. 2016;145(1):35-45.
130. Li N, Franceschi S, Howell-Jones R, Snijders PJ, Clifford GM. Human papillomavirus type distribution in 30,848 invasive cervical cancers worldwide: Variation by geographical region, histological type and year of publication. Int J Cancer. 2011;128(4):927-35.
131. Basu P, Banerjee D, Mittal S, Dutta S, Ghosh I, Chowdhury N, et al. Sensitivity of APTIMA HPV E6/E7 mRNA test in comparison with hybrid capture 2 HPV DNA test for detection of high risk oncogenic human papillomavirus in 396 biopsy confirmed cervical cancers. Journal of medical virology. 2016;88(7):1271-8.
132. Cook DA, Smith LW, Law J, Mei W, van Niekerk DJ, Ceballos K, et al. Aptima HPV Assay versus Hybrid Capture((R)) 2 HPV test for primary cervical cancer screening in the HPV FOCAL trial. Journal of clinical virology : the official publication of the Pan American Society for Clinical Virology. 2017;87:23-9.
133. Reid JL, Wright TC, Jr., Stoler MH, Cuzick J, Castle PE, Dockter J, et al. Human papillomavirus oncogenic mRNA testing for cervical cancer screening: baseline and longitudinal results from the CLEAR study. Am J Clin Pathol. 2015;144(3):473-83.
134. Monsonego J, Hudgens MG, Zerat L, Zerat J-C, Syrjänen K, Halfon P, et al. Evaluation of oncogenic human papillomavirus RNA and DNA tests with liquid-based cytology in primary cervical cancer screening: The FASE study. International Journal of Cancer. 2011;129(3):691-701.
135. Tang S, Tao M, McCoy JP, Jr., Zheng ZM. The E7 oncoprotein is translated from spliced E6*I transcripts in high-risk human papillomavirus type 16- or type 18-positive cervical cancer cell lines via translation reinitiation. Journal of virology. 2006;80(9):4249-63.
136. Forslund O, Lindqvist P, Haadem K, Czeglédy J, Göran Hansson B. HPV 16 DNA and mRNA in cervical brush samples quantified by PCR and microwell hybridization. Journal of virological methods. 1997;69(1):209-22.
137. Cricca M, Venturoli S, Leo E, Costa S, Musiani M, Zerbini M. Molecular analysis of HPV 16 E6I/E6II spliced mRNAs and correlation with the viral physical state and the grade of the cervical lesion. Journal of medical virology. 2009;81(7):1276-82.
138. Schmitt M, Dalstein V, Waterboer T, Clavel C, Gissmann L, Pawlita M. The HPV16 transcriptome in cervical lesions of different grades. Molecular and Cellular Probes. 2011;25(5):260-5.
139. Nakagawa S, Yoshikawa H, Yasugi T, Kimura M, Kawana K, Matsumoto K, et al. Ubiquitous presence of E6 and E7 transcripts in human papillomavirus-positive cervical carcinomas regardless of its type. Journal of medical virology. 2000;62(2):251-8.
140. Liu S, Minaguchi T. Separate analysis of human papillomavirus E6 and E7 messenger RNAs to predict cervical neoplasia progression. 2018;13(2):e0193061.
141. Shen Y, Li Y, Ye F, Wang F, Lu W, Xie X. Identification of suitable reference genes for measurement of gene expression in human cervical tissues. Analytical Biochemistry. 2010;405(2):224-9.

142. Daud II, Scott ME. Validation of Reference Genes in Cervical Cell Samples from Human Papillomavirus-Infected and -Uninfected Women for Quantitative Reverse Transcription-PCR Assays. Clinical and Vaccine Immunology. 2008;15(9):1369-73.
143. de Campos RP, Schultz IC, de Andrade Mello P, Davies S, Gasparin MS, Bertoni APS, et al. Cervical cancer stem-like cells: systematic review and identification of reference genes for gene expression. Cell biology international. 2018;42(2):139-52.
144. Leitão MdCG, Coimbra EC, Lima RdCPd, Guimarães MdL, Heráclio SdA, Silva Neto JdC, et al. Quantifying mRNA and MicroRNA with qPCR in Cervical Carcinogenesis: A Validation of Reference Genes to Ensure Accurate Data. PLOS ONE. 2014;9(11):e111021.
145. Moser N, Rodriguez-Manzano J, Lande TS, Georgiou P. A Scalable ISFET Sensing and Memory Array With Sensor Auto-Calibration for On-Chip Real-Time DNA Detection. IEEE Transactions on Biomedical Circuits and Systems. 2018;12(2):390-401.
146. Toumazou C, Shepherd LM, Reed SC, Chen GI, Patel A, Garner DM, et al. Simultaneous DNA amplification and detection using a pH-sensing semiconductor system. Nature Methods. 2013;10:641.
147. Yu L-S, Rodriguez-Manzano J, Malpartida-Cardenas K, Sewell T, Bader O, Armstrong-James D, et al. Rapid and Sensitive Detection of Azole-Resistant Aspergillus fumigatus by Tandem Repeat Loop-Mediated Isothermal Amplification. The Journal of Molecular Diagnostics. 2019;21(2):286-95.
148. Malpartida-Cardenas K, Miscourides N, Rodriguez-Manzano J, Yu LS, Baum J, Georgiou P. Quantitative and rapid Plasmodium falciparum malaria diagnosis and artemisinin-resistance detection using a CMOS Lab-on-Chip platform. bioRxiv. 2019:638221.
149. Notomi T, Okayama H, Masubuchi H, Yonekawa T, Watanabe K, Amino N, et al. Loop-mediated isothermal amplification of DNA. Nucleic Acids Res. 2000;28(12):E63.
150. Nagamine K, Hase T, Notomi T. Accelerated reaction by loop-mediated isothermal amplification using loop primers. Molecular and Cellular Probes. 2002;16(3):223-9.
151. Minnucci G, Amicarelli G, Salmoiraghi S, Spinelli O, Guinea Montalvo ML, Giussani U, et al. A novel, highly sensitive and rapid allele-specific loop-mediated amplification assay for the detection of the JAK2V617F mutation in chronic myeloproliferative neoplasms. Haematologica. 2012;97(9):1394-400.
152. Vasquez AM, Zuluaga L, Tobon A, Posada M, Velez G, Gonzalez IJ, et al. Diagnostic accuracy of loop-mediated isothermal amplification (LAMP) for screening malaria in peripheral and placental blood samples from pregnant women in Colombia. Malaria journal. 2018;17(1):262.
153. Hagiwara M, Sasaki H, Matsuo K, Honda M, Kawase M, Nakagawa H. Loop-mediated isothermal amplification method for detection of human papillomavirus type 6, 11, 16, and 18. Journal of medical virology. 2007;79(5):605-15.
154. Satoh T, Matsumoto K, Fujii T, Sato O, Gemma N, Onuki M, et al. Rapid genotyping of carcinogenic human papillomavirus by loop-mediated isothermal amplification using a new automated DNA test (Clinichip HPV). Journal of virological methods. 2013;188(1-2):83-93.
155. Edgar RC. MUSCLE: multiple sequence alignment with high accuracy and high throughput. Nucleic Acids Res. 2004;32(5):1792-7.
156. Olmedo-Nieva L, Munoz-Bello JO, Contreras-Paredes A, Lizano M. The Role of E6 Spliced Isoforms (E6*) in Human Papillomavirus-Induced Carcinogenesis. Viruses. 2018;10(1).
157. Kwok S, Kellogg DE, McKinney N, Spasic D, Goda L, Levenson C, et al. Effects of primer-template mismatches on the polymerase chain reaction: Human immunodeficiency virus type 1 model studies. Nucleic Acids Research. 1990;18(4):999-1005.
158. Ayyadevara S, Thaden JJ, Shmookler Reis RJ. Discrimination of Primer 3'-Nucleotide Mismatch by Taq DNA Polymerase during Polymerase Chain Reaction. Analytical Biochemistry. 2000;284(1):11-8.

159. Malpartida-Cardenas K, Miscourides N, Rodriguez-Manzano J, Yu LS, Moser N, Baum J, et al. Quantitative and rapid Plasmodium falciparum malaria diagnosis and artemisinin-resistance detection using a CMOS Lab-on-Chip platform. Biosens Bioelectron. 2019;145:111678.
160. Jamasb S. An analytical technique for counteracting drift in ion-selective field effect transistors (ISFETs). IEEE Sensors Journal. 2004;4(6):795-801.
161. Wang HY, Kim G, Cho H, Kim S, Lee D, Park S, et al. Diagnostic performance of HPV E6/E7, hTERT, and Ki67 mRNA RT-qPCR assays on formalin-fixed paraffin-embedded cervical tissue specimens from women with cervical cancer. Experimental and molecular pathology. 2015;98(3):510-6.
162. Heselmeyer-Haddad K, Sommerfeld K, White NM, Chaudhri N, Morrison LE, Palanisamy N, et al. Genomic amplification of the human telomerase gene (TERC) in pap smears predicts the development of cervical cancer. The American journal of pathology. 2005;166(4):1229-38.
163. Alameda F, Espinet B, Corzo C, Munoz R, Bellosillo B, Lloveras B, et al. 3q26 (hTERC) gain studied by fluorescence in situ hybridization as a persistence-progression indicator in low-grade squamous intraepithelial lesion cases. Human pathology. 2009;40(10):1474-8.
164. Caraway NP, Khanna A, Dawlett M, Guo M, Guo N, Lin E, et al. Gain of the 3q26 region in cervicovaginal liquid-based pap preparations is associated with squamous intraepithelial lesions and squamous cell carcinoma. Gynecologic oncology. 2008;110(1):37-42.
165. Zheng X, Liang P, Zheng Y, Yi P, Liu Q, Han J, et al. Clinical significance of hTERC gene detection in exfoliated cervical epithelial cells for cervical lesions. International journal of gynecological cancer : official journal of the International Gynecological Cancer Society. 2013;23(5):785-90.
166. Gurrala R, Lang Z, Shepherd L, Davidson D, Harrison E, McClure M, et al. Novel pH sensing semiconductor for point-of-care detection of HIV-1 viremia. Scientific reports. 2016;6:36000.
167. Francois P, Tangomo M, Hibbs J, Bonetti EJ, Boehme CC, Notomi T, et al. Robustness of a loop-mediated isothermal amplification reaction for diagnostic applications. FEMS Immunol Med Microbiol. 2011;62(1):41-8.
168. Barber RD, Harmer DW, Coleman RA, Clark BJ. GAPDH as a housekeeping gene: analysis of GAPDH mRNA expression in a panel of 72 human tissues. Physiological Genomics. 2005;21(3):389-95.
169. Zappacosta R, Sablone F, Pansa L, Buca D, Buca D, Rosini S. Analytic and Diagnostic Performances of Human Papillomavirus E6/E7 mRNA Test on up-to 11-Year-Old Liquid-Based Cervical Samples. A Biobank-Based Longitudinal Study. International journal of molecular sciences. 2017;18(7).
170. Luo L, Nie K, Yang MJ, Wang M, Li J, Zhang C, et al. Visual detection of high-risk human papillomavirus genotypes 16, 18, 45, 52, and 58 by loop-mediated isothermal amplification with hydroxynaphthol blue dye. Journal of clinical microbiology. 2011;49(10):3545-50.

CHAPTER 3 Validation of a novel lab-on-a-chip methodology using clinical samples

3.1 Introduction

A “see and treat” approach for cervical intraepithelial neoplasia at colposcopy sometimes identifies an early stage cervical cancer (Ia or small volume Ib1) where most of the tumour may have been excised by diagnostic knife cone biopsy or large loop excision of the transformation zone (LLETZ). However, it is important to establish the presence and extent of any residual disease as this crucially determines subsequent surgical management. Determining the presence and extent of residual tumour currently relies on high-resolution imaging. MRI is performed using an endovaginal receiver coil at my institution The Royal Marsden(4.3.3) to achieve high spatial resolution images and facilitate residual tumour delineation. Although the technique is highly sensitive, its specificity for tumours of <1.7cm^3 after cone biopsy or LLETZ is around 70% because of confounding appearances from scarring and fibrosis (91). Molecular information on the presence of tumour DNA or high-risk HPV DNA/RNA at the time of MRI could potentially increase the sensitivity and specificity for identifying small tumours.

Apart from the need for molecular technologies to supplement imaging in the early detection of cervical cancer, they also could aid decision making in later stage disease. In patients with larger volume disease treated with hysterectomy, it is vitally important to monitor the excision margin at the vaginal vault, as 70% of recurrences occur within the pelvis (171). Here, too, interpretation of MRI is

limited by scarring and fibrosis at the vaginal vault. With sensitive MRI techniques such as diffusion-weighted and R2* imaging, post-treatment, post-surgical or post radiation therapy appearances mean that the negative predictive value for diagnosing early recurrence is around 85% (172). However, even when done optimally (high field strength scanner, multichannel receivers), MRI only achieves a resolution of the order of several cubic millimeters, so that early recurrence is missed. In equivocal cases, repeat scans or biopsies are recommended. Moreover, lack of consensus over optimal surveillance methods following treatment of cervical cancer means that by the time they are recognized, recurrences are often late, symptomatic and difficult to manage. Thus, successfully developing molecular techniques that are translatable to the clinic could potentially positively influence not only the early detection of cervical cancer but also its management at multiple points in the patient pathway.

The work described in Chapter 2 shows the development and validation of the DNA and RNA tumour markers and demonstrates the accuracy of these molecular markers in *in vitro* and *ex vivo* systems. This work in this chapter focuses on translating the use of this technology into the clinic.

3.2 Aims

These were two-fold:

- Firstly, in a retrospective clinical study, to establish the value of HPV testing in addition to MRI for detecting cervical cancer prior to definitive surgical treatment.

- Secondly, in a prospective pilot clinical study, to establish the sensitivity and specificity of LOC assay for detecting cervical cancer (HPV DNA/RNA and hTERT TERC and Myc testing).
- I did this using cytology samples from patients with early stage (FIGO 2009 1b1 or earlier) cervical cancer referred for endovaginal MRI prior to fertility-sparing surgery and validated the results by comparing them with those from a conventional qPCR platform.
- I also established the diagnostic benefit of the LOC testing in patients with endovaginal MRI scans that were negative vs. positive for tumour.

3.3 Establishing the clinical value of HPV testing in addition to MRI for detecting cervical cancer prior to definitive surgical treatment

3.3.1 Retrospective clinical study

Between January 2010 and June 2019, the Royal Marsden Hospital Gynaecological surgery database recorded 257 cases who were treated surgically for cervical cancer (39 cone biopsies, 102 radical trachelectomies and 116 radical hysterectomies). Of these, 84 had a type specific DNA (n=82) and/or RNA (n=55) test (Abbott RealTi*m*e High Risk HPV DNA assay (173) and/or the PreTect HPV-Proofer E6/E7 mRNA assay (174) analysed by The Doctor's Laboratory Ltd) and 79 had an MRI prior to curative surgery (70 with an endovaginal coil).

Imaging was classed as positive or negative for tumour from the MRI report: tumour was regarded as being present if explicitly stated so on the report or if the report indicated that it was highly probable. All other cases were regarded as being negative for tumour on MRI. The reported tumour volume on MRI

(measured as the total tumour area delineated multiplied by the slice thickness) and the presence or absence of parametrial or lymph node involvement also was noted.

HPV DNA, HPV RNA and MRI performed at diagnosis individually had high sensitivity for detecting disease. MRI was the most sensitive (90.9%) followed by HPV DNA (88.2%) and RNA (87.2%). Removal of cases with residual high-grade dysplasia only (n=5) resulted in the sensitivity of MRI rising further to 96.2%. The DNA and RNA based tests revealed a superior specificity (80.8% and 81.8%) compared with MRI (30.4%) (Table 3.1).

Of the 16 cases in whom a false positive MRI was present, an HPV DNA test was available in 15. Of these, 14 (93%) were negative, so correctly predicting the absence of residual tumour. The mean volume of predicted tumour of the 16 false positive cases on MRI was 0.21cm^3 (range 0.02-0.8cm^3). This indicates the potential value of HPV DNA testing for confirming the presence or absence of residual disease in patients with low volume tumours on MRI.

	HPV DNA	HPV RNA	MRI
n=	82	55	79
False negative	6	5	5
True Positive	45	34	50
True negative	21	9	7
False positive	5	2	16
Sensitivity (%)	88.24	87.18	90.91
Specificity (%)	80.77	81.82	30.43
Positive predictive value (%)	90.00	94.44	75.76
Negative predictive value (%)	77.78	64.29	58.33

Table 3-1 Performance of HPV DNA/RNA typing and MRI for detecting cervical cancer following diagnostic cone biopsy/ LLETZ

3.3.2 Prospectively establishing the sensitivity and specificity of LOC technology using cytology samples

3.3.2.1 Study Design

The MODULAR (MOlecular Diagnostics Using a novel LAb-on-a-chip and MRI for detecting cervical cancer) study was a prospective pilot study designed and implemented by myself. It was conducted in accordance with the Declaration of Helsinki (1964), and local R&D, Ethics Committee and Health Research Authority (HRA) approval. Written informed consent was obtained from each patient. Patients were studied in 3 groups 1) new diagnosis of cervical cancer 2) recurrence of cervical cancer 3) non-cancer (normal) controls.

All patients with early cervical cancer referred to the Gynaecological Oncology Unit at The Royal Marsden Hospital and patients previously treated for early cervical cancer with evidence of recurrence on imaging were invited to participate. Women attending St George's Hospital "Test of cure" colposcopy clinic after a previous treatment for high grade CIN or a follow up 1 year after a diagnosis of CIN1, who were judged to have a normal cervix on colposcopic examination and confirmed to be HPV negative and cytological normal(were invited to participate. The HPV status of participants was known after recruitment had taken place and was a key determinant of the patients sample usage.

Inclusion criteria:

- Patients with early stage (FIGO 2009 Ib1 or earlier) cervical cancer (squamous or adenocarcinoma on histology) being considered for curative surgery.

- Patients treated for cervical cancer (squamous or adenocarcinoma on histology) with cytologically or histologically confirmed local recurrent disease.
- Patients with normal cervix at colposcopic examination.

Exclusion Criteria:

- MRI incompatibility Ferromagnetic metal implants, claustrophobia ()
- Neuroendocrine or unusual histological subtypes.
- Abnormal cervix seen at colposcopic examination (for Normal cervix cohort only).

Withdrawal criteria:

- Unable to obtain adequate cytology for assessment of tumour markers on lab-on-a-chip.
- Unable to obtain histology/ cytology for validation of tumour presence/ absence
- Inability to tolerate MRI examination.
- In Normal cohort - HPV positive cytology sample

A cervical specimen was taken using the Cervex broom-type brush and suspended in PreservCyt collection mediumeither at an out-patient visit or prior to an examination under anaesthesia (EUA) in all study subjects with cancer and stored as per manufacturers guidelines. In those patients with a normal cervix at colposcopy, the sample was taken as part of the colposcopic examination. The procedure involved the insertion of a speculum and taking a

swab from the cervix and/ or vaginal vault for tumour marker and HPV assessment. Additionally, a separate, sequential, cervical swab sample was examined conventionally to assess for cytology and HPV DNA and RNA typing as per Royal Marsden standard clinical practice.

3.3.2.2 Patient cohort

Between August 2018 and June 2019, 44 patients were prospectively recruited to the MODULAR study. 27 patients had newly diagnosed cervical cancer (primary disease), 3 patients had recurrent cervical cancer and 14 patients were non-cancer (normal) controls. Mean age and BMI were 35.1 years (range 25-51 years) and 23.7 (range 16.9-35.5) respectively.

In the primary disease group, initial diagnosis was made with a LLETZ in 20 patients and with punch biopsy in the remaining 7. Squamous cell carcinoma (SCC) was diagnosed in 17 patients and adenocarcinoma in 10 patients, with grade of disease distributed between well, moderate and poor differentiated in 5, 14 and 4 cases respectively (4 patients were not graded on histology). Lymphovascular space invasion was present in 7 cases, absent in 17 cases and not mentioned in 3. 8 patients had radical hysterectomy, 11 patients had radical trachelectomy two of which followed neoadjuvant chemotherapy, 6 patients had a cone biopsy and 2 patients underwent primary chemoradiotherapy following adverse findings at examination under anaesthesia.

Of the 27 cases with primary disease, 21 had tumour present on MRI (6 had no evidence of tumour on MRI). Of those with tumour present, 19 had surgery and 2 had primary chemoradiotherapy. Of 19 MRI positive patients who went to surgery, 17 were confirmed as containing tumour at subsequent surgical histology. Patients (n=4) who received either neoadjuvant chemotherapy or primary chemoradiotherapy had their study cervical swab taken prior to treatment and were included in the analysis on the basis of their positive diagnostic biopsies. In the 6 patients who were negative for tumour on MRI, 5 cases had no residual disease on histology and 1 case had residual disease. Therefore, there were 22 cases with primary disease that were positive for tumour (17 with positive MRI, 1 with negative MRI and 4 treated with neoadjuvant chemotherapy or chemoradiotherapy) (Figure 3.3)

As there were only 3 patients with recurrent disease, I combined the assessment of their tumour markers with the primary disease group. Therefore, the total number of patients with a positive diagnosis of cervical cancer were 25. The total number of patients with a diagnosis of cervical cancer but negative on final histology was 7 (2 positives on MRI and 5 negatives on MRI).

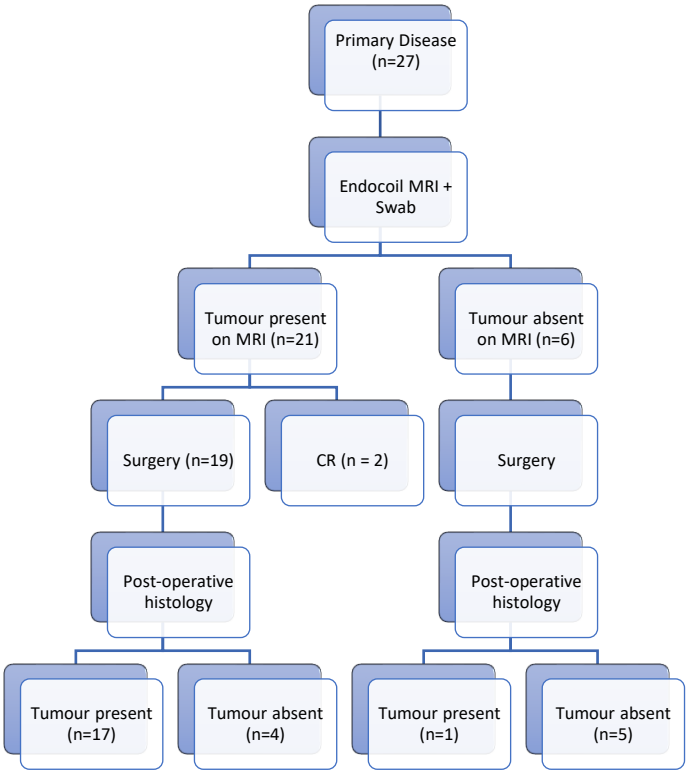

Figure 3-1 Management and histological status in patients with newly diagnosed cervical cancer recruited to the MODULAR study

3.3.2.3 DNA/ RNA marker yield

Following DNA/RNA extraction the mean yield of DNA and RNA was 31.79ng/uL and 57.37ng/uL respectively with a mean 260/280 ratio of 1.62 and 2.01 indicating pure RNA was successfully extracted albeit with likely contamination remaining in the DNA samples. The extracted nucleic acid yield was insufficient in 1 patient, so they were excluded from further analysis.

In the normal control group mean yield of DNA and RNA was 43.28ng/uL and 56.07ng/uL respectively with a mean 260/280 ratio of 1.28 and 1.98, suggesting

that RNA extraction was successful, however some contaminants remained in the DNA samples.

3.3.2.4 Comparing LOC assay with PCR assays

3.3.2.4.1 HPV

27 patients with newly diagnosed or recurrent cervical cancer had HPV typing performed by The Doctors Laboratory (TDL) The test used was the Abbott RealTi*m*e High Risk HPV DNA assay and/or the PreTect HPV-Proofer E6/E7 mRNA assay, which I considered to be the gold-standard. This PCR test assesses for 14 possible HR- HPV DNA types and 5 HR-HPV RNA types. This testing identified 19 patients who were positive for HPV DNA and/or RNA, (12 Type 16, 5 Type 18, 1 Type 45 and 1 Type 31). 7 patients were negative for the presence of HPV DNA or RNA and in 1 case the results of the test were missing. As the LOC analysis only tested for HPV type 16 and 18, the performance of HPV testing between the LOC assay and TDL PCR was assessed only for these subtypes. Patients who were positive for Type 45 and 31 were not included in the comparative analysis.

The comparative performance of the LOC assay HPV DNA and mRNA type specific markers with their TDL PCR counterparts showed that of the 12 HPV-16 cases detected by TDL PCR, 10 were detected with the LOC assay Type 16 DNA primers. In one case, the LOC was positive for HPV-16 with no HPV DNA detected on TDL PCR. Of the 10 HPV-16 mRNA detected by TDL PCR, 7 were detected by the LOC assay primers. Sensitivity and specificity for HPV-16 DNA

on LOC assay compared to TDL PCR was 83.3% and 75% respectively, and for HPV-16 RNA was 63.6% and 100% respectively.

The HPV 18 DNA pH-LAMP primers agreed with the 5 positive TDL PCR Type 18 cases, however there was evidence of primer-dimer formation in PCR negative cases. True Type 18 cases were positive in less than 8 minutes but typically showed primer-dimer formation after 20 minutes. The LOC assay Type 18 mRNA detected all 5 Type 18 mRNA detected by the TDL PCR. There were no false positives on LOC assay HPV-18 mRNA.

3.3.2.4.2 Tumour markers

With hTERT the PCR test agreed with the findings from the hTERT LOC assay in all but two samples. The TERC/GAPDH DNA copy number PCR test was only successfully recorded in 19 of 28 samples and 9 of these had either differing technical replicates or a wide standard deviation between replicates. Similarly, with the MYC PCR assay a result wasn't recorded in 6 samples and had differing technical replicates or with wide standard deviation in 10 cases.

3.3.2.5 Sensitivity and specificity of LOC assay and MRI for cancer detection

MYC/GAPDH relative expression was recorded in all 28 patients on LOC assay and achieved a sensitivity of 58.8% and a specificity of 100% at a threshold relative expression of 0.155 for tumour detection. (Figure 3.4)

Relative TERC/GAPDH DNA copy number was successfully recorded in 24 cases on LOC and achieved a sensitivity of 40% and specificity of 100% for tumour detection. (Figure 3.5)

hTERT recorded a result in only 14 cases on the LOC test. In the normal controls it was positive at the outer limit of detection in 7 cases with a mean Ct of 42.9 minutes. Therefore, this was used as a Ct threshold for a positive result in the cervical cancer cases where it yielded a sensitivity of 45.5% and specificity of 100% for tumour detection.

To evaluate the performance of the combined markers within the LOC assay in detecting residual disease two scenarios were applied. In the first, tumour was considered present if any tumour marker was present with or without HPV positivity and tumour absent if all tumour markers were absent regardless of the presence or not of HPV. Using these criteria, the LOC assay correctly predicted the presence of 14 tumours (true positive) and missed 4 tumours (false negative). There were 10 correct predictions of no residual disease (true negative) and no tumours incorrectly predicted as being present (false positive). This gave the LOC assay a sensitivity of 77.8%, specificity of 100%, positive predictive value of 100% and a negative predictive value of 71.4%. In the second scenario, tumour was considered present if any tumour marker or HPV was present, and tumour was considered absent if all tumour markers and HPV were absent. Using these criteria, the LOC scheme correctly predicted the presence of 17 tumours (true positive) and missed 1 tumour (false negative). There were 7 correct predictions of no residual disease (true negative) and 3 tumours incorrectly predicted as being present (false positive). This gave the LOC assay a sensitivity of 94.4%, specificity of 70%, positive predictive value of 85% and a negative predictive value of 87.5%.

Endovaginal MRI correctly predicted the presence of 15 tumours (true positive) and missed 1 tumour (false negative). There were 4 correct predictions of no residual disease (true negative) and 4 tumours incorrectly predicted as being present (false positive). This gave the MRI a sensitivity of 93.8%, specificity of 50%, positive predictive value of 78.9% and a negative predictive value of 80%.

3.3.3 Establishing the diagnostic benefit of the LOC testing in patients with endovaginal MRI scans that are negative vs. positive for tumour

In the MR positive patients, 3 patients were negative on all tumour marker and HPV tests, correctly recognising 2 of the 4 false positives on MRI. In the MRI negative patients, 3 patients were positive on at least 1 tumour marker or HPV test, correctly recognising the single false negative case on MRI. Taken together therefore MRI and LOC correctly identified tumour in 15 of 16 cases and excluded it in 5 of 8 cases.

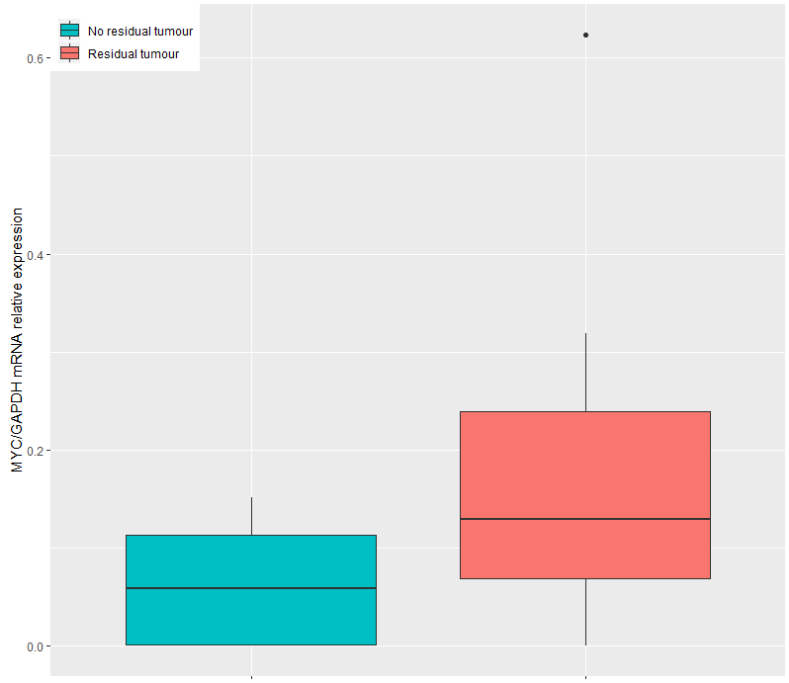

Figure 3-2 Boxplot of relative expression of MYC/GAPDH mRNA between normal and residual tumour group

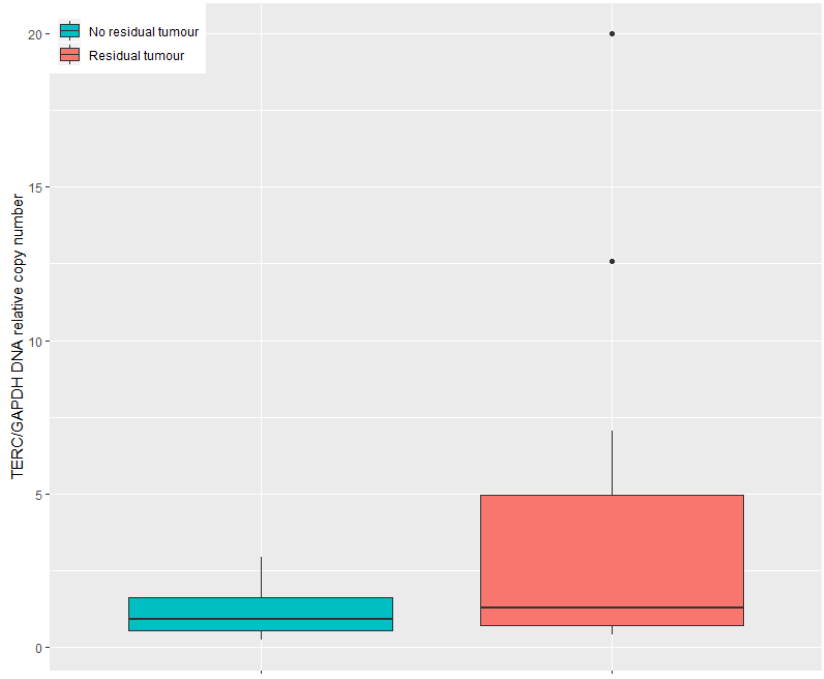

Figure 3-3 Boxplot of relative copy number of TERC to GAPDH DNA in no residual tumour and residual tumour group

3.4 Discussion

This data indicates the feasibility of performing HPV and tumour marker testing using LOC technology and indicates its current accuracy in comparison to standard PCR systems. The ability to perform multiple marker testing at point-of-care demonstrates the added value of this type of molecular testing in the diagnostic pathway of patients with early stage, small volume cervical cancers following cone biopsy or LLETZ, who undergo MRI for determining the presence and extent of residual disease prior to definitive surgery. The time to positive (TTP) of less than 25 minutes on the LOC platform for all tests further demonstrates the true point-of-care potential of this system to deliver rapid, accurate results in a portable platform.

3.4.1 Added value of HPV testing in diagnostic pathway of cervical cancer

In the last decade advances in reducing the burden of cervical cancer have been made. The HPV vaccination programme and switching to primary HPV screening present opportunities to dramatically reduce if not extinguish cervical cancer in the decades to come (175). Cytological assessment has previously been the mainstay but suffers from a poor false negative rate, with evidence that almost 30% of invasive carcinomas follow a falsely negative cytology result (29). HPV DNA testing is very sensitive (~95%) but lacks the specificity (30-50%) required to be used as a sole screening tool to determine treatment(176). However, with appropriate triage tests initial evidence from large randomised trials suggest a 60-70% protection is conferred with HPV DNA screening

compared with cytology alone and may allow an extension of the screening interval to 5 years (46, 177)

There are a wide range of commercially available HPV detection assays which are based on different techniques such as target amplification (mainly PCR), signal amplification, and probe amplification (178). There are a dozen HPV assays which have been clinically validated either through randomised trials or international equivalency criteria (48, 49, 179). HPV E6/E7 mRNA tests (as described here) have superior specificity to HPV DNA tests (176). Overexpression of HPV E6 and E7 mRNAs has been evaluated as a marker for the transition from a productive infection to an abortive infection that eventually promotes cell transformation.

Approaches also have been adopted to combine HPV DNA testing with cytology (180) to optimise the sensitivity and specificity of cancer detection and to avoid overload of colposcopy services given the relatively high prevalence in the 25-30 year old group. In the UK screening programme for example, a HPV DNA positive result is followed by a cytology analysis and if this is abnormal colposcopy is performed. If the cytology is normal a re-screen in performed in 12 months. If HPV persistence remains at 2 years or reflex cytology is abnormal at each stage a referral to colposcopy is made.. Alternative triage strategies include HPV genotyping to determine HPV 16/18 status as these types are associated most often with CIN2+, especially in younger women. This approach, however is not likely to be useful for older women as other HPV types are typically related to CIN2+ (181).

In these cases, utilization of HPV mRNA might provide substantial improvements in specificity for cancer detection in patients at high risk of invasive disease.

In areas with limited cervical screening programmes and without the high quality, well-resourced colposcopic service seen in developed countries, however, the benefit of a rapid, low-cost, point-of-care approach to cervical screening could potentially be transformational. It would provide the opportunity for developing countries to skip over several hurdles which developed countries have encountered in establishing their screening programmes (182). An approach utilising a LOC which would allow for rapid determination of HPV DNA status with genotyping available may well provide an excellent solution in low-resource settings. The potential ability to deliver molecular based triage tests would allow an opportunity to improve the specificity of the HPV DNA test and reduce the overtreatment rate in a test and treat programme (33, 183).

3.4.2 Utility of tumour marker testing in cervical cancer

The three pH-LAMP tests (hTERT mRNA, MYC mRNA and TERC DNA) each had poor sensitivity but excellent specificity for predicting the presence of residual tumour. The need for three pH-LAMP nucleic tests is warranted to cover a range of possible scenarios; comparison between these showed that all 3 were positive in 1 case, 2 were positive in 6 cases and 1 was positive in 7 cases. The poor sensitivity of the tumour marker tests is counteracted by having the HPV markers included on the chip, as their sensitivity for detecting cancer was high. Jointly utilising HPV and tumour marker testing and interpreting the tumour marker status on those with positive HPV results would help differentiate

the true positives from those with an indeterminate result that require further investigation. Conversely, it is also true that the few false negative cases seen with HPV DNA testing may be successfully detected by a positive tumour marker status.

Other markers could be considered for inclusion on multiplexed chip technology in future. Because the expression of HPV viral E7 leads to an increase of cyclin-dependent kinase inhibitor p16 (p16INK4a), p16 would be a possible candidate. However, as p16 overexpression, fundamentally is a marker of HPV infection, I chose not to select it for the current study. It provides a similar sensitivity and specificity profile to the HPV markers. A meta-analysis of seventeen studies showed a pooled sensitivity and specificity of p16INK4a to detect CIN2 or worse in patients with squamous intraepithelial lesions was 83.8% and 65.7% respectively (184).

DNA methylation of several human genes has been shown to be also a relevant event for cervical carcinoma development. The use of differential methylation hybridization using a pilot methylation array allowed the identification of SOX1, NKX6-1, PAX1, WT1, and LMX1A as frequently methylated genes in cervical cancer and precursor lesions(185) . In future, optimal marker selection and methods to identify DNA methylation may substantially improve the sensitivity of the tumour marker testing.

3.4.3 Patient recruitment limitations

Recruitment of patients with newly diagnosed cervical cancer and those with a diagnosis of no disease was straightforward in an oncology or colposcopy clinic respectively and exceeded expectation. The patients were recruited over 10

months. However, recruitment of patients with recurrent disease was more difficult. This was largely due to the smaller numbers of patients with recurrent disease referred for surgical treatment, and the difficulty with obtaining consent for a diagnostic study at a time in the patient pathway when they were receiving devastating news about the recurrence of their disease. I approached 6 patients with recurrent cancer, 3 of whom agreed. Additional vaginal examinations and swabs from patients post radiation therapy is also uncomfortable and seen by many patients as an unacceptable added intervention. In future, obtaining this material at the time of pelvic exenteration may be more clinically acceptable. Amalgamation of the newly diagnosed and recurrent cervical cancer into a single group meant that the assessment of this technique for diagnosing recurrent disease *per se* could not be established.

3.5 Summary

- The sensitivity and specificity of HPV 16 and 18 DNA and RNA compared to MRI for early detection of cervical cancer has been established in a retrospective study (HPV DNA 88.2% and 80.8%; HPV RNA 87.2% and 81.8% and MRI 96.2% and 30.4%)
- The LOC LAMP assays have been prospectively trialled using cytology samples from patients with newly diagnosed and recurrent cervical cancer and in normal controls.
- The sensitivity and specificity for HPV-16 DNA on LOC assay compared to TDL PCR was 83.3% and 75% respectively, and for HPV-16 RNA was 63.6% and 100% respectively.

- The sensitivity for hTERT, TERC and MYC were 45.5, 40.0 and 58.8% respectively and specificities were 100%, 100% and 100% respectively.
- The addition of LOC testing to endovaginal MRI in Stage 1b1 or earlier cervical cancer reduced the identification of false negative and false positive cases.

3.6 References

29. Spence AR, Goggin P, Franco EL. Process of care failures in invasive cervical cancer: systematic review and meta-analysis. Preventive medicine. 2007;45(2-3):93-106.
33. Kelly H, Mayaud P, Segondy M, Pant Pai N, Peeling RW. A systematic review and meta-analysis of studies evaluating the performance of point-of-care tests for human papillomavirus screening. Sexually Transmitted Infections. 2017;93(S4):S36-S45.
46. Ronco G, Dillner J, Elfström KM, Tunesi S, Snijders PJ, Arbyn M, et al. Efficacy of HPV-based screening for prevention of invasive cervical cancer: follow-up of four European randomised controlled trials. Lancet. 2014;383(9916):524-32.
48. Meijer CJ, Berkhof H, Heideman DA, Hesselink AT, Snijders PJ. Validation of high-risk HPV tests for primary cervical screening. Journal of clinical virology : the official publication of the Pan American Society for Clinical Virology. 2009;46 Suppl 3:S1-4.
49. Arbyn M, Snijders PJ, Meijer CJ, Berkhof J, Cuschieri K, Kocjan BJ, et al. Which high-risk HPV assays fulfil criteria for use in primary cervical cancer screening? Clinical microbiology and infection : the official publication of the European Society of Clinical Microbiology and Infectious Diseases. 2015;21(9):817-26.
91. Downey K, Jafar M, Attygalle AD, Hazell S, Morgan VA, Giles SL, et al. Influencing surgical management in patients with carcinoma of the cervix using a T2- and ZOOM-diffusion-weighted endovaginal MRI technique. British journal of cancer. 2013;109(3):615-22.
171. Peiretti M, Zapardiel I, Zanagnolo V, Landoni F, Morrow CP, Maggioni A. Management of recurrent cervical cancer: a review of the literature. Surg Oncol. 2012;21(2):e59-66.
172. Mahajan A, Engineer R, Chopra S, Mahanshetty U, Juvekar SL, Shrivastava SK, et al. Role of 3T multiparametric-MRI with BOLD hypoxia imaging for diagnosis and post therapy response evaluation of postoperative recurrent cervical cancers. Eur J Radiol Open. 2016;3:22-30.
173. Hesselink AT, Meijer CJLM, Poljak M, Berkhof J, van Kemenade FJ, van der Salm ML, et al. Clinical validation of the Abbott RealTime High Risk HPV assay according to the guidelines for human papillomavirus DNA test requirements for cervical screening. Journal of clinical microbiology. 2013;51(7):2409-10.
174. Ratnam S, Coutlee F, Fontaine D, Bentley J, Escott N, Ghatage P, et al. Clinical performance of the PreTect HPV-Proofer E6/E7 mRNA assay in comparison with that of the Hybrid Capture 2 test for identification of women at risk of cervical cancer. Journal of clinical microbiology. 2010;48(8):2779-85.
175. Simms KT, Steinberg J, Caruana M, Smith MA, Lew J-B, Soerjomataram I, et al. Impact of scaled up human papillomavirus vaccination and cervical screening and the potential for global elimination of cervical cancer in 181 countries, 2020–99: a modelling study. The Lancet Oncology. 2019;20(3):394-407.
176. Arbyn M, Ronco G, Anttila A, Meijer CJ, Poljak M, Ogilvie G, et al. Evidence regarding human papillomavirus testing in secondary prevention of cervical cancer. Vaccine. 2012;30 Suppl 5:F88-99.
177. Rebolj M, Rimmer J, Denton K, Tidy J, Mathews C, Ellis K, et al. Primary cervical screening with high risk human papillomavirus testing: observational study. BMJ (Clinical research ed). 2019;364:l240.
178. Luhn P, Wentzensen N. HPV-based Tests for Cervical Cancer Screening and Management of Cervical Disease. Curr Obstet Gynecol Rep. 2013;2(2):76-85.
179. Arbyn M, Depuydt C, Benoy I, Bogers J, Cuschieri K, Schmitt M, et al. VALGENT: A protocol for clinical validation of human papillomavirus assays. Journal of clinical virology : the official publication of the Pan American Society for Clinical Virology. 2016;76 Suppl 1:S14-s21.

180. Tornesello ML, Buonaguro L, Giorgi-Rossi P, Buonaguro FM. Viral and cellular biomarkers in the diagnosis of cervical intraepithelial neoplasia and cancer. Biomed Res Int. 2013;2013:519619.
181. Tidy JA, Lyon R, Ellis K, Macdonald M, Palmer JE. The impact of age and high-risk human papillomavirus (hrHPV) status on the prevalence of high-grade cervical intraepithelial neoplasia (CIN2+) in women with persistent hrHPV-positive, cytology-negative screening samples: a prospective cohort study. Bjog. 2020.
182. Jeronimo J, Bansil P, Lim J, Peck R, Paul P, Amador JJ, et al. A Multicountry Evaluation of careHPV Testing, Visual Inspection With Acetic Acid, and Papanicolaou Testing for the Detection of Cervical Cancer. International Journal of Gynecological Cancer. 2014;24(3):576-85.
183. Campos NG, Tsu V, Jeronimo J, Mvundura M, Kim JJ. Estimating the value of point-of-care HPV testing in three low- and middle-income countries: a modeling study. BMC cancer. 2017;17:791.
184. Roelens J, Reuschenbach M, von Knebel Doeberitz M, Wentzensen N, Bergeron C, Arbyn M. p16INK4a immunocytochemistry versus human papillomavirus testing for triage of women with minor cytologic abnormalities: a systematic review and meta-analysis. Cancer cytopathology. 2012;120(5):294-307.
185. Lai HC, Lin YW, Huang TH, Yan P, Huang RL, Wang HC, et al. Identification of novel DNA methylation markers in cervical cancer. Int J Cancer. 2008;123(1):161-7.

CHAPTER 4 Prognostic biomarkers in low volume cervical cancers suitable for trachelectomy: utilising radiomic features derived from T2- and diffusion-weighted MRI

4.1 Introduction

4.1.1 Prognostic biomarkers in early stage, low volume cervical tumours suitable for trachelectomy

Stage 1 cervical cancer is primarily treated with hysterectomy, although less radical surgical options (cone biopsy, trachelectomy) are considered where fertility preservation is desirable (186-189). Decisions regarding the type and extent of surgery and the subsequent need for adjuvant therapy depend on tumour resectability and the risk of recurrence. Biomarkers that predict more advanced disease (parametrial extension, lymph node metastasis) and recurrence are of paramount importance for selecting the most appropriate treatment options. In tumours >2cm in longest dimension, pre-operative tumour volume is a powerful adverse prognostic factor associated with reduced overall survival (190, 191). Other prognostic factors, such as tumour type, grade, lymphovascular space invasion (LVSI) and depth of stromal invasion are derived from a biopsy (192-195), and therefore may not represent the tumour in its entirety.

4.1.2 Potential of imaging-derived prognostic biomarkers

Prognostic biomarkers derived from imaging a cervical tumour would be more representative of the whole tumour and so are potentially preferable or additive to information from biopsy. They have potential to provide prognostic information and enable selection of the optimal surgical management at the outset in Stage 1 disease.

Magnetic Resonance imaging is routinely used to detect and stage cervical cancer, where T2-W and diffusion-weighted (DW) imaging form the mainstay of diagnostic sequences (79, 196). Derivation of an apparent diffusion coefficient (ADC) from the DW images (85) and analysis of first order histogram distribution of ADC values has been shown to predict histological subtype (86, 87), staging (88), parametrial invasion (89), LVSI (90) the response to chemo-radiotherapy (197) and to aid surgical decision-making (91). However, these first-order statistical quantitative imaging data remain limited in their prediction of likely recurrence (92). It is possible to refine image analysis and convert the T2-W (93) and DW (94) imaging data into a high-dimensional feature space using algorithms to extract a more extensive set of statistical features within the data. This type of analysis, referred to as “radiomics” (cf 1.7), requires that the data have a high signal-to-noise ratio to reduce error in the analysis from image noise; this is achievable in cervical cancer using an endovaginal MRI technique (95).

4.2 Aim

To identify radiomic features of cervical cancers on endovaginal MRI that differ between tumours below and above the volume threshold of eligibility for

trachelectomy (less or greater than 4.19 cm^3, equivalent to a 2cm diameter spherical tumour volume) and to determine their value in predicting lymph node metastasis and recurrence in patients in the low-volume tumour group. A 2cm diameter tumour is typically the threshold for fertility sparing surgery such as trachelectomy (187).

4.3 Methods

4.3.1 Study Design

I analysed data from a single-institution that recruited patients prospectively within an institutional review board (IRB) approved research study to document imaging features of cervical cancer indicative of poor outcome. (NCT01937533). This included patients with histologically confirmed cervical cancer, presumed Stage 1 or 2 (FIGO 2009 (52). Patients were imaged with an endovaginal MRI technique between March 2011 and October 2018 and were potentially suitable for surgical management (trachelectomy or hysterectomy). All patients gave written consent for use of their data. All patients were treated with curative intent with either surgery or chemoradiation following MRI and staging investigations. Surgical options included cold-knife cone, trachelectomy or hysterectomy depending on their suitability for fertility preservation and their desire for continued fertility. A pelvic lymphadenectomy was performed in all cases.

Clinico-pathological metrics recorded in each case were tumour volume, type, grade, LVSI, parametrial invasion, Depth of Invasion and lymph node metastasis. Patients were followed up for median of 35 months (3-92). Median time to recurrence was 7 months (3-62 months).

4.3.2 Study participant selection

378 consecutive patients were imaged over the defined study period. In 98 cases, tumour was not identified on MRI while in 127 cases tumour was poorly identified and volume was <0.07 cm^3, (62 of these had negative histology). Of the remaining 153 patients, 10 had non-cervical origin tumours on histology, 12 had histology other than squamous or adenocarcinoma (clear cell or neuroendocrine histology), 2 had metastatic disease, in 3 the whole tumour was not within the imaged field-of-view, and 1 did not have a diffusion-weighted images (**Figure 4.1**). These 28 exclusions resulted in 125 patients with histologically confirmed residual squamous-or adeno carcinomas that could be defined on MRI and were therefore eligible for analysis. No patients had to be excluded on the grounds of image artefact degrading the data. In patients who underwent primary surgery, the post-operative histological diagnosis was taken as the gold-standard. In those who received chemoradiation therapy, their pre-treatment histological diagnosis was taken as the gold-standard. In assessing lymph node status, surgical pathology was the reference gold-standard in those undergoing surgery, and imaging (MRI or PET-CT) was the reference gold-standard in those treated with chemoradiation.

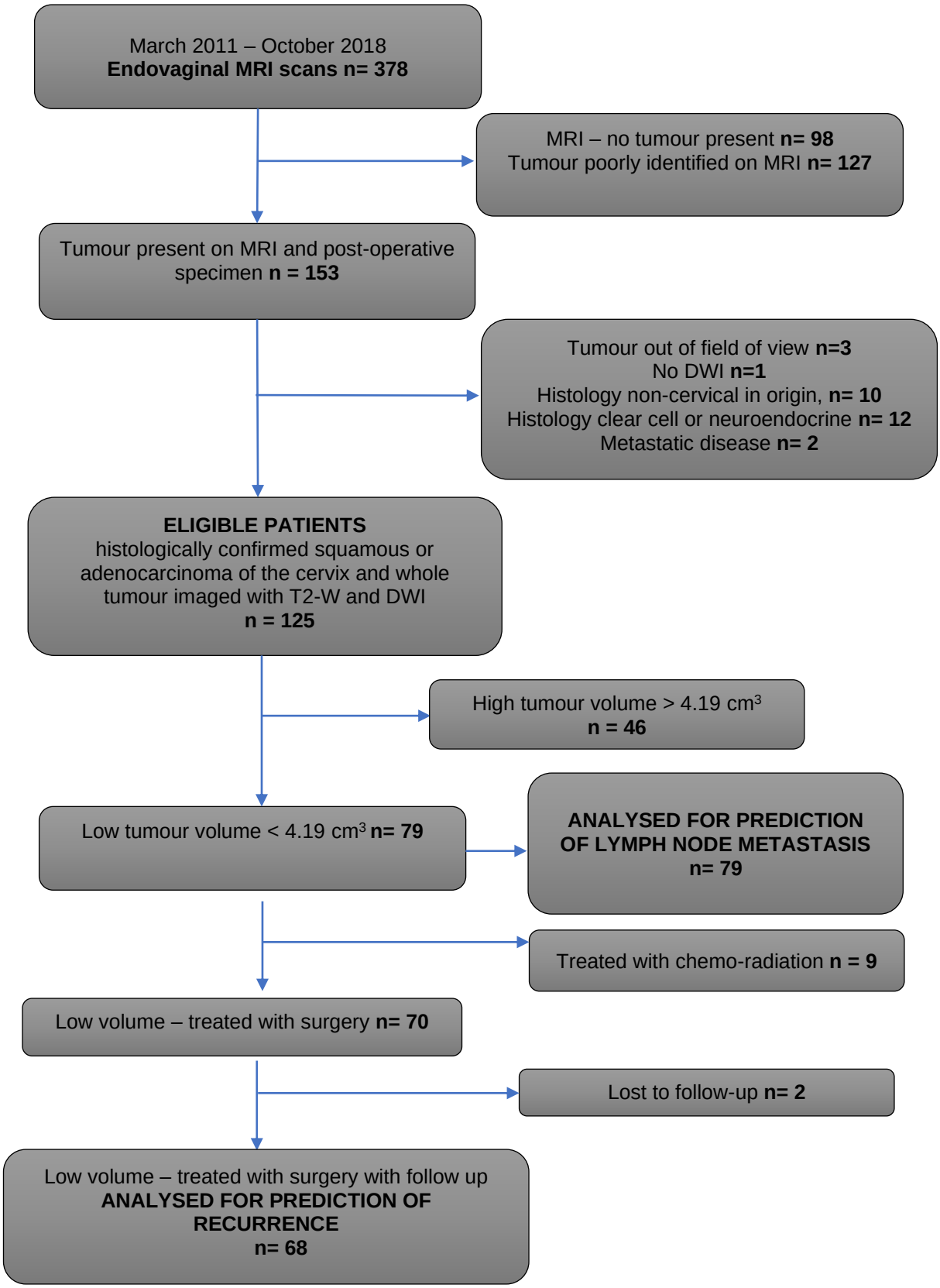

Figure 4-1 Flow chart of study criteria

4.3.3 MRI

4.3.3.1 Scanning procedure

All scans were performed on a 3.0 Tesla Philips Achieva (Best, The Netherlands) with a dedicated in-house developed 37 mm ring-design solenoidal receiver coil that has been previously described and extensively used for assessing early stage cervical cancer at the Royal Marsden Hospital (**Figure 4.2**) (20, 21, 24).

Figure 4-2 Ring design solenoidal Endovaginal receiver coil used for imaging

Cervical position was determined at vaginal examination, after which the coil was inserted and placed around the cervix by the radiologist. Image distortion from susceptibility artefacts were reduced by aspiration of vaginal air via a 4 mm diameter tube (Ryles; Pennine Healthcare, London, England). The administration of Hyoscine butyl bromide (Buscopan) 20 mg IM decreased artefacts from bowel peristalsis.

4.3.3.2 MRI protocol

T2-W images were obtained in three planes orthogonal to the cervix: TR/TE 2750/80 ms (coronal and axial) and 2500/80 ms (sagittal); field of view (FOV) 100 mm x 100 mm; acquired voxel size 0.42 x 0.42 x 2 mm; reconstructed voxel size 0.35 x 0.35 x 2 mm; slice thickness 2 mm; slice gap 0.1 mm; 24 coronal and 22 sagittal slices; number of signal averages (NSA) 2. Additionally,

matched Zonal Oblique Multislice (ZOOM) diffusion-weighted images (DWI) were acquired: TR/TE 6500/54 ms; b-values 0, 100, 300, 500, 800 s/mm^2; FOV 100 x 100 mm; acquired voxel size 1.25 x 1.25 x 2 mm; reconstructed voxel size 0.45 x 0.45 x 2 mm; slice thickness 2 mm, slice gap 0.1 mm; 24 slices, NSA 1. ADC maps were automatically generated by the scanner software. These were compared with T2-W images to identify the presence and extent of a tumour within the cervix. Mass-lesions disrupting the normal cervical epithelial architecture that were intermediate signal-intensity on T2-W images with corresponding restriction on the ADC maps were recognized as tumour (**Figure 4.3**).

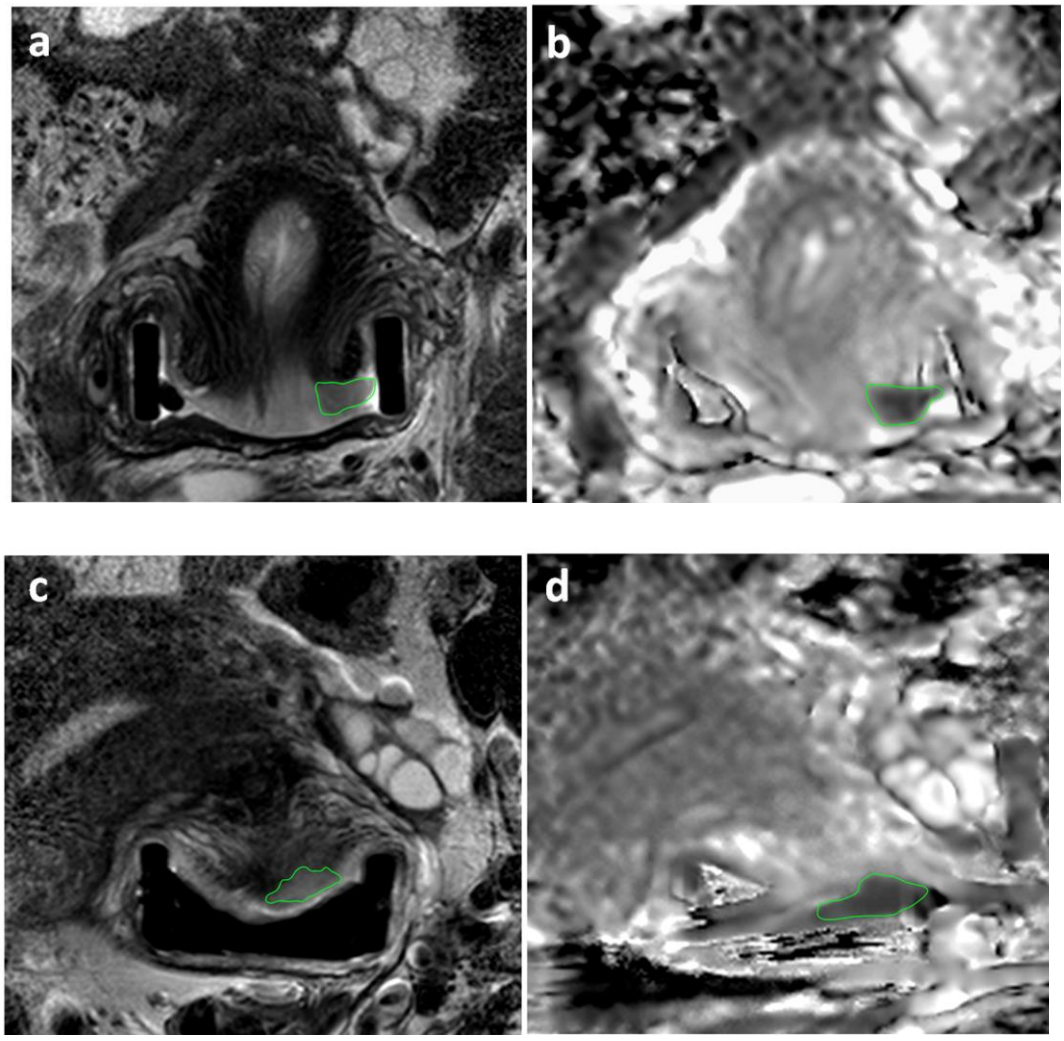

Figure 4-3 T2-W (a) and ADC map (b) in a 33- year old patient with a 0.8 cm3 volume tumour that had high dissimilarity (0.808). Regions-of-interest delineate the tumour. The intermediate signal-intensity tumour on the T2-W imaging (arrow) is restricted in diffusion on the ADC maps (arrow). Tumour was confined to the cervix, and the patient remains disease-free following trachelectomy. T2-W (c) and ADC map (d) in a 26 year old patient with a 0.9 cm^3 volume tumor that had low dissimilarity (0.489). The intermediate signal-intensity tumor on the T2-W imaging (c) is restricted in diffusion on the ADC maps (d). Regions-of-interest delineate the tumor. Tumor was confined to the cervix, but despite negative nodes on surgical histology, the patient recurred centrally after 9 months.

4.3.3.3 Analysis: extraction of texture features

Scans were anonymised (DicomBrowser, Neuroinformatics Research Group, Washington University, St Louis, MO) and transferred to an XNAT(198, 199) image repository. Images were imported into OsiriX (Pixmeo SARL, Bernex, Switzerland) and 2D regions-of-interest (ROI) were drawn by a radiologist, (25 years' experience) on the coronal T2-W and ADC maps on every slice demonstrating tumour (**Figure 4.3**). 2D ROI contours were aggregated using a

custom Python script, integrated into OsiriX via pyOsirix (200) and exported as a single 3D volume (VOI) in DICOM RT-STRUCT format, which was then uploaded to XNAT. Custom in-house software (MATLAB, MathWorks, Natick, MA) was used to extract Grey Level Co-occurrence Matrix (GLCM) features (Haralick texture analysis (201, 202)) from the both the T2-W images and ADC maps.

4.3.4 Statistical analysis

Statistical analysis was performed with *R* (R Core Team (2019), Vienna, Austria. http://www.R-project.org). Correlations between features indicated 10 distinct feature clusters by creating a dissimilarity measure from a distance matrix (**Figure 4.4**).

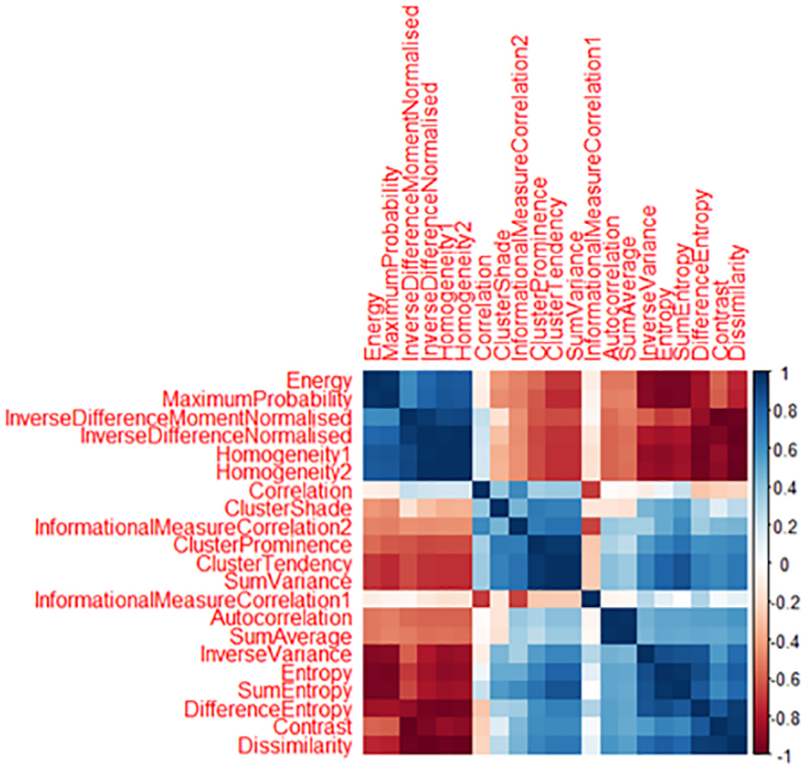

Figure 4-4 Heatmap of correlations between Haralick features

Several of the texture features were very highly correlated (r=0.97-1) and were successfully clustered. The feature with the greatest dynamic range from each cluster was selected for investigation (**Table 4.1**): these were Dissimilarity, Contrast, Energy, Entropy, ClusterProminence, ClusterShade, InverseVariance, Correlation, Autocorrelation and InformationalMeasureCorrelation2. Contrast and Entropy, although not clustered with Dissimilarity and Energy respectively, were highly correlated (R>0.9), and were removed.

Texture feature colour coded by cluster	**Dynamic range**
InverseVariance	**14.18**
Energy	**13.43**
MaximumProbability	7.62
Entropy	**4.87**
SumEntropy	4.24
Autocorrelation	**8.05**
SumAverage	2.95
Contrast	**106.39**
InverseDifferenceMomentNormalised	1.06
Dissimilarity	**39.41**
DifferenceEntropy	11.29
Homogeneity2	2.11
Homogeneity1	1.89
InverseDifferenceNormalised	1.17
Correlation	**16.47**
InformationalMeasureCorrelation1	0.13
ClusterShade	**-2.52**
ClusterProminence	**177.40**
ClusterTendency	36.30
SumVariance	36.30
InformationalMeasureCorrelation2	**3.14**

Table 4-1 Clusters of Haralick features that are significantly correlated and their dynamic ranges

A Shapiro-Wilk test was performed to test for normality. Features did not have a normal distribution were compared with non-parametric tests. A Mann-Whitney (*U*) test with Bonferroni correction was applied to assess the differences in texture features between tumours greater than or less than 4.19 cm^3 on T2-W imaging (volume threshold of eligibility for trachelectomy, designated as high-volume and low-volume tumours). A p-value <0.05 was taken to be significant. Stepwise logistic regression was used to determine which combination of features from each category (ADC-radiomics, T2-W-radiomics and clinico-pathological metrics) were indicative of lymph node metastasis or recurrence. The recurrence analysis was done in 2 scenarios i) in all patients with low-volume tumours using adjuvant therapy as a feature in the model; ii) in only those patients who did not receive adjuvant therapy. The logistic regression coefficients were used to combine the features identified from each scenario to generate Receiver operating characteristic (ROC) curves for ADC-radiomic features and for T2-W radiomic features predicting recurrence in low-volume tumours. These were compared with the ROC curve of the clinico-pathological features identified in both scenarios using the Akaike information criteria (AIC). Further improvements in predicting recurrence were investigated by combining the features identified in the ADC-radiomic and T2-W radiomic models with the clinico-pathological features and evaluated with a Chi-square test. A bootstrap resampling (n=1000) procedure was performed to obtain estimates of optimism in the regression models to provide a bias-corrected AUC value through a Somers' D rank correlation metric whereby AUC = (1 + Somers D)/2. The rms: Regression Modelling Strategies R package, version 5.1-0 was used.

4.4 Results

4.4.1 Patient demographics and clinical characteristics

Eligible patients were aged between 24-89 years (mean 38.4 years) at primary treatment. Initial diagnosis was made with biopsy in 77 patients and large loop excision of the transformation zone (LLETZ) in 48 patients. Biopsies confirming the presence of cancer were not large or deep enough to confirm tumour grade in 1 case or LVSI in 7.

Of 125 patients, 79 were low-volume (range 0.26 – 4.17 cm^3, mean 1.3 ± 1.2 cm^3); 70 were treated surgically and 9 with chemoradiation. Forty-six were high-volume (range 4.2-56.1 cm^3, mean 15.3 ± 11.7 cm^3); 7 were treated surgically and 39 with chemoradiation. Of the 79 patients with low-volume tumours 70 were treated surgically, 2 patients did not have follow-up data, so that prediction of lymph node metastases was modelled on 79 patients and recurrence was modelled on 68 patients (**Figure 4.1**). Patient and tumour characteristics in those with high- and low-volume tumours are detailed in **Table 4.2**.

For the recurrence analysis, 54 of 68 patients in the low-volume group did not receive adjuvant therapy. Fourteen patients in the low-volume group received adjuvant therapy following surgery because of adverse features: 5 had unexpected lymph node metastases, 3 had unexpected extension of tumour to the parametrium, 1 had a 0.5 mm margin to the parametrium at surgical histology, 1 had spread to the vaginal cuff and 4 met 2 of the Sedlis criteria (LVSI) and deep stromal invasion). There were 7 recurrences overall: 5 in 54 patients who had not and 2 in14 in patients who had received adjuvant therapy.

	All tumours n=125	High volume >4.19cm^3 n=46	Low volume <4.19cm^3 n=68 (Recurrence)	Low volume <4.19cm^3 n=79 (Lymph node)
Age, mean (range)	38.4 (65.0)	43.0 (64.0)	35.5 (38.0)	35.6 (38.0)
BMI, mean (range)	25.7 (36.3)	26.2 (36.3)	25.5 (32.6)	25.4 (32.9)
FIGO stage, n				
1	59.2 (74)	5	91.2 (62)	87.3 (69)
2	40.8 (51)	41	8.8 (6)	12.7 (10)
Histological subtype, %				
Squamous	61.6 (77)	78.3 (36)	51.5 (35)	51.9 (41)
Adenocarcinoma	38.4 (48)	21.7 (10)	48.5 (33)	48.1 (38)
Grade % patients (n)				
1 or 2	55.2 (69)	52.2 (24)	57.4 (39)	57.0 (45)
3	43.2 (54)	43.5 (20)	42.6 (29)	43.0 (34)
Unknown	1.6 (2)	4.3 (2)	0	0
LVSI, % patients (n)				
Positive	27.2 (34)	15.2 (7)	35.3 (24)	34.2 (27)
Negative	65.6 (82)	67.4 (31)	64.7 (44)	64.6 (51)
Unknown	7.2 (9)	17.4 (8)	0	1.2 (1)
Depth of Invasion,	7.1 (20.4)	6.0 (19.0)	7.3 (20.4)	7.4 (20.4)
Parametrial invasion %				
Positive	32.8 (41)	76.1 (35)	4.4 (3)	7.6 (6)
Negative	67.2 (84)	23.9 (11)	95.6 (65)	92.4 (73)
Lymph node				
Positive	31.2 (39)	58.7 (27)	8.8 (6)	15.2 (12)
Negative	68.8 (86)	41.3 (19)	91.2 (62)	84.8 (67)
Treatment, % patients				
Surgery	61.6 (77)	15.2 (7)	100 (68)	88.6 (70)
Chemoradiation	38.4 (48)	84.8 (39)	0	11.4 (9)
Surgery, % patients (n)				
Cold Knife Cone CKC	0	0	0	0
Trachelectomy	48.1 (37)	14.3 (1)	50 (34)	51.4 (36)
Hysterectomy	51.9 (40)	85.7 (6)	50 (34)	48.6 (34)
Adjuvant treatment				
Yes	23.4 (18)	28.6 (2)	20.6 (14)	22.9 (16)
Recurrence, % patients				
Yes	16.0 (20)	26.1 (12)	10.3 (7)	10.1 (8)*

No	78.4 (98)	65.2 (30)	89.7 (61)	86.1 (68)
Unknown	5.6 (7)	8.7 (4)	0	3.8 (3)

*Table 4-2 Patient characteristics for all tumours and for low- and high-volume tumour sub-groups (*1 treated with chemoradiotherapy) Data available for Recurrence group n=68, Lymph node group n=79.*

4.4.2 Differences in texture features based on tumour volume and clinico-pathological metrics

The number of voxels in the T2-W images ranged from 17441-209892 in the high-volume tumours (median 38597) to 107-17324 in the low-volume tumours (median 2207 for n=68, 2750 for n=79). The number of voxels in the ADC maps ranged from 10497-140650 in the high-volume tumours (median 26812) to 75-13294 in the low-volume tumours (median 1754 for n=68, 1927 for n=79).

From heat-maps of correlated texture features, ten texture feature clusters were identified (**Table 4.1**). After Bonferroni correction, 6 texture features on both ADC maps and T2-W images (**Table 4.3**) remained significantly different between the high- and low-volume tumours, namely Dissimilarity, Energy, ClusterShade, ClusterProminence, InverseVariance and Autocorrelation. An additional feature on T2-W imaging (Correlation) differed between groups (**Table 4.3**).

In low-volume tumours, Dissimilarity and Energy differed in patients without and with LVSI. However, none of the Haralick features from ADC maps or T2-W images differed between adeno- and squamous cancers, low and high-grade tumours, or those with negative vs. positive lymph node status.

		Median low volume N=79	IQR low volume N=79	Median high volume N=46	IQR high volume	Adjusted p-value
Dissimilarity	ADC	0.64	0.28	0.35	0.17	1.22E-11
	T2W	0.49	0.32	0.25	0.12	4.31E-14
Energy	ADC	0.15	0.11	0.30	0.21	3.76E-09
	T2W	0.20	0.13	0.34	0.2	7.55E-10
InverseVariance	ADC	0.41	0.08	0.29	0.13	2.84E-11
	T2W	0.38	0.12	0.23	0.10	9.61E-13
ClusterProminence	ADC	29.33	40.77	10.52	10.11	5.95E-08
	T2W	22.66	24.14	8.03	6.50	1.49E-09
ClusterShade	ADC	2.82	3.62	1.26	1.42	3.84E-03
	T2W	2.29	2.28	1.18	1.30	0.02
Autocorrelation	ADC	11.41	5.68	9.13	4.64	0.02
	T2W	11.65	8.69	6.08	3.64	8.22E-09
Informational Measure Correlation2	ADC	0.63	0.21	0.54	0.07	0.08
	T2W	0.67	0.16	0.68	0.22	1
Correlation	ADC	0.44	0.18	0.47	0.07	0.89
	T2W	0.55	0.23	0.62	0.26	0.03

Table 4-3 Texture features derived from ADC maps and T2-W images showing differences between low- and high- volume tumours

4.4.3 Clinico-pathological features as predictors of lymph node metastasis or recurrence

4.4.3.1 As predictors of lymph node metastasis

The AUCs and 95% CI for individual clinico-pathological features for predicting lymph node metastasis in all low-volume tumours (n=79) were: (tumour type (0.560 [0.403-0.718]), grade (0.606 [0.465-0.748]), LVSI (0.591 [0.433-0.749]) , Depth of Invasion (0.546 [0.311-0.781 and T2-W tumour volume (0.649 [0.455-0.843]).

Regression modelling indicated that tumour type and LVSI were indicative of lymph node metastasis (AUC=0.631, CI = 0.444-0.817 and AIC 69.17).

4.4.3.2 As predictors of recurrence

The AUCs and 95% CI for individual clinico-pathological features for predicting recurrence in all low-volume tumours (n=68) regardless of adjuvant therapy were: (tumour type (0.548 [0.340-0.756]), grade (0.501 [0.294-0.709]), LVSI (0.537 [0.347-0.728]) , Depth of Invasion (0.553 [0.291-0.814]), lymph node metastasis (0.530 [0.386-0.675]) and T2-W tumour volume (0.691 [0.448-0.934]). Adjuvant treatment had an AUC of 0.544 [0.357-0.732]. When patients receiving adjuvant therapy were excluded (n=54), the AUCs were: tumour type (0.555 [0.305-0.805]), grade (0.504 [0.254-0.754]), LVSI (0.633 [0.570-0.695]), Depth of Invasion (0.510 [0.214-0.807]), lymph node metastasis (0.510 [0.490-0.530]) and T2-W tumour volume (0.629 [0.327-0.931]). Regression modelling which included adjuvant therapy as a confounding feature indicated that volume and Depth of Invasion were indicative of recurrence (AUC=0.766 CI 0.562-

0.970), but that when patients who received adjuvant therapy were excluded, LVSI alone was predictive of recurrence (AUC= 0.633 95% CI 0.570-0.695). Combining T2-W volume, Depth of Invasion and LVSI predicted recurrence in all 68 low-volume tumours with an AUC 0.794 (95% CI 0.617- 0.971) and AIC of 45.684.

4.4.4 Texture features from ADC maps

4.4.4.1 As predictors of lymph node metastasis

When considering 79 patients with low-volume disease, the texture features Dissimilarity, Energy, InverseVariance, ClusterProminence, ClusterShade, Autocorrelation and Volume derived from ADC maps had an AUC of 0.716, 0.654, 0.650, 0.664, 0.561, 0.445 and 0.647 for predicting lymph node metastasis. (Figure 4.5, Table 4.4). When all low-volume tumours were considered, a regression model indicated that no combination of texture features improved prediction of lymph node metastasis over and above the performance of Dissimilarity. Combining metrics from ADC maps and clinic-pathological models (addition of LVSI and Type) improved the prediction significantly. (AUC 0.713, CI 0.617-0.916, AIC 64.25, p = 0.009)

4.4.4.2 As predictors of recurrence

When considering all 68 patients with low-volume disease, the texture features Dissimilarity, Energy, InverseVariance, ClusterProminence, ClusterShade, Autocorrelation and volume derived from ADC maps had an AUC of 0.775, 0.635, 0.674, 0.646, 0.508, 0.665 and 0.672, respectively for predicting recurrence. (Figure 4.6, Table 4.5). A regression model indicated that when combined, Dissimilarity and Energy were contributory to prediction of

recurrence (AUC=0.864, 95% CI =0.772-0.956, AIC 41.044). However, when patients who had adjuvant therapy were excluded, only Dissimilarity was predictive of recurrence (AUC=0.853, 95% CI=0.725-0.981).

Combining metrics predictive of recurrence from ADC-radiomic and clinico-pathological models (Dissimilarity and Energy with T2-W volume+Depth of Invasion+LVSI) significantly improved prediction of recurrence in all 68 low-volume tumours (AUC=0.916, 95% CI 0.837-0.994, with 100% sensitivity, 77% specificity, p=0.006, AIC=39.638, **Table 4**) compared to the combined clinico-pathological model of T2-W volume+Depth of Invasion+LVSI.

Examples of tumours with high Dissimilarity, and low Energy vs. low Dissimilarity and high Energy respectively are illustrated **in Figure 1**.

4.4.5 Texture features from T2-W imaging

4.4.5.1 As predictors of lymph node metastasis

When considering 79 patients with low-volume disease, the texture features Dissimilarity, Energy, InverseVariance, ClusterProminence, ClusterShade, Autocorrelation, Correlation and Volume derived from T2-W images had an AUC of 0.689, 0.611, 0.709, 0.468, 0.721, 0.682, 0.746 and 0.649 for predicting lymph node metastasis. (Figure 4.5, Table 4.4). When combined in a regression model InverseVariance, ClusterProminence and ClusterShade predicted lymph node metastasis more successfully. (AUC = 0.821, 95% CI = 0.666-0.975, AIC = 59.75) Combining metrics from T2-W and clinic-pathological models (addition of LVSI and Type) improved the prediction significantly. (AUC 0.786, CI 0.707-0.997, AIC 58.81, p = 0.001)

4.4.5.2 As predictors of recurrence

When considering patients with low-volume disease, the texture features Dissimilarity, Energy, InverseVariance, ClusterProminence, ClusterShade, Autocorrelation, Correlation and Volume derived from T2-W images individually had an area under the curve (AUC) of 0.609, 0.604,0.671, 0.607, 0.628, 0.536, 0.511 and 0.691 respectively for predicting recurrence (**Table 4.5**). When all low-volume tumours were considered, a regression model indicated that no combination of features improved prediction of recurrence. When patients who had adjuvant therapy were excluded, Dissimilarity, Clusterprominence and InverseVariance together were predictive of recurrence (AUC=0.837, 95% CI=0.698-0.976). These features applied to all 68 patients gave an AUC of 0.808 (95% CI=0.690-0.926, AIC=49.193).

Combining metrics predictive of recurrence from T2-W-radiomic and clinico-pathological models (Dissimilarity, ClusterProminence and InverseVariance with LVSI+Depth of Invasion+T2-W volume) did not significantly improve prediction of recurrence in low-volume tumours (AUC=0.906, 95% CI 0.822-0.991, p= 0.09, AIC=45.128, **Table 4.5**) compared to the combined clinico-pathological model of T2-W volume+Depth of Invasion+LVSI.

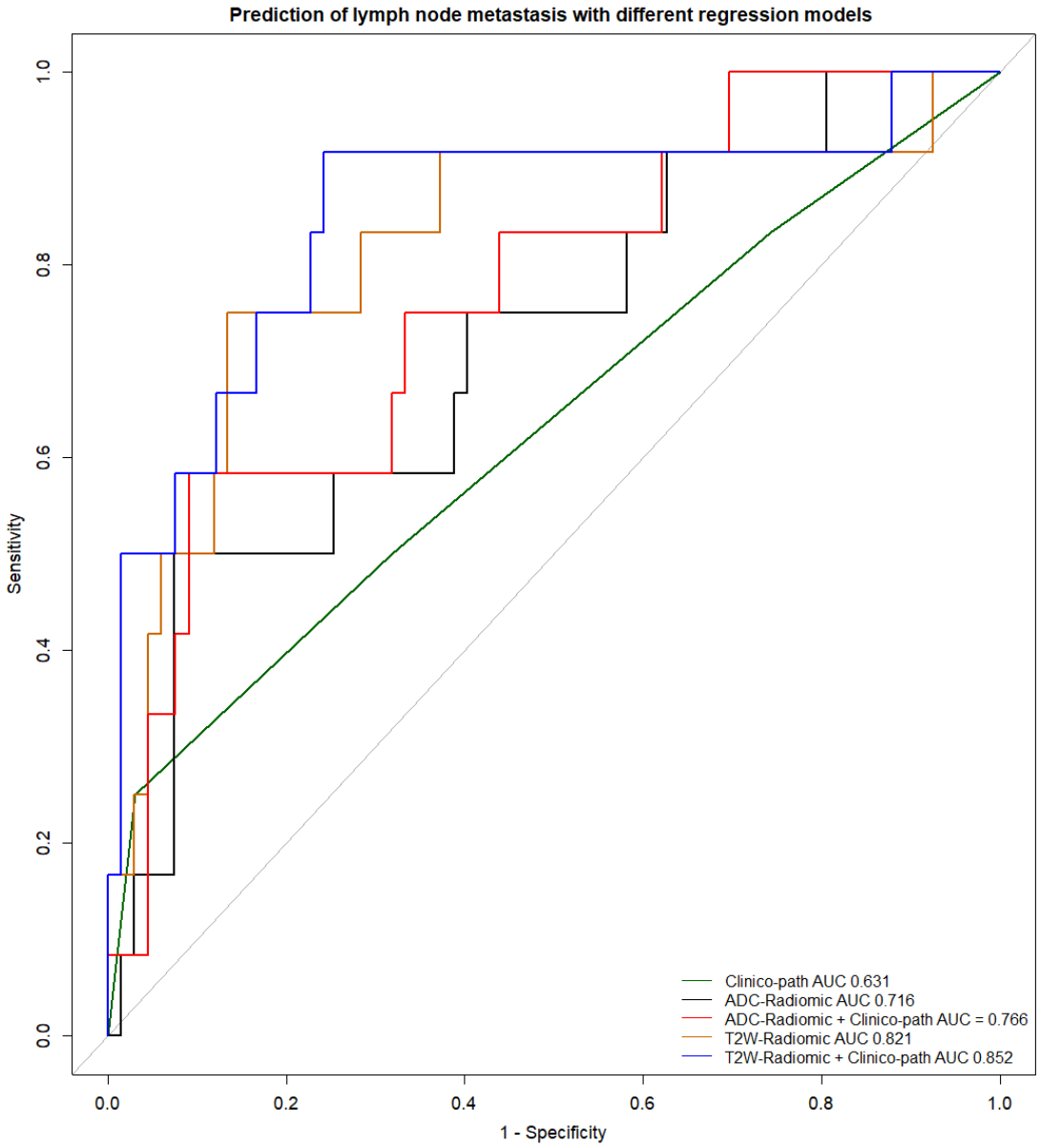

Figure 4-5 Receiver Operating Curves showing sensitivity and specificity for prediction of lymph node metastasis by texture features in 79 patients with low-volume tumours. Clinico-path model includes LVSI and tumour type, ADC Radiomic model includes Dissimilarity, T2W Radiomic model includes InverseVariance, ClusterProminence and ClusterShade.

Texture	From	AUC (CI)	Threshold	Sensitivity	Specificity
Dissimilarity	ADC map	0.716	0.428	50	92.5
	T2-W image	0.689	0.311	50	92.5
Energy	ADC map	0.654	0.218	58.3	77.6
	T2-W image	0.611	0.279	41.7	85.1
Cluster prominence	ADC map	0.664	16.515	66.7	74.6
	T2-W image	0.468	22.552	58.3	52.2
Inverse variance	ADC map	0.65	0.40	66.7	65.7
	T2-W image	0.709	0.324	66.7	79.1
Auto-correlation	ADC map	0.445	11.427	58.3	52.2
	T2-W image	0.682	9.679	75	64.2
Correlation	ADC map	-	-	-	-
	T2-W image	0.746	0.597	83.3	73.1
ClusterShade	ADC map	0.561	2.209	66.7	59.7
	T2-W image	0.721	2.469	91.7	64.2
Information MeasureCor	ADC map	0.419	0.666	57.1	60.7
	T2-W image	-	-	-	-
Volume	ADC map	0.647	2877.471	50	85.1
	T2-W image	0.649	2471.788	50	86.6

Table 4-4 Texture features derived from ADC maps and T2-W images in 79 low-volume tumours as predictors of lymph node metastasis

	AUC	CI	Corrected AUC	AIC	Resid. Df	Resid. Dev	Df	Deviance	p Value*
Clinico-pathological	0.631	0.444-0.817	0.572	69.17	75	63.170	-	-	-
ADC-Radiomic	0.716	0.551-0.882	0.714	64.61	77	-	-	-	-
T2W-Radiomic	0.821	0.666-0.975	0.778	59.75	75	-	-	-	-
ADC-Radiomic +Clinico-pathological	0.766	0.617-0.916	0.713	64.25	74	56.252	1	6.9173	0.009
T2W-Radiomic +Clinico-pathological	0.852	0.707-0.997	0.786	58.81	72	46.805	3	16.364	0.001

*Table 4-5 Regression models in prediction of lymph node metastasis with bootstrap corrected AUC and Chi-Square test of model differences. The reduction in AIC when T2W-radiomic or ADC-radiomic and clinico-pathological features are combined compared to clinico-pathological features alone is indicative of the improvement of the combined model *p- value of nested model compared to clinico-pathological model*

Texture	From	AUC (CI)	Threshold	Sensitivity	Specificity
Dissimilarity	ADC map	0.775	0.635	100	61
	T2-W	0.609	0.318	43	89
Energy	ADC map	0.635	0.178	71	61
	T2-W	0.604	0.235	71	67
Cluster prominence	ADC map	0.646	53.789	100	33
	T2-W	0.607	12.113	43	85
Inverse variance	ADC map	0.674	0.443	100	38
	T2-W	0.665	0.349	71	66
Auto-correlation	ADC map	0.665	11.978	100	41
	T2-W	0.628	8.921	100	38
Correlation	ADC map	-	-	-	-
	T2-W	0.536	0.524	71	57
ClusterShade	ADC map	0.508	5.75	100	23
	T2-W	0.511	3.474	86	26
InformationMeasureCorrela	ADC map	-	-	-	-
	T2-W	-	-	-	-
Volume	ADC map	0.672	1292.136	71	64
	T2-W	0.691	1248.191	71	64

Table 4-6 Texture features derived from ADC maps and T2-W images in 68 low-volume tumours as predictors of recurrence

	AUC	CI	Corrected AUC	AIC	Resid. Df	Resid. Dev	Df	Deviance	p Value*
Clinico-pathological	0.794	0.617-0.971	0.708	45.684	64	37.684	-	-	-
ADC-Radiomic	0.864	0.772-0.956	0.824	41.044	65	-	-	-	-
T2W-Radiomic	0.808	0.690-0.926	0.716	49.193	65	-	-	-	-
ADC-Radiomic +Clinico-pathological	0.916	0.837-0.994	0.840	39.638	63	27.638	2	10.046	0.006
T2W-Radiomic +Clinico-pathological	0.906	0.822-0.991	0.822	45.128	61	31.128	3	6.556	0.086

*Table 4-7 Regression models in prediction of recurrence with bootstrap corrected AUC and Chi-Square test of model differences. The reduction in AIC when ADC-radiomic and clinico-pathological features are combined compared to clinico-pathological features alone is indicative of the improvement of the combined model. *p- value of nested model compared to clinico-pathological model*

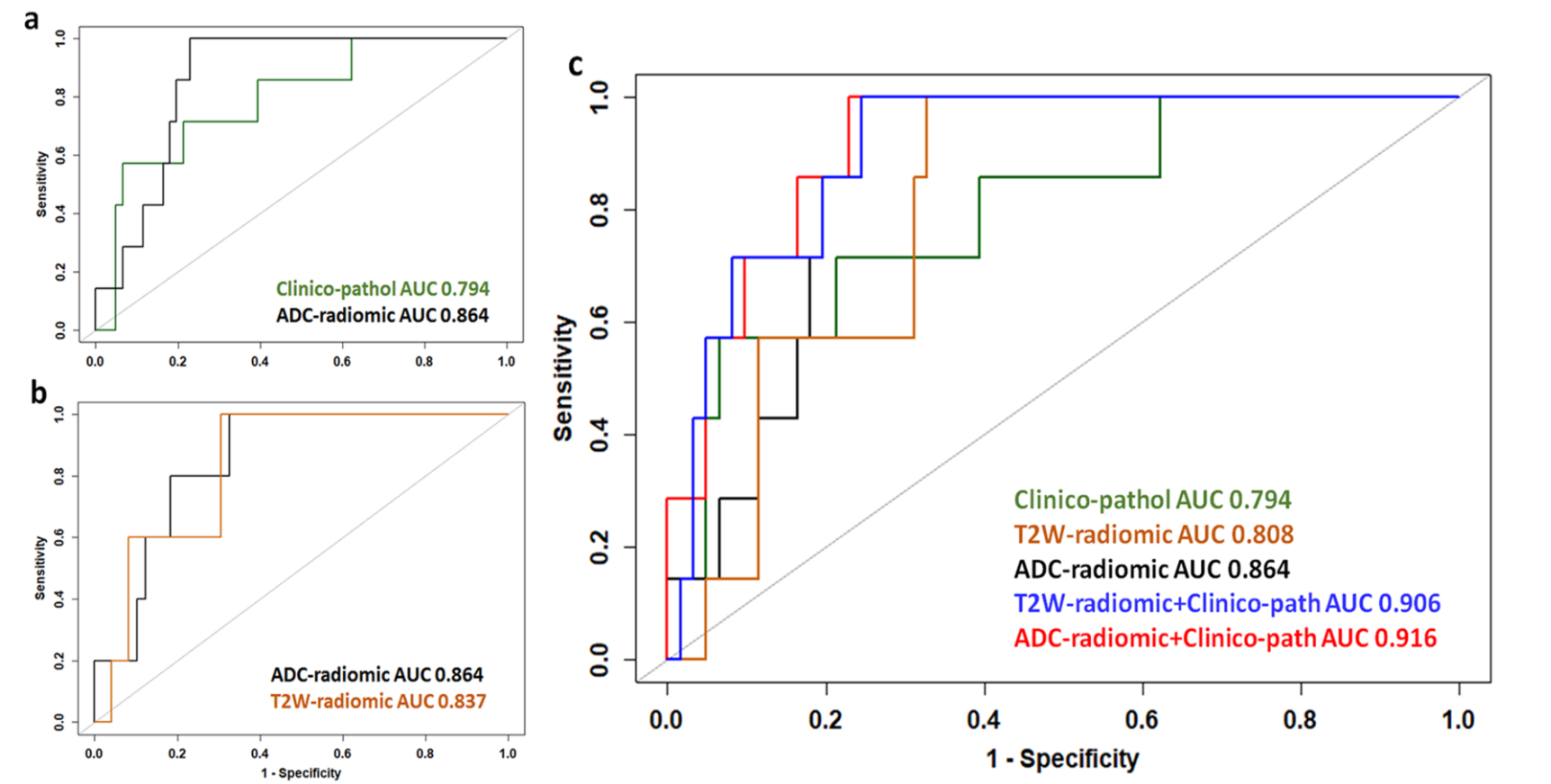

Figure 4-6 Receiver Operating Curves showing sensitivity and specificity for prediction of recurrence by texture and clinic-pathological features (a) in 68 patients with low-volume tumours where use of adjuvant therapy is included in the model; (b) in 54 patients who did not receive adjuvant therapy; and (c) in all 68 patients using features identified in both a and b (Dissimilarity, Energy for ADC-radiomics; Dissimilarity, ClusterProminence, InverseVariance for T2-W-radiomics; and Volume, Depth of Invasion, LymphoVascular Space Invasion for clinico-pathological features). In a, no combination of T2-W features was significantly superior to individual features. In b, of the clinico-pathological features, LVSI alone was predictive of recurrence, In c, the optimal prediction of recurrence is shown by a combination of ADC-radiomic an clinico-pathological features.

4.4.6 Validation of logistic regression models

4.4.6.1 As predictors of lymph node metastasis

Bias-corrected AUCs generated through a bootstrap resampling process showed reductions in AUC from 0.716 to 0.714 for the ADC-radiomic model (Dissimilarity), from 0.821 to 0.778 for the T2-W radiomic model (ClusterShade, InverseVariance and ClusterProminence) and from 0.631 to 0.572 for the clinico-pathological model (Tumour type and LVSI). The combined radiomic and clinico-pathological models were corrected from 0.766 to 0.713 (ADC-radiomic and clinico-pathological features) and from 0.852 to 0.786 (T2-W-radiomic and clinico-pathological features). **Table 4.5**

4.4.6.2 As predictors of recurrence

Bias-corrected AUCs generated through a bootstrap resampling process showed reductions in AUC from 0.864 to 0.824 for the ADC-radiomic model (Dissimilarity and Energy), from 0.808 to 0.716 for the T2-W radiomic model (Dissimilarity, InverseVariance and ClusterProminence) and from 0.794 to 0.718 for clinico-pathological model (T2-W volume, depth of invasion and LVSI). The combined radiomic and clinico-pathological models were corrected from 0.916 to 0.840 (ADC-radiomic and clinico-pathological features) and from 0.906 to 0.822 (T2-W-radiomic and clinico-pathological features). **Table 4.7**

4.5 Discussion

4.5.1 Utility of radiomic features in planning management

This data highlights the potential of texture feature analysis for predicting recurrence with potential to influence the surgical management of patients with early stage, low-volume cervical cancer. It means that surgical management can be altered, or appropriate patient counselling provided at the outset because the use of adjuvant therapy can be anticipated. The utility of such information would be particularly valuable in a young patient population seeking to retain fertility and minimize therapy. For instance, to avoid the toxicity of lymphadenectomy followed by adjuvant chemoradiation, patients with “good” radiomic features may elect to have sentinel node biopsy prior to curative treatment (surgery or chemoradiation). Additionally, patients could be counselled as to the need for adjuvant therapy at the outset. In larger tumours, where volume is a strong predictive factor of recurrence (203) and survival (58) , the utility of additional radiomic analyses in altering management remains to be established.

4.5.2 Radiomic differences between high and low volume cervical tumours

My data has identified the radiomic features from ADC maps and T2-W images that differ between high- and low-volume cervical tumours and shown that these features individually and in combination are useful for predicting parametrial extension, lymph node metastasis and recurrence in low-volume tumours. Patients in the high- and low--volume tumour groups were well matched by age, and although the low-volume tumours were by definition lower stage, there were

more adenocarcinomas and LVSI in this group, both of which adversely affect outcome. Radiomic differences between high and low-volume tumours were largely similar for both the ADC and T2-W data although regression models identified different combinations of features as being contributory to prediction of recurrence in each case. Moreover, although radiomic features differed between tumours with and without LVSI, they did not differ between other histological parameters of poor prognosis (type, grade, Depth of Invasion, LN metastasis), indicating that they are likely to be independent.

A strength of this study was the derivation of the data using an endovaginal receiver coil, particularly in small volume tumours where it was possible to obtain a minimum of 100 voxels. This provided a substantial boost in SNR (95) and was invaluable for the assessment of the ADC data where external array imaging in the low-volume tumours would have limited the voxel numbers and precluded meaningful ADC feature analysis.

Other retrospective studies have reported radiomic features derived from MRI and ^{18}FDG-positron emission tomography (PET) scans of locally advanced cervical cancer treated with chemoradiotherapy. Radiomics features such as entropy from ADC maps and grey level non-uniformity from PET, respectively, have been shown to be independent predictors of recurrence and loco-regional control in these larger volume tumours with significantly higher prognostic power than usual clinical parameters (204) .This supports our findings where these features are shown to differ between high- and low-volume tumours and to be predictive of recurrence in the low-volume tumour group.

The greater tendency to decreased Dissimilarity in larger tumours, indicates that grey levels in adjacent pixels were similar in larger tumours. Energy, which is a

measure of textural uniformity, and is highest when grey level distribution has either a constant or a periodic form, also was higher in larger tumours. A previous prospective study has confirmed the reproducibility of these features and their lack of dependence on regional ROI selection within the tumour (205), nevertheless we used whole tumour analysis in our study. A study by Hao et al has shown that radiomic analysis of the tumour periphery is informative in differentiating those likely to recur from those that do not (206), but the tumour volume in their cohort was high and patients were treated with chemoradiation. My data interrogates the differences in features between high- vs. low-volume tumours across the entire tumour volume and uses these features to recognize low- volume tumours with potentially poor prognosis. It confirms for the first time using radiomic analysis, that as cervical tumours grow, they tend to become texturally less dissimilar and more homogenous. This may well reflect the transition from a morphology where tumour elements are interspersed with normal cervical glandular elements and stroma in smaller tumours to more homogenous sheets of malignant cells as tumours increase in size and de-differentiate.

4.5.3 Comparison of ADC and T2-W radiomic features

T2W-radiomic features were less good than the ADC-radiomic features for predicting recurrence but were better than ADC in predicting lymph node metastasis. It may well be that the distribution of water within a tumour indicative of tumour architecture is associated more with lymph node metastasis, while the ADC features indicative of cellular density of tumours are associated more with recurrence. T2-W data also was affected by signal-

intensity variations across the image, particularly in the presence of an endovaginal coil, which was not an issue with the quantified ADC from diffusion-weighted images, which may have reduced its sensitivity for predicting recurrence. ADC-radiomics when combined with clinico-pathological features offered significant improvements for prediction of recurrence, however the T2-W-radiomics did not as the model over-fitted the data.

4.5.4 Adjuvant therapy as a confounding factor

The application of adjuvant therapy as a confounding factor represented an analysis dilemma: removal of patients with low-volume tumours on MRI who went on to receive adjuvant chemotherapy would have biased the sample and made it unrepresentative of the final application. On the other hand, retaining these patients in the analysis, potentially weakened the model because patients with MRI radiomics features indicative of a recurrence after surgery will have that recurrence prevented by the adjuvant treatment. My solution was to perform both sets of analyses. As predicted, when the patients who received adjuvant therapy were removed, the AUC of the model increased, but at the cost of a smaller sample size.

4.5.5 Study limitations

This work has several limitations. First it is a single site study with a relatively small sample size, albeit from a quaternary referral gynaecological oncology centre which sees and treats a high volume of patients. The models haven't yet been validated in an independent patient sample and this will be required to provide further evidence of the applicability of this technique.

Second, the recurrence rate was low (~10%) but is in keeping with expectations in this early stage, potentially curable disease. Even with a larger sample size, it would not have been possible to avoid such an imbalance between the recurrence and no-recurrence classes. Taken together, these factors lead to a model based on a small number of recurrences and the consequent risk of overfitting from the combined model, with a possibly over-optimistic value for the combined-model AUC. However, we show that for *single-feature* models *any one* of the ADC radiomic features Dissimilarity, Energy, InverseVariance, ClusterProminence, Autocorrelation or ADC volume performed better than the highest-scoring “clinico-pathological” features (T2-W volume and LVSI). Furthermore, when considering models based on just *two* features, the radiomic model (ADC Dissimilarity and Energy, AUC=0.864) compared well with the clinical model (T2-W volume and Depth of invasion, AUC=0.766).

Third, patients were often diagnosed following a LLETZ biopsy which may remove a significant volume of disease, thus affecting the assessment at their staging MRI and confounding our results; this was the case in 1 patient in our study group. Nevertheless, in a clinical setting a LLETZ or cone biopsy is performed as part of the normal clinical pathway prior to MRI and imaging prior to a diagnostic LLETZ or cone biopsy is unlikely, making our results more applicable in a clinical workflow. In future, when determining the utility of radiomic features combined with other clinical and histologic assessments, use of MRI plus LLETZ volume is desirable.

Finally, the current poor availability of endovaginal MRI limits radiomic assessments of low-volume tumours more widely. However, if further accumulation of cases confirms the predictive power of this model and that high

SNR enables its implementation, this will provide a justification for more widespread use of this MRI technique at specialist centres offering trachelectomy. Alternatively, improvements of SNR in non-endovaginal MRI may be required.

4.6 Conclusions

In patients with low-volume tumours, ADC-radiomic texture analysis is potentially a useful predictor of tumour recurrence. This can substantially impact the treatment planning and counselling of patients with low-volume tumours seeking fertility preservation. The regression model derived from this data requires validation in a test set. It should then be possible to set thresholds for the relevant radiomic and clinical factors and to use these in a nomogram to predict the likelihood of recurrence in a clinical setting.

4.7 References

52. Pecorelli S, Zigliani L, Odicino F. Revised FIGO staging for carcinoma of the cervix. International Journal of Gynecology & Obstetrics. 2009;105(2):107-8.

58. Soutter WP, Hanoch J, D'Arcy T, Dina R, McIndoe GA, DeSouza NM. Pretreatment tumour volume measurement on high-resolution magnetic resonance imaging as a predictor of survival in cervical cancer. BJOG. 2004;111(7):741-7.

79. Cibula D, Pötter R, Planchamp F, Avall-Lundqvist E, Fischerova D, Haie Meder C, et al. The European Society of Gynaecological Oncology/European Society for Radiotherapy and Oncology/European Society of Pathology guidelines for the management of patients with cervical cancer. Radiotherapy and Oncology. 2018;127(3):404-16.

85. Guan Y, Shi H, Chen Y, Liu S, Li W, Jiang Z, et al. Whole-Lesion Histogram Analysis of Apparent Diffusion Coefficient for the Assessment of Cervical Cancer. J Comput Assist Tomogr. 2016;40(2):212-7.

86. Downey K, Riches SF, Morgan VA, Giles SL, Attygalle AD, Ind TE, et al. Relationship between imaging biomarkers of stage I cervical cancer and poor-prognosis histologic features: quantitative histogram analysis of diffusion-weighted MR images. AJR Am J Roentgenol. 2013;200(2):314-20.

87. Winfield JM, Orton MR, Collins DJ, Ind TE, Attygalle A, Hazell S, et al. Separation of type and grade in cervical tumours using non-mono-exponential models of diffusion-weighted MRI. Eur Radiol. 2017;27(2):627-36.

88. Guan Y, Li W, Jiang Z, Zhang B, Chen Y, Huang X, et al. Value of whole-lesion apparent diffusion coefficient (ADC) first-order statistics and texture features in clinical staging of cervical cancers. Clin Radiol. 2017;72(11):951-8.

89. Woo S, Kim SY, Cho JY, Kim SH. Apparent diffusion coefficient for prediction of parametrial invasion in cervical cancer: a critical evaluation based on stratification to a Likert scale using T2-weighted imaging. Radiol Med. 2017.

90. Yang W, Qiang JW, Tian HP, Chen B, Wang AJ, Zhao JG. Minimum apparent diffusion coefficient for predicting lymphovascular invasion in invasive cervical cancer. J Magn Reson Imaging. 2017;45(6):1771-9.

91. Downey K, Jafar M, Attygalle AD, Hazell S, Morgan VA, Giles SL, et al. Influencing surgical management in patients with carcinoma of the cervix using a T2- and ZOOM-diffusion-weighted endovaginal MRI technique. British journal of cancer. 2013;109(3):615-22.

92. Payne GS, Schmidt M, Morgan VA, Giles S, Bridges J, Ind T, et al. Evaluation of magnetic resonance diffusion and spectroscopy measurements as predictive biomarkers in stage 1 cervical cancer. Gynecologic oncology. 2010;116(2):246-52.

93. Hou Z, Li S, Ren W, Liu J, Yan J, Wan S. Radiomic analysis in T2W and SPAIR T2W MRI: predict treatment response to chemoradiotherapy in esophageal squamous cell carcinoma. Journal of thoracic disease. 2018;10(4):2256-67.

94. Wang Q, Li Q, Mi R, Ye H, Zhang H, Chen B, et al. Radiomics Nomogram Building From Multiparametric MRI to Predict Grade in Patients With Glioma: A Cohort Study. J Magn Reson Imaging. 2019;49(3):825-33.

95. Gilderdale DJ, deSouza NM, Coutts GA, Chui MK, Larkman DJ, Williams AD, et al. Design and use of internal receiver coils for magnetic resonance imaging. Br J Radiol. 1999;72(864):1141-51.

186. Shepherd JH, Spencer C, Herod J, Ind TE. Radical vaginal trachelectomy as a fertility-sparing procedure in women with early-stage cervical cancer-cumulative pregnancy rate in a series of 123 women. Bjog. 2006;113(6):719-24.

187. Bentivegna E, Gouy S, Maulard A, Chargari C, Leary A, Morice P. Oncological outcomes after fertility-sparing surgery for cervical cancer: a systematic review. The Lancet Oncology. 2016;17(6):e240-e53.

188. Laios A, Kasius J, Tranoulis A, Gryparis A, Ind T. Obstetric Outcomes in Women With Early Bulky Cervical Cancer Downstaged by Neoadjuvant Chemotherapy to Allow for Fertility-Sparing Surgery: A Meta-analysis and Metaregression2018. 1 p.
189. Naik R, Cross P, Nayar A, Mayadevi S, Lopes A, Godfrey K, et al. Conservative surgical management of small-volume stage IB1 cervical cancer. Bjog. 2007;114(8):958-63.
190. Alfsen GC, Kristensen GB, Skovlund E, Pettersen EO, Abeler VM. Histologic subtype has minor importance for overall survival in patients with adenocarcinoma of the uterine cervix. Cancer. 2001;92(9):2471-83.
191. Horn L-C, Bilek K, Fischer U, Einenkel J, Hentschel B. A cut-off value of 2cm in tumor size is of prognostic value in surgically treated FIGO stage IB cervical cancer. Gynecologic oncology. 2014;134(1):42-6.
192. Halle MK, Ojesina AI, Engerud H, Woie K, Tangen IL, Holst F, et al. Clinicopathologic and molecular markers in cervical carcinoma: a prospective cohort study. American journal of obstetrics and gynecology. 2017;217(4):432.e1-.e17.
193. Burke TW, Hoskins WJ, Heller PB, Bibro MC, Weiser EB, Park RC. Prognostic factors associated with radical hysterectomy failure. Gynecologic oncology. 1987;26(2):153-9.
194. Kato T, Takashima A, Kasamatsu T, Nakamura K, Mizusawa J, Nakanishi T, et al. Clinical tumor diameter and prognosis of patients with FIGO stage IB1 cervical cancer (JCOG0806-A). Gynecologic oncology. 2015;137(1):34-9.
195. Samlal RA, van der Velden J, Ten Kate FJ, Schilthuis MS, Hart AA, Lammes FB. Surgical pathologic factors that predict recurrence in stage IB and IIA cervical carcinoma patients with negative pelvic lymph nodes. Cancer. 1997;80(7):1234-40.
196. Roh HJ, Kim KB, Lee JH, Kim HJ, Kwon YS, Lee SH. Early Cervical Cancer: Predictive Relevance of Preoperative 3-Tesla Multiparametric Magnetic Resonance Imaging. International journal of surgical oncology. 2018;2018:9120753.
197. Meng J, Zhu L, Zhu L, Wang H, Liu S, Yan J, et al. Apparent diffusion coefficient histogram shape analysis for monitoring early response in patients with advanced cervical cancers undergoing concurrent chemo-radiotherapy. Radiat Oncol. 2016;11(1):141.
198. Marcus DS, Olsen TR, Ramaratnam M, Buckner RL. The Extensible Neuroimaging Archive Toolkit: an informatics platform for managing, exploring, and sharing neuroimaging data. Neuroinformatics. 2007;5(1):11-34.
199. Doran SJ, d'Arcy J, Collins DJ, Andriantsimiavona R, Orton M, Koh DM, et al. Informatics in radiology: development of a research PACS for analysis of functional imaging data in clinical research and clinical trials. Radiographics : a review publication of the Radiological Society of North America, Inc. 2012;32(7):2135-50.
200. Blackledge MD, Collins DJ, Koh DM, Leach MO. Rapid development of image analysis research tools: Bridging the gap between researcher and clinician with pyOsiriX. Computers in biology and medicine. 2016;69:203-12.
201. Wibmer A, Hricak H, Gondo T, Matsumoto K, Veeraraghavan H, Fehr D, et al. Haralick texture analysis of prostate MRI: utility for differentiating non-cancerous prostate from prostate cancer and differentiating prostate cancers with different Gleason scores. Eur Radiol. 2015;25(10):2840-50.
202. Haralick RM, Shanmugam K, Dinstein I. Textural Features for Image Classification. IEEE Transactions on Systems, Man, and Cybernetics. 1973;SMC-3(6):610-21.
203. Sethi TK, Bhalla NK, Jena AN, Rawat S, Oberoi R. Magnetic resonance imaging in carcinoma cervix--does it have a prognostic relevance. Journal of cancer research and therapeutics. 2005;1(2):103-7.
204. Lucia F, Visvikis D, Desseroit MC, Miranda O, Malhaire JP, Robin P, et al. Prediction of outcome using pretreatment (18)F-FDG PET/CT and MRI radiomics in locally advanced cervical cancer treated with chemoradiotherapy. European journal of nuclear medicine and molecular imaging. 2018;45(5):768-86.

205. Liu Y, Zhang Y, Cheng R, Liu S, Qu F, Yin X, et al. Radiomics analysis of apparent diffusion coefficient in cervical cancer: A preliminary study on histological grade evaluation. J Magn Reson Imaging. 2018.
206. Hao H, Zhou Z, Li S, Maquilan G, Folkert MR, Iyengar P, et al. Shell feature: a new radiomics descriptor for predicting distant failure after radiotherapy in non-small cell lung cancer and cervix cancer. Physics in Medicine & Biology. 2018;63(9):095007.

CHAPTER 5 Conclusions and future work

The work developed in this thesis has shown the potential capability of a lab-on-a-chip device which can detect nucleic acid markers of both HPV infection and the host genomic consequences of persistent HPV effect resulting in malignancy. Coupled with endovaginal MRI, we have shown the LOC assay can improve the detection and classification of patients with and without residual tumour prior to curative treatment for early stage cervical cancer. We are at the pilot stage of development and have tested the assay and device on a small cohort of patients, albeit prospectively recruited. Several further developments and testing processes are required prior to the utilisation of this technique being realised.

5.1 Technical advancements required

Currently, the time it takes to set up each LOC experiment would preclude the testing of each MODULAR sample with each marker as this would be over 200 individual experiments. The next step in the development of this system is the construction and testing of a microfluidic platform which is able to compartmentalise the prepared sample into several chambers, each with their own pH-LAMP tumour marker primer set, to allow an array of tests to be performed on-chip at once. This process has already begun to be tested by colleagues at Imperial College London, by 3D printing a microfluidic chamber which allows to compartmentalise the LOC array into two distinct testing areas. This has been successfully trialled as part of their development of a COVID-19 LOC test platform (207).

There are several aspects which require development to allow for multiplexing of several markers per sample. The microfluidic will need to reliably distribute equal volumes of the lysate to the chip array. There needs to be a solid seal between chambers to avoid cross-contamination of the lysate with different primer sets. The reaction mixture and primer sets need to be optimised for lyophilisation so that assay specific chips can be used and stored easily. A component of multiplexing which could be utilised is being developed by my colleagues at Imperial College London whereby simultaneous absolute quantification using standard curves employing only a single channel or detector platform through establishing multi-dimentional standard curves of the multiplexed targets (208, 209).

Similarly, a sample preparation component will also need to be developed as I used existing bench-based DNA/RNA extraction methods to provide the highest quality nucleic acid samples to be tested. A method, either heat or chemical lysis, will need to be developed which allows for the direct testing of the lysed cervical cell samples delivered via a microfluidic platform as described above. As the cervical swab sample predominantly consists of exfoliated cells, mucous and occasionally small amounts of blood this process should, in comparison to cell-free DNA testing in blood, be relatively straightforward to deliver.

5.2 Further testing

5.2.1 LOC device

Once development of the LOC device is completed a number of testing phases will need to be completed prior to its ultimate use. The MODULAR samples have not yet been validated on the LOC device as explained above and this would need to take place to ensure that the lower cellularity of a cytological

sample, and therefore lower concentration of nucleic acids available to detect the markers in, compared with the solid tumour samples the LOC device has been currently tested on. The LOC assay performed with high analytical sensitivity on the Lightcycler benchtop platform and so it is unlikely that the LOC device would have a dramatically different comparative sensitivity.

The HPV DNA LAMP primers used in the experiments were drawn from Luo et al (170) but certainly did not perform as well as expected, especially HPV Type 18. Alternative primer sets would need to be tested and validated either from existing published work or designed in-house.

The tumour markers used were only tested against the presence or absence of tumour. If the LOC device were to be used in the setting of a point of care screening tool, predominantly as a HPV DNA or RNA primary screen with additional nucleic acid based molecular triage markers, a detailed examination of the triage markers used would need be made to determine the ability to discriminate pre-malignant lesions from normal or CIN1 for example. The device and included HPV DNA/RNA primer sets would need to be validated against the Meijer criteria or more likely the VALGENT criteria, as genotyping would be an integral advantage the device would offer a multiplex detection capability.

A large scale prospective trial whereby a comparison against clinically validated assays used as part of a nationwide screening programme were used to determine the relative sensitivity and specificity of the LOC assay and device.

The careHPV test which is aimed at the LMIC setting does not yet conform to the Meijer criteria as its relative sensivity is inferior to HC2 (33). This would need to be performed firstly in the confines of a laboratory environment to provide optimal experimental conditions prior to its testing at the point-of-care,

perhaps in a prospective trial in partnership with a LMIC looking to provide a low-cost screening programme. The LOC approach would meet the ASSURED (**A**ffordable, **S**ensitive, **S**pecific, **U**ser-friendly, **R**apid and robust, **E**quipment-free and **D**eliverable to end-users) criteria set out by the World Health Organization (210).

5.2.2 Radiomic analysis from endovaginal MRI

The radiomic analysis predicting the risk of lymph node metastasis or recurrence was developed on a single cohort of patients and the risk of overfitting the model on training data is a key consideration of the usefulness and applicability of the technique. We attempted to ameliorate the risk with our strategy of bootstrapping but ultimately applying the radiomic analysis on a entirely separate validation cohort would be the true test of the technique. A validation cohort of patients have been identified as they were recruited following the cessation of my project and this work will be able to be validated once enough time has elapsed to allow the recurrence data to mature. This is likely to be at least 2 years as the majority of recurrences in early cervical cancer occur by this period. If the validation process confirms the success of the technique it would open up the possibility of significant avenues of future work.

The endovaginal MRI technique is limited to two institutions and so a retrospective analysis of patients across the country would not be possible. A prospective trial encompassing a collaboration of a number of institutions with high-throughput of early cervical cancer would be needed to truly validate the work.

An opportunity to combine the power of HPV DNA testing and endovaginal MRI to detect residual disease could potentially allow a change in the treatments offered to patients with early cervical cancer. Following the publication of the LACC trial (211) a shift from minimally invasive approaches to performing radical hysterectomy has occurred due to the increased risk of recurrence following a minimal access approach. The SUCCOR study has suggested the uterine manipulator as the culprit in this discrepancy in recurrence risk (212). However, in the original oral presentation by Chiva et al suggested that those who had previous conisation or no residual disease did not have a discrepant recurrence risk (213). A formal publication on this particular suggestion is awaited. This potentially allows for the utilisation of HPV testing in combination with endovaginal MRI to predict residual disease prior to surgical treatment choice and allow for the selection of minimal access surgery in those patients judged not to have residual disease. This would allow the potential morbidity of an open approach to be reduced.

5.3 Competing technologies

Current HPV “self-test” kits are based on detection of antibodies to HPV strains and primarily detect high-risk strains. Therefore, they are dependent on the host immune reaction to the presence of the HPV and may be falsely negative, especially in the acute phase of the infection. Direct detection of viral DNA or even RNA is therefore being actively pursued.

There are other descriptions of electrochemical chip biosensors for detection of HPV DNA. One such electrochemical system uses 16 gold working electrodes arranged in a four by four distribution on a borosilicate glass chip measuring 21 mm × 23 mm. Each working electrode (1 mm × 1 mm) is placed between a

silver pseudo reference (0.2 mm × 1 mm) and a gold counter electrode of the same size in order to create 16 planar electrochemical cells. The assay is based on co-immobilisation of HPV E7 and E6 thiolated probes with backfiller, a hybridisation process and electrochemical detection (214). The limits of detection are described in the pM range and are sufficient for most real RNA/DNA samples, but the system is bulky and not easily adaptable to population screening. In another system, target HPV DNA is captured via magnetic bead-modified DNA probes, followed by an antidigoxigenin-peroxidase detection system at screen-printed carbon electrode chips, with eight samples measurable simultaneously (215). In comparison, the system described in this work uses a lab-on-chip cartridge that performs on-chip real-time DNA amplification and is able to detect viral DNA by loop-mediated isothermal amplification. This simplifies sample preparation, readout of multiplexed DNA /RNA and is also potentially adaptable to high throughput as required for screening applications.

5.4 Future direction incorporating molecular and imaging diagnostics into an early detection pathway for cervical cancer

Cervical cancer screening involves detecting and treating the preinvasive phase on a cytology sample from the cervix. This is offered to women aged 25-64 years in the NHS. Uptake (the proportion of screening invitees for whom a screening test result is recorded) is the most important factor in determining the success of a screening programme (216, 217). Women from ethnic minorities and deprived subgroups have consistently shown lower uptake over decades of screening (218, 219) because health literacy is an important determinant in uptake. A quarterly coverage report (March 2019) produced by public Health

England (220) indicated that 70.2% of women aged 25-49 years had an adequate screening test recorded in the last 3.5 years (compared to 73.7% in March 2011) and that 76.4% of women aged 50-64 years had an adequate screening test recorded in the previous 5.5 years in the quarter ending March 2019 (compared to 80.1% in March 2011), showing that screening attendance is gradually declining. Lowest uptake is in London regions where screening attendance is consistently <60%. Media campaigns, particularly around celebrity experiences, can have a profound short-term effect, but cannot sustain improvement.

The opportunity for self-collecting cervico-vaginal cells at home and returning the sample for HPV testing is easy and private, so has the potential to increase screening participation. However, it is vital that detection rates of self-collected and clinic-collected samples are equivalent. There is a growing evidence base, mainly from high-income countries that indicates increased screening participation with self-testing. Three trials in the UK reported a small (2%) increase in uptake (221-223). A meta-analysis of 33 studies (29 RCTs and 4 observational studies) that included 369 017 participants (93% from high-income countries) examined HPV self-sampling in comparison to standard-of-care (eg, smear cytology, visual inspection with acetic acid, clinician-collected HPV testing) and showed a greater screening uptake among HPV self-sampling participants compared with control (RR: 2.13, 95% CI 1.89 to 2.40) (224). Meta-analyses also have shown comparable detection rates of high-risk HPV infections between self and physician-collected tests (225, 226). As HPV self-testing kits are now becoming available, a recently opened trial in North and East London is sending women who fail to attend screening a self-test HPV kit.

Those who test positive will be invited for cytological screening. A proposal for a pathway incorporating self-testing coupled with endovaginal MRI for early detection of cervical cancer is outlined in **Figure 5.1**

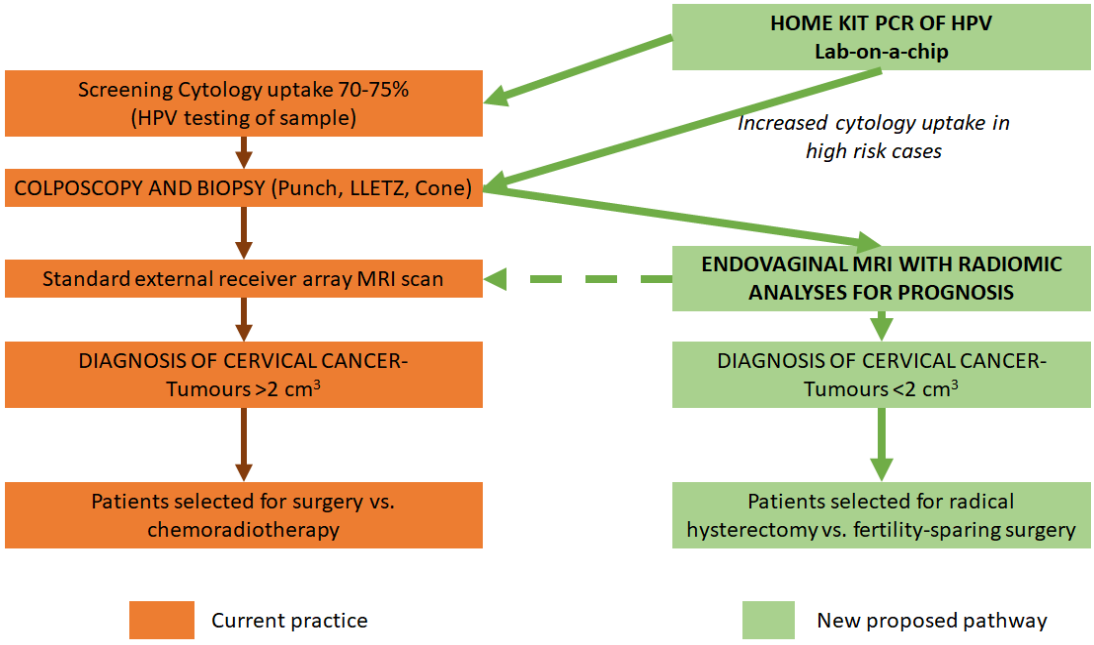

Figure 5-1Proposal for an early detection pathway incorporating lab-on-a-chip and endovaginal MRI

Cost-effectiveness remains at the centre of the debate around self-sampling. Nevertheless, a systematic review of 16 studies (9 modelled in European screening programs, 6 targeted women who were underscreened for cervical cancer, and 5 modelled in low- and middle-income countries) demonstrated that the most commonly identified driver of HPV self-sampling cost-effectiveness was the level of increase in cervical cancer screening attendance (227). In future, lower HPV self-sampling material and testing costs and higher sensitivity to detect cervical precancer should increase cost-effectiveness particularly in populations with severe under-screeners, or where no screening programmes currently exist. The lab-on-a-chip described in this work is a strong candidate to meet these requirements: it offers advantages of a simple read-out system of multiple HPV types, whereby the sample could potentially be taken to a local

pharmacy or GP surgery for instant results, and is robust enough to be used in the developing world. Moreover, if combined with tumour DNA/RNA testing it would quickly identify not only those who needed referral for cytology screening, but also those who could be referred directly to colposcopic services. Patients with small tumours on clinical examination/ colposcopy and who wish to retain fertility could then be referred to national centres offering an endovaginal MRI service, where prognostic evaluation of small tumours could be done on radiological whole-tumour evaluation as well as on histological samples prior to planning appropriate surgery.

5.5 Future direction incorporating molecular and imaging diagnostics into a “test for cure” pathway for cervical cancer

An attempt to eradicate cervical cancer from the population would require more drastic colposcopic surveillance measures, which are intensive, invasive and unlikely to meet patient acceptability. It is in this scenario that the use of self-sampling HPV tests, coupled with tests for tumour DNA, could be transformative, particularly when following-up patients in whom CIN has been completely excised from the cervix and who have had negative endovaginal MRI. Regular, repeat HPV tests in this population would ensure that re-colposcopy was done early to treat CIN when HPV re-testing became positive, so that progression to invasive disease did not occur. A proposal for a potential

"test for cure" pathway is outlined in **Figure 5.2**

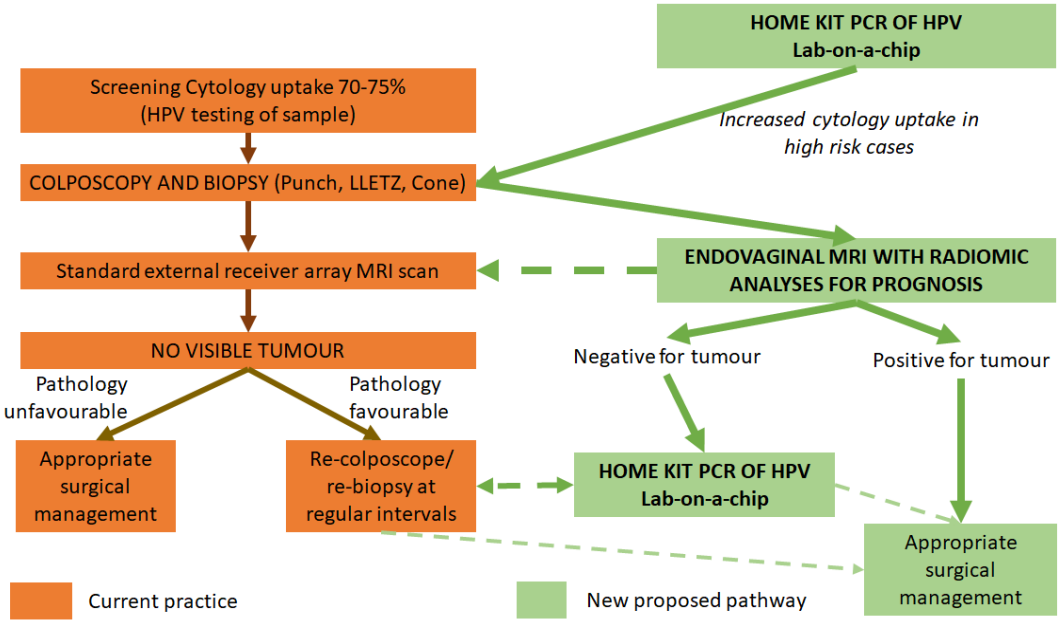

Figure 5-2 Proposal for a "test for cure" pathway incorporating lab-on-a-chip and endovaginal MRI

As with the early detection pathway, it would be important to implement self-collection of samples in a "test for cure" pathway as it has proven more acceptable than clinic attendance (80.0% vs. 56.7% uptake in a trial randomising women to either self-collection or clinic attendance, (228). Importantly, in a small subset of these patients where HPV testing was possible from both self-collected and clinic samples, the sensitivity and specificity of the self-collected vs the clinic collected samples as a reference was 100% and 94.1% respectively (228).

Although PCR based analyses have substantially lower sensitivities (88%) than immunohistochemistry and in-situ hybridization techniques (97%) (229), kits such as the *care*HPV test (230) with a sensitivity and specificity of 85.7% and 83.1% respectively may be considered sufficiently accurate for screening low-resource regions, but may be insufficiently effective when aiming for HPV eradication. The new lab-on-a-chip device described here which uses robust,

smarter read-outs of viral DNA/ RNA through real-time amplification, in a location closer to home may well provide a more robust and effective system when implementing HPV and tumour nucleic acid testing in a “test for cure” scenario.

5.6 References

33. Kelly H, Mayaud P, Segondy M, Pant Pai N, Peeling RW. A systematic review and meta-analysis of studies evaluating the performance of point-of-care tests for human papillomavirus screening. Sexually Transmitted Infections. 2017;93(S4):S36-S45.
170. Luo L, Nie K, Yang MJ, Wang M, Li J, Zhang C, et al. Visual detection of high-risk human papillomavirus genotypes 16, 18, 45, 52, and 58 by loop-mediated isothermal amplification with hydroxynaphthol blue dye. Journal of clinical microbiology. 2011;49(10):3545-50.
207. Rodriguez-Manzano J, Malpartida-Cardenas K, Moser N, Pennisi I, Cavuto M, Miglietta L, et al. A handheld point-of-care system for rapid detection of SARS-CoV-2 in under 20 minutes. medRxiv. 2020:2020.06.29.20142349.
208. Rodriguez-Manzano J, Moniri A, Malpartida-Cardenas K, Dronavalli J, Davies F, Holmes A, et al. Simultaneous Single-Channel Multiplexing and Quantification of Carbapenem-Resistant Genes Using Multidimensional Standard Curves. Anal Chem. 2019;91(3):2013-20.
209. Moniri A, Rodriguez-Manzano J, Malpartida-Cardenas K, Yu LS, Didelot X, Holmes A, et al. Framework for DNA Quantification and Outlier Detection Using Multidimensional Standard Curves. Anal Chem. 2019;91(11):7426-34.
210. Peeling RW, Holmes KK, Mabey D, Ronald A. Rapid tests for sexually transmitted infections (STIs): the way forward. Sexually Transmitted Infections. 2006;82(suppl 5):v1-v6.
211. Ramirez PT, Frumovitz M, Pareja R, Lopez A, Vieira M, Ribeiro R, et al. Minimally Invasive versus Abdominal Radical Hysterectomy for Cervical Cancer. N Engl J Med. 2018;379(20):1895-904.
212. Chiva L, Zanagnolo V, Querleu D, Martin-Calvo N, Arévalo-Serrano J, Căpîlna ME, et al. SUCCOR study: an international European cohort observational study comparing minimally invasive surgery versus open abdominal radical hysterectomy in patients with stage IB1 cervical cancer. International Journal of Gynecologic Cancer. 2020:ijgc-2020-001506.
213. Chiva L, Zanagnolo V, Kucukmetin A, Chakalova G, Raspagliesi F, Narducci F, et al. SUCCOR study. An international european cohort observational study comparing minimally invasive surgery versus open abdominal radical hysterectomy in patients with stage IB1 (FIGO 2009, <4 cm) cervical cancer operated in 2013–2014. International Journal of Gynecologic Cancer. 2019;29(Suppl 4):A1-A2.
214. Civit L, Fragoso A, O'Sullivan CK. Electrochemical biosensor for the multiplexed detection of human papillomavirus genes. Biosens Bioelectron. 2010;26(4):1684-7.
215. Bartosik M, Durikova H, Vojtesek B, Anton M, Jandakova E, Hrstka R. Electrochemical chip-based genomagnetic assay for detection of high-risk human papillomavirus DNA. Biosens Bioelectron. 2016;83:300-5.
216. Barratt A, Mannes P, Irwig L, Trevena L, Craig J, Rychetnik L. Cancer screening. J Epidemiol Community Health. 2002;56(12):899-902.
217. Parkin DM, Tappenden P, Olsen AH, Patnick J, Sasieni P. Predicting the impact of the screening programme for colorectal cancer in the UK. J Med Screen. 2008;15(4):163-74.
218. Downs LS, Smith JS, Scarinci I, Flowers L, Parham G. The disparity of cervical cancer in diverse populations. Gynecologic oncology. 2008;109(2 Suppl):S22-30.
219. Moser K, Patnick J, Beral V. Inequalities in reported use of breast and cervical screening in Great Britain: analysis of cross sectional survey data. BMJ (Clinical research ed). 2009;338:b2025.
220. programme Ncs. Cervical screening: quaterly coverage data reports 2019 2019 [updated 26th February 2020. Available from: https://www.gov.uk/government/publications/cervical-screening-quarterly-coverage-data-reports-2019.
221. Cadman L, Wilkes S, Mansour D, Austin J, Ashdown-Barr L, Edwards R, et al. A randomized controlled trial in non-responders from Newcastle upon Tyne invited to return a

self-sample for Human Papillomavirus testing versus repeat invitation for cervical screening. J Med Screen. 2015;22(1):28-37.
222. Kitchener HC, Gittins M, Rivero-Arias O, Tsiachristas A, Cruickshank M, Gray A, et al. A cluster randomised trial of strategies to increase cervical screening uptake at first invitation (STRATEGIC). Health Technol Assess. 2016;20(68):1-138.
223. Szarewski A, Cadman L, Mesher D, Austin J, Ashdown-Barr L, Edwards R, et al. HPV self-sampling as an alternative strategy in non-attenders for cervical screening - a randomised controlled trial. British journal of cancer. 2011;104(6):915-20.
224. Yeh PT, Kennedy CE, de Vuyst H, Narasimhan M. Self-sampling for human papillomavirus (HPV) testing: a systematic review and meta-analysis. BMJ Glob Health. 2019;4(3):e001351.
225. Snijders PJ, Verhoef VM, Arbyn M, Ogilvie G, Minozzi S, Banzi R, et al. High-risk HPV testing on self-sampled versus clinician-collected specimens: a review on the clinical accuracy and impact on population attendance in cervical cancer screening. Int J Cancer. 2013;132(10):2223-36.
226. Petignat P, Faltin DL, Bruchim I, Tramer MR, Franco EL, Coutlee F. Are self-collected samples comparable to physician-collected cervical specimens for human papillomavirus DNA testing? A systematic review and meta-analysis. Gynecologic oncology. 2007;105(2):530-5.
227. Malone C, Barnabas RV, Buist DSM, Tiro JA, Winer RL. Cost-effectiveness studies of HPV self-sampling: A systematic review. Preventive medicine. 2020;132:105953.
228. Williams DL, Hagensee M, Gao R, Barnhill D, Fontham ETH. The accuracy and validity of HPV testing through self-collection with tampons for cervical cancer screening. Translational Cancer Research. 2016:S993-S9.
229. Benevolo M, Vocaturo A, Caraceni D, French D, Rosini S, Zappacosta R, et al. Sensitivity, specificity, and clinical value of human papillomavirus (HPV) E6/E7 mRNA assay as a triage test for cervical cytology and HPV DNA test. Journal of clinical microbiology. 2011;49(7):2643-50.
230. Ying H, Jing F, Fanghui Z, Youlin Q, Yali H. High-risk HPV nucleic acid detection kit-the careHPV test -a new detection method for screening. Scientific reports. 2014;4:4704.

CHAPTER 6 AppendicesReaction mixes

6.1.1 LAMP reaction mix for experiments performed in a conventional qPCR platform

The LAMP mix contained the following:2.4μL of Betaine (stock at 5M), 1.5 μL of isothermal buffer, 0.9 μL of MgSO4 (stock at 100 mmol/L), 0.375μL of bovine serum albumin (20 mg/mL), 2.1 μL of dNTPs (stock at 10 mmol/L), 0.375 μL of Syto 9 (20 mmol/L stock) (Thermo FisherScientific,Waltham,MA), 0.6 μL of Bst 2.0DNApolymerase (8000 U/mL) (New England Biolabs, Hitchin, UK), 1.5 μL of 10Xprimer mixture (20 mmol/L BIP/FIP, 10 mmol/L loop forward and back primer, and 2.5 mmol/L B3/F3) (Integrated DNA Technologies), 3 μL of synthetic DNA (Integrated DNA Technologies) template solution, and enough nuclease-free water to bring the volume to 15 μL. Each solution was split into 5 μL reactions (triplicates) on a 96-well PCR plate and heated at 63C for 40 minutes.

6.1.2 pH-LAMP reaction conditions for lab-on-a-chip DNA markers

The pH-LAMP mix for DNA markers contained the following:2.4μL of Betaine (stock at 5M), 1.5 μ/L of customised isothermal buffer(pH 8.5-9), 0.9 μ/L of MgSO4 (stock at 100 mmol/L), 0.9μL of bovine serum albumin (20 mg/mL), 0.84 μL of dNTPs (stock at 25 mmol/L), 0.375 μL of Syto 9 (20 mmol/L stock) (Thermo FisherScientific,Waltham,MA), 0.375 μL of sodium hydroxide (0.2M), 0.04 μL of Bst 2.0DNApolymerase (120,000 U/mL) (New England Biolabs, Hitchin, UK), 1.5 μL of 10Xprimer mixture (20 mmol/L BIP/FIP, 10 mmol/L loop forward and back primer, and 2.5 mmol/L B3/F3) (Integrated DNA

Technologies), 3 μL of synthetic DNA (Integrated DNA Technologies) template solution, and enough nuclease-free water to bring the volume to 15 μL. Each solution was split into 5-μL reactions (triplicates) on a 96-well PCR plate and heated at 63C for 40 minutes.

6.1.3 pH-LAMP reaction conditions for lab-on-a-chip RNA markers

The pH-LAMP mix for RNA markers contained the following:2.4μL of Betaine (stock at 5M), 1.5 μ/L of customised isothermal buffer (pH 8.5-9), 0.9 μ/L of MgSO4 (stock at 100 mmol/L), 0.9μL of bovine serum albumin (20 mg/mL), 0.84 μL of dNTPs (stock at 25 mmol/L), 0.375 μL of Syto 9 (20 mmol/L stock) (Thermo FisherScientific,Waltham,MA), 0.375 μL of sodium hydroxide (0.2M), 0.375 μL of SuperScript® III RT/Platinum® Taq (Thermo FisherScientific,Waltham,MA), 0.15 μL of RNaseOUT™ Recombinant Ribonuclease Inhibitor (Thermo FisherScientific,Waltham,MA), 0.04 μL of Bst 2.0DNApolymerase (120,000 U/mL) (New England Biolabs, Hitchin, UK), 1.5 μL of 10Xprimer mixture (20 mmol/L BIP/FIP, 10 mmol/L loop forward and back primer, and 2.5 mmol/L B3/F3) (Integrated DNA Technologies), 3 μL of synthetic DNA or RNA (Integrated DNA Technologies) template solution, and enough nuclease-free water to bring the volume to 15 μL. Each solution was split into 5-μL reactions (triplicates) on a 96-well PCR plate and heated at 63^{o}C for 40 minutes.

6.2 TERC DNA

6.2.1 Primer screen 10^6 copy/reaction

Primer Option	Time to positive (mins)	Error(mins)
C0D	6.60	0.06
C1D	12.93	0.09
C2D	10.44	0.23
C3D	27.93	0.27
C4D	7.53	0.29

Primer option C0D and C4D were taken forward to the dilution screen stage.

6.2.2 Dilution screen

Copies/reaction	C0D TTP(mins)	Error (mins)	C4D TTP (mins)	Error (mins)
10^6	7.09	0.18	8.65	0.21
10^5	8.57	0.10	10.64	0.22
10^4	10.16	0.10	12.69	0.05
10^3	11.70	0.21	14.62	0.32
10^2	14.80	0.64	16.52	0.64
10^1	23.27	7.67	20.32	3.62
10^0	41.43	0.00	32.06	10.49

6.2.3 C4 with added loop primer screen

Primer Option	TTP (mins)	Error(mins)
C4L	5.74	0.06
C4	7.22	0.01
C0	6.45	0.01

6.2.4 C4 with added loop dilution comparison

Copies/reaction	C4 Loop TTP(min)	Error(mins)	C4 TTP(mins)	C0 TTP(mins)
10^4	8.00	0.10	12.69	10.16
10^3	9.30	0.20	14.62	11.70
10^2	10.15	0.23	16.52	14.80
10^1	11.95	0.15	20.32	23.27
10^0	33.38	13.40	32.06	41.43

6.3 hTERT RNA

6.3.1 Primer screen

Primer Option	Time to positive (mins)	Error(mins)
T_0	5.76	0.10
T_1	10.12	0.03
T_3	10.52	0.07
T_4	22.16	0.12
T_5	16.04	0.25

6.3.2 Dilution screen

Copies/reaction	T_0 TTP (mins)	Error (mins)	T_1 TTP (mins)	Error (mins)
10^8	5.61	0.13	9.87	0.17
10^7	7.08	0.12	12.17	0.09
10^6	8.52	0.22	13.89	0.16
10^5	9.60	0.06	16.30	0.16
10^4	11.04	0.13	17.63	0.93
10^3	12.91	1.45	21.65	1.63
10^2	-	-	-	-
10^1	-	-	-	-
10^0	-	-	-	-

Primer set T_0 and T_1 were taken forward to the dilution screen stage. The T_0 primer set outperformed the T_1 set but its copy detection limit was 10^3 copies per reaction.

6.4 MYC

6.4.1 Dilution screen

Copies/reaction	MYC_Op1 TTP(mins)	Error(mins)
10^6	6.26	0.41
10^5	7.51	0.07
10^4	9.22	0.06
10^3	10.58	0.19

10^2	11.81	0.59
10^1	14.98	1.95
10^0	-	-

6.5 GAPDH DNA

6.5.1 Primer screen

Primer Option	Time to positive (mins)	Error(mins)
GD_Op1_d	7.10	0.14
GD_Op_2d	5.19	0.12
GD_Op_3d	11.63	0.27
GD_Op_4d	8.24	0.06
GD_Op_5d	5.65	0.11

6.5.2 Dilution screen

Copies/reaction	Op2 TTP (mins)	Error (mins)	Op5 TTP (mins)	Error (mins)
10^4	6.84	0.22	7.60	0.08
10^3	8.13	0.32	8.93	0.22
10^2	9.98	0.12	10.21	0.60
10^1	11.33	0.12	17.51	5.30
10^0	13.62	0.86	-	-

Options 2 and 5 were taken forward for dilution screening. Both primer sets selected following screening were highly sensitive, however Option 2 was more efficient.

6.6 GAPDH RNA

6.6.1 Primer screen

Primer Option	Time to positive (mins)	Error(mins)
GR_1D	5.93	0.13
GR_2D	6.50	0.16
GR_3D	13.61	0.19
GR_4D	5.82	0.07

6.6.2 Dilution screen

Copies/reaction	GR1 TTP (mins)	Error (mins)	GR4 TTP (mins)	Error (mins)
10^6	6.44	0.16	5.83	0.06
10^5	7.16	0.21	6.93	0.19
10^4	8.46	0.08	8.14	0.22
10^3	9.64	0.46	9.35	0.17
10^2	13.41	3.43	11.95	1.23
10^1	23.38	0.00	12.76	1.17
10^0	40.76	0.00	-	-

Option 1 and 4 was taken forward to dilution screening. Both sets selected performed well, however Option 4 was both more sensitive and efficient.

6.7 HPV 16

6.7.1 Primer screen

Primer Option	Time to positive (mins)	Error(mins)
Op_1d	3.58	0.24
Op_2d	4.85	0.10
Op_3d	11.29	0.34
Op_4d	4.41	0.08

Options 1 and 4 were very fast and were taken forward to the dilution screen.

Option 1 was both more efficient and sensitive so was chosen.

6.7.2 Dilution screen

Copies/reaction	Op1 TTP (mins)	Error (mins)	Op4 TTP (mins)	Error (mins)
10^4	5.65	0.12	6.84	0.05
10^3	6.58	0.10	8.74	0.04
10^2	7.28	0.08	10.23	0.17
10^1	8.76	0.47	12.86	1.33
10^0	11.96	3.42	-	-

6.8 HPV 18

6.8.1 Primer screen

Primer Option	Time to positive (mins)	Error(mins)
18_Op_1	6.13	0.07
18_Op_2	11.57	0.09

18_Op_3	6.41	0.04
18_Op_4	5.66	0.02

Option 3 and 4 were taken forward to dilution screening; option 4 was chosen as it was more efficient and had similar sensitivity.

6.8.2 Dilution screen

Copies/reaction	Op3 TTP (mins)	Error (mins)	Op4 TTP (mins)	Error (mins)
10^4	10.93	0.31	9.27	0.34
10^3	12.75	0.11	11.02	0.15
10^2	14.30	0.62	13.08	0.24
10^1	18.67	0.00	-	-
10^0	-	-	-	-

6.9 HPV 45

6.9.1 Primer screen

Primer Option	Time to positive (mins)	Error(mins)
45_Op_1	11.90	0.03
45_Op_2	9.85	0.17
45_Op_3	5.46	0.07
45_Op_4	6.67	0.12

Option 3 and 4 were taken forward to dilution screening and Option 3 was chosen as it was more sensitive and efficient.

6.9.2 Dilution screen

Copies/reaction	Op3 TTP (mins)	Error (mins)	Op4 TTP (mins)	Error (mins)
10^4	9.41	0.23	11.80	0.18
10^3	10.49	0.18	13.63	0.27
10^2	13.17	1.06	15.66	0.55
10^1	13.72	0.84	-	-
10^0	-	-	-	-

6.10 HPV 58

6.10.1 Primer screen

Primer Option	Time to positive (mins)	Error(mins)
58_Op_1	7.06	0.07
58_Op_2	5.86	0.04
58_Op_3	3.54	0.09
58_Op_4	9.51	0.11

Option 2 and 3 were taken forward to dilution screening stage despite Option 2 having some evidence of primer dimer formation. Option 3 was more efficient and sensitive and so was chosen.

6.10.2 Dilution screen

Copies/reaction	Op2 TTP (mins)	Error (mins)	Op3 TTP (mins)	Error (mins)

10^4	7.93	0.19	5.50	0.07
10^3	9.40	0.14	6.20	0.39
10^2	11.06	0.12	6.78	0.03
10^1	15.37	1.96	8.58	0.55
10^0	33.92	1.12	11.73	1.96

6.11 HPV primer additional screening

6.11.1 All HPV types against non-splice sequence

HPV type	Non-splice sequence Time to positive (mins)	Error(mins)	Splice sequence Time to positive (mins)	Error(mins)
16d	6.17	0.05	3.58	0.24
18d	16.62	1.08	6.13	0.07
45d	7.97	0.12	5.46	0.07
58d	11.55	0.96	3.54	0.09

6.11.2 Data for all HPV types against non-splice sequences with single loop primer removed

Primer Option	Time to positive (mins)	Error(mins)
16_minus_Loop	33.57	8.85
18_ minus_Loop	38.43	0.86
45_ minus_Loop	39.77	0.94
58_ minus_Loop	20.35	1.64

6.11.3 HPV 18 Option screen

Primer Option vs splice/full sequence	Time to positive (mins)	Error(mins)
18_Op1_splice	11.45	0.30
18_Op1_full	27.30	1.92
18_Op2_splice	10.90	0.92
18_Op2_full	25.74	2.22

Option 2 was chosen to be screened with the mismatch FIP primer components. Option 18_2_3n, 18_2_3.1 and 18_2_4n will be tested in a dilution screen. There is amplification occurring in the full sequence, however it is unstable with a wide error. It is likely to disappear in the presence of the spliced version as it will consume the primers long before an inefficient amplification of the full sequence can occur.

6.11.4 HPV 18 Option 2 Mismatch screen

18_2_3n_splice	10.36	0.12
18_2_3n_full	24.61	1.91
18_2_3.1_splice	10.87	0.23
18_2_3.1_full	30.60	6.26
18_2_3.2_splice	-	-
18_2_3.2_full	-	-
18_2_4n_splice	10.69	0.33

18_2_4n_full	31.15	6.10
18_2_4.1_splice	12.45	0.23
18_2_4.1_full	27.72	1.94
18_2_4.2_splice	29.94	2.80
18_2_4.2_full	-	-

6.11.5 HPV 45 Mismatch screen

45_3N_splice	8.20	0.08
45_3N_full	26.71	10.70
45_3.1_splice	8.65	0.19
45_3.1_full	31.82	1.73
45_3.2_splice	22.68	0.82
45_3.2_full	43.75	0.00
45_4N_splice	19.34	0.56
45_4N_full	-	-
45_4.1_splice	8.73	0.19
45_4.1_full	36.71	6.32
45_4.2_splice	12.71	0.09
45_4.2_full	35.64	0.00

6.11.6 HPV 58 Mismatch screen

58op3_3n_splice	5.19	0.25
58op3_3n_full	16.52	2.35

58op3_3.1_splice	6.94	0.29
58op3_3.1_full	14.86	0.33
58op3_3.2_splice	10.36	0.10
58op3_3.2_full	9.96	0.12
58op3_4n_splice	6.69	0.20
58op3_4n_full	16.30	3.13
58op3_4.1_splice	8.19	0.19
58op3_4.1_full	11.04	0.08
58op3_4.2_splice	15.97	0.14
58op3_4.2_full	22.14	0.03